National technical university of Ukraine
«Igor Sikorsky Kyiv polytechnic institute»
Ministry of education and science of Ukraine

National technical university of Ukraine
«Igor Sikorsky Kyiv polytechnic institute»
Ministry of education and science of Ukraine

Qualification scientific work
as a manuscript

SHUKURLU ELNUR

UDC 622.271

DISSERTATION

SCIENTIFIC SUBSTANTIATION OF THE TECHNOLOGY OF EXPLOSIVE DEMAND OF GOLD-BEARING QUARTZITE

184 Mining
18 Production and Technologies

Submitted in fulfillment of the requirements for the degree of Doctor of Philosophy

The dissertation contains the results of the author's original research. Any use of ideas, results, or texts of other authors is duly referenced to the relevant sources.

________________ E.Shukurlu

Supervisor - ZUIEVSKA Natalia, doctor of technical sciences, professor

Kyiv - 2026

ABSTRACT

SHUKURLU E. Scientific substantiation of the technology of explosive demand of gold-bearing quartzite. – Qualification scientific work as a manuscript.

Dissertation for the degree of Doctor of Philosophy in Specialty 184 “Mining” (18 - Production and Technologies). — National Technical University of Ukraine “Igor Sikorsky Kyiv Polytechnic Institute”, Kyiv, 2026.

In the dissertation, a new solution to an urgent scientific and technical problem is presented, namely the scientific substantiation of an improved technology for the explosive fragmentation of gold-bearing quartzites based on an enhanced composition of foam stemming, using mathematical modelling and geographic information systems to optimize the directions of mining operations.

The current stage of development of the gold-mining industry in Azerbaijan is relatively new; however, it is already characterized by an active increase in production, expansion of the mineral resource base, and the opening of new open pits for the extraction of gold-bearing quartzite-containing rocks. Under such conditions, the application of modern geoinformation technologies becomes particularly relevant, as they make it possible to substantiate the directions of mining development, refine reserves, and optimize the volumes of rock mass extraction. At the same time, the significant volumes of gold-bearing rock mass fragmentation determine the need to improve the efficiency of drilling-and-blasting operations while ensuring the required particle-size distribution of the blasted rock. This is because the quality of fragmentation directly affects loading, transportation, and subsequent crushing processes, as well as overall production costs.

Considering the possible consequences of blasting operations in open pits, one of the main technological tasks in the development of gold-bearing quartzites is to ensure the required fragmentation of the rock mass and to minimize the negative environmental impact. If blasting operations cannot be avoided, it is necessary to implement modern, scientifically substantiated organizational and technological measures aimed at achieving the required quality of rock mass fragmentation and reducing the environmental burden.

In this dissertation, this task is solved by selecting an effective stemming material and conducting mathematical modelling aimed at evaluating the ejection time of the stemming from the borehole charge. Therefore, the research carried out in the dissertation and the obtained scientific and practical results are undoubtedly relevant.

Chapter 1 substantiates the relevance of the study in the context of the strategic importance of gold deposit development for the mining industry of Azerbaijan. It is shown that increasing the efficiency and environmental safety of mining operations requires the use of modern tools for investigation and optimization of extraction processes, including the integration of geodetic monitoring with GIS technologies. Geodetic monitoring provides high-accuracy spatial data necessary for surface condition control, deposit parameterization, and analysis of changes within the mining area, whereas GIS technologies make it possible to integrate, process and interpret these data, build three-dimensional models, estimate mineral reserves, and forecast the consequences of mining operations. The dissertation develops a methodology for analyzing a gold deposit and assessing the prospectivity of mining direction based on geodetic monitoring and GIS, using the Tulallar deposit (Azerbaijan) as a case study and applying Surfer and Google Earth software tools.

Chapter 2 examines the role of stemming as one of the key elements of the borehole charge structure, which determines the efficiency of explosive energy utilization. It is shown that reliable stemming ensures the retention of detonation products within the borehole during the critical stage of gas expansion, thereby increasing the initial pressure and the duration of the action of explosive gases on the rock mass. This contributes to the improvement of crack formation, displacement, and fragmentation of the rock mass, while also reducing unproductive energy losses into the atmosphere.

It is substantiated that stemming performs not only the technological function of ensuring fragmentation quality but also prevents the premature release of gases from the borehole, which may lead to incomplete detonation, increased toxicity of post-blast gases, uncontrolled flyrock from the collar zone, and intensification of the air blast wave. In this regard, stemming should be considered an important factor not only in the efficiency of explosive rock breaking but also in the safety and environmental performance of drilling-and-blasting operations.

The chapter also establishes that the efficiency of stemming is determined not only by its length but also by its mechanical properties, structure, and geometry. The physical behavior of stemming during blasting is analyzed, including successive stages of shock compression, decompression, free movement, and ejection, which together determine the duration of borehole sealing and the time of pressure action on the surrounding rock mass.

It is shown that optimal stemming should be technologically convenient to use and capable of delayed deformation under the action of expanding gases, thereby ensuring an extended retention time of detonation products. It is noted that traditional clay-sand mixtures remain a widely used solution due to their plasticity and adhesion; however, for short boreholes, improved stemming designs have significant potential. The presented analytical and numerical estimates confirm that even a slight increase in the retention time of detonation products can significantly improve blasting results, in particular by increasing fragmentation efficiency and reducing the specific consumption of explosive material.

Special attention in the chapter is paid to the environmental aspect of stemming application. It is shown that, under open-pit mining conditions, the choice of stemming material significantly affects not only the particle-size distribution of the blasted rock mass but also the level of dust-and-gas emissions during mass blasting. In this regard, modern approaches to stemming improvement are focused on achieving two interrelated objectives: extending the retention time of detonation products to improve fragmentation and reducing dust-and-gas emissions through the use of materials capable of absorbing dust and neutralizing harmful gases.

In this context, foam stemming is identified as a promising direction, as it ensures longer pressure retention, reduces the spread of the dust-and-gas cloud, improves muckpile characteristics, and may contribute to increasing the productivity of excavation and loading equipment. It is established that further improvement of foam stemming materials, including through the addition of 5% chalk, is a scientifically and practically justified direction for increasing the efficiency and environmental performance of blasting operations in open pits.

In the third chapter, a numerical model of explosive loading in a gold-bearing quartzite massif was developed and implemented using the ANSYS Explicit Dynamics software package. As a result of the modeling, it was established that the decisive factor influencing the efficiency of explosive rock fragmentation is not so much the peak pressure value, but rather the duration of detonation product retention within the borehole. It was shown that, for both stemming variants, the maximum pressure of the detonation products is similar in magnitude; however, the subsequent pressure decay differs significantly. In the case of sand stemming, the pressure decreases much more rapidly, indicating earlier gas escape and the loss of part of the explosive energy. In contrast, in the case of foam stemming, a slower pressure decrease is observed, which means a longer preservation of the force effect on the borehole walls and the surrounding rock mass.

An important scientific result of this chapter is the establishment of a polynomial relationship describing the variation of detonation product pressure over time for the two types of stemming. The obtained approximation made it possible to move from a qualitative analysis of the pressure curves to a quantitative assessment of the energy effect of the explosion. It was on the basis of these polynomial relationships that the average pressure values, the average forces exerted by the detonation products on the stemming, and the work of the detonation products along the stemming ejection path were determined. Thus, the polynomial approximation served not only as a tool for describing the dynamics of the process, but also as a basis for further engineering calculations characterizing the efficiency of explosive energy utilization.

The quantitative assessment showed that the average pressure in the case of foam stemming is higher than that in the case of sand stemming and, accordingly, the average force exerted by the detonation products on the stemming is also greater. The calculations showed that the average force in the case of foam stemming increases by approximately 41% compared with sand stemming. This indicates that, when foam stemming is used, a significantly larger portion of the explosion energy is directed toward fragmentation of the rock mass rather than being lost due to premature gas escape from the borehole.

The analysis of the stress state of the rock mass showed that foam stemming forms a more favorable stress distribution pattern. While in the case of sand stemming the explosive effect is concentrated mainly along the borehole axis, the use of foam stemming provides a wider and more uniform radial propagation of the affected zone. The effective area of stress distribution in the foam-stemming model is larger, which creates better conditions for uniform crack development and subsequent quartzite fragmentation.

Chapter 4 summarizes the theoretical and applied aspects of controlling the quality of explosive rock fragmentation under open-pit mining conditions and substantiates the expediency of applying modern approaches to regulating the particle-size distribution of the blasted rock mass. It is shown that fragmentation quality is determined by the combined influence of geological and structural factors, in particular the physical and mechanical properties of rocks, fracturing, blockiness, and layering of the rock mass, as well as bench geometry, drilling parameters, charge design, initiation schemes, and unloading conditions. It has been established that, due to the multifactorial nature of the process, universal theoretical prediction of fragmentation without taking into account the actual heterogeneity of the rock mass and without verification based on the results of industrial or field blasts is limited. This confirms the need to combine calculation-based approaches with systematic monitoring of the actual results of drilling-and-blasting operations.

It has been confirmed that the requirements for the quality of explosive fragmentation are determined primarily by the parameters of mining, haulage, and crushing-and-screening equipment, while the main evaluation criteria are the yield of oversized fractions, the average fragment size, and the uniformity of the particle-size distribution.

Within the framework of this chapter, field studies were carried out on the use of foam stemming as an alternative to traditional sand stemming during the fragmentation of gold-bearing quartzites. A comparison of the two technological variants showed that the use of foam stemming provides a noticeable improvement in fragmentation performance. In particular, it was established that when foam stemming was used, the yield of oversized fractions decreased to 5%, whereas when conventional sand stemming was used, this indicator was 9%. Thus, the application of foam stemming made it possible to reduce the percentage yield of oversized material by 4%, which confirms its higher technological efficiency compared with traditional sand stemming.

To ensure the objectivity of the comparison, the chapter applied a methodology of digital photo analysis of the particle-size distribution using specialized software. Unlike traditional methods of visual assessment or manual measurement, digital photo analysis makes it possible to promptly obtain quantitative fragmentation characteristics, including the average fragment size, the proportion of oversized material, and distribution uniformity indicators, as well as to expand the sample by analyzing multiple photographs. Importantly, this methodology is suitable for field conditions, does not require interruption of the production process, and can be used to form a statistical database for further optimization of drilling-and-blasting parameters.

Keywords: drilling and blasting, borehole charge, stemming, sand stemming, foam stemming, detonation products, pressure dynamics, pressure retention, stress–strain state, rock fragmentation, particle size distribution (PSD), oversized fractions, numerical simulation, ANSYS Explicit Dynamics, WipFrag.

АНОТАЦІЯ

ШУКЮРЛЮ Е. Наукове обґрунтування технології вибухового подрібнення золотоносних кварцитів. – Кваліфікаційна наукова праця на правах рукопису.

Дисертація на здобуття наукового ступеня доктора філософії за спеціальністю 184 – «Гірництво». – Національний технічний університет України «Київський політехнічний інститут імені Ігоря Сікорського», Київ, 2026.

В дисертаційній роботі представлено нове рішення актуальної науково-технічної задачі з наукового обгрунтування удосконаленої технології вибухового подрібнення золотоносних кварцитів на основі поліпшеного складу пінної забивки шляхом математичного моделювання та з використанням геоінформаційних систем для оптимізації напрямків гірничо-видобувних робіт.

Сучасний етап розвитку золотодобувної галузі Азербайджану є відносно новим, однак уже характеризується активним нарощуванням видобутку, розширенням мінерально-сировинної бази та відкриттям нових кар’єрів для розробки золоторудних кварцитовмісних порід. У таких умовах особливої актуальності набуває застосування сучасних геоінформаційних технологій, які дають змогу обґрунтовувати напрями розвитку гірничих робіт, уточнювати запаси та оптимізувати обсяги виймання гірської маси. Водночас значні обсяги подрібнення золоторудної маси зумовлюють необхідність підвищення ефективності буро-вибухових робіт із забезпеченням заданого гранулометричного складу підірваної породи, оскільки якість фрагментації безпосередньо впливає на процеси навантаження, транспортування та подальшого дроблення, а також на загальні виробничі витрати.

З огляду на можливі наслідки вибухових робіт у кар’єрах, однією з основних технологічних задач під час розробки золотоносних кварцитів є забезпечення необхідної фракційності гірської маси та мінімізація негативного впливу на навколишнє середовище. У разі неможливості відмови від ведення вибухових робіт необхідно впроваджувати сучасні, науково обґрунтовані організаційно-технологічні заходи, спрямовані на досягнення необхідної якості подрібнення гірської маси та зменшення екологічного навантаження. В дисертації ця задача

вирішується за рахунок вибору ефективного матеріалу забійки з проведенням математичного моделювання, направленого на оцінку часу вильоту забійки свердловинного заряду. Тому дослідження, які проведені в дисертаційній роботі, і отримані наукові та практичні результати є безумовно актуальними.

У першому розділі обґрунтовано актуальність досліджень у контексті стратегічного значення розробки золоторудних родовищ для гірничої промисловості Азербайджану. Показано, що підвищення ефективності та екологічної безпеки гірничих робіт потребує застосування сучасних інструментів аналізу й планування, зокрема поєднання геодезичного моніторингу з ГІС-технологіями. Геодезичний моніторинг забезпечує високоточне отримання просторових даних для контролю стану поверхні, параметризації родовища та аналізу змін у зоні видобутку, тоді як ГІС-технології дозволяють інтегрувати, обробляти та інтерпретувати ці дані, будувати тривимірні моделі, оцінювати запаси і прогнозувати наслідки гірничих робіт. У роботі розроблено методику аналізу золоторудного родовища та оцінювання перспективності напрямку ведення гірничих робіт на основі геодезичного моніторингу і ГІС на прикладі родовища Tulallar (Азербайджан) із використанням програмних продуктів Surfer і Google Earth.

У розділі 2 розглянуто роль забійки як одного з ключових елементів конструкції свердловинного заряду, що визначає ефективність використання енергії вибуху. Показано, що надійна забійка забезпечує утримання продуктів детонації в межах свердловини на критичному етапі розширення газів, завдяки чому підвищуються початковий тиск і тривалість дії вибухових газів на масив порід. Це сприяє покращенню процесів тріщиноутворення, зміщення та дроблення гірської маси, а також зменшує непродуктивні втрати енергії в атмосферу. Обґрунтовано, що забійка виконує не лише технологічну функцію забезпечення якості дроблення, а й запобігає передчасному виходу газів зі свердловини, що може спричиняти неповну детонацію, підвищення токсичності післявибухових газів, неконтрольований викид уламків із пригирлової зони та посилення повітряної ударної хвилі. У зв’язку з цим забійку слід розглядати як важливий чинник не лише ефективності вибухового руйнування, але й безпеки та екологічності буро-вибухових робіт.

У розділі також встановлено, що ефективність забійки визначається не тільки її довжиною, а й механічними властивостями, структурою та геометрією. Проаналізовано фізичну поведінку забійки в процесі вибуху, яка включає послідовні стадії ударного стискання, розрідження, вільного руху та викиду, що в сукупності визначають тривалість герметизації свердловини та час дії тиску на навколишній масив. Показано, що оптимальна забійка має бути технологічною у використанні та здатною до уповільненої деформації під дією газів, що розширюються, забезпечуючи подовження часу утримання продуктів детонації. Відзначено, що традиційні глинисто-піщані суміші завдяки своїй пластичності та адгезії залишаються поширеним рішенням, однак для коротких свердловин значний потенціал мають удосконалені конструкції забійки. Наведені аналітичні й числові оцінки підтверджують, що навіть незначне збільшення часу утримання продуктів детонації може суттєво покращувати результати вибуху, зокрема підвищувати ефективність дроблення та знижувати питомі витрати вибухової речовини.

Окрему увагу в розділі приділено екологічному аспекту застосування забійки. Показано, що в умовах кар’єрного видобутку вибір матеріалу забійки істотно впливає не лише на гранулометричний склад підірваної маси, а й на рівень пилогазових викидів під час масових вибухів. У зв’язку з цим сучасні підходи до вдосконалення забійки орієнтовані на досягнення двох взаємопов’язаних цілей: подовження часу утримання продуктів детонації для покращення дроблення, та зниження пилогазових викидів шляхом використання матеріалів, здатних поглинати пил і нейтралізувати шкідливі гази. У цьому контексті перспективним напрямом визначено пінну забійку, яка забезпечує триваліше утримання тиску, зменшує поширення пилогазової хмари, покращує характеристики розвалу та може сприяти підвищенню продуктивності виймально-навантажувального обладнання. Встановлено, що подальше вдосконалення пінних забійкових матеріалів, у тому числі за рахунок додавання 5% крейди є науково і практично обґрунтованим напрямом підвищення ефективності, та екологічності вибухових робіт у кар'єрах.

У третьому розділі розроблено та реалізовано чисельну модель вибухового навантаження в масиві золотоносних кварцитів із використанням програмного комплексу ANSYS Explicit Dynamics. У результаті моделювання встановлено, що вирішальним фактором, який впливає на ефективність вибухового руйнування гірської породи, є не стільки пікове значення тиску, скільки тривалість утримання продуктів детонації в межах свердловини. Показано, що для обох варіантів забійки максимальний тиск продуктів детонації є близьким за величиною, однак подальше зниження тиску суттєво відрізняється. У випадку піщаної забійки тиск зменшується значно швидше, що свідчить про більш ранній вихід газів і втрату частини енергії вибуху. Натомість у випадку пінної забійки спостерігається повільніше зниження тиску, що означає триваліше збереження силового впливу на стінки свердловини та навколишній гірський масив.

Важливим науковим результатом цього розділу є встановлення поліноміальної залежності, яка описує зміну тиску продуктів детонації в часі для двох типів забійки. Отримана апроксимація дала змогу перейти від якісного аналізу кривих тиску до кількісної оцінки енергетичного ефекту вибуху. Саме на основі цих поліноміальних залежностей було визначено середні значення тиску, середні сили впливу продуктів детонації на забійку, а також роботу продуктів детонації вздовж шляху викидання забійки. Таким чином, поліноміальна апроксимація стала не лише інструментом опису динаміки процесу, а й основою для подальших інженерних розрахунків, що характеризують ефективність використання енергії вибуху.

Кількісна оцінка показала, що середній тиск у випадку пінної забійки є вищим, ніж у випадку піщаної забійки, а відповідно, більшою є і середня сила впливу продуктів детонації на забійку. Розрахунки показали, що середня сила у випадку пінної забійки зростає приблизно на 41% порівняно з піщаною забійкою. Це свідчить про те, що при застосуванні пінної забійки значно більша частина енергії вибуху спрямовується на дроблення гірського масиву, а не втрачається внаслідок передчасного виходу газів зі свердловини.

Аналіз напруженого стану гірського масиву показав, що пінна забійка формує більш сприятливу картину розподілу напружень. Якщо у випадку піщаної забійки вибуховий вплив концентрується переважно вздовж осі свердловини, то застосування пінної забійки забезпечує ширше та більш рівномірне радіальне поширення зони впливу. Ефективна площа їх розподілу в моделі з пінною забійкою є більшою, що створює кращі умови для рівномірного розвитку тріщин і подальшого дроблення кварцитів.

Розділ 4 узагальнює теоретичні та прикладні аспекти керування якістю вибухового дроблення гірських порід в умовах відкритої розробки родовищ і обґрунтовує доцільність застосування сучасних підходів до регулювання гранулометричного складу підірваної гірської маси. Показано, що якість дроблення визначається сукупною дією геологічних і структурних факторів, зокрема фізико-механічними властивостями порід, тріщинуватістю, блочністю та шаруватістю гірського масиву, а також геометрією уступу, параметрами буріння, конструкцією заряду, схемами ініціювання та умовами розвантаження. Встановлено, що через багатофакторний характер процесу універсальне теоретичне прогнозування дроблення без урахування фактичної неоднорідності гірського масиву та без перевірки за результатами промислових або польових вибухів є обмеженим. Це підтверджує необхідність поєднання розрахункових підходів із систематичним моніторингом фактичних результатів буро-вибухових робіт.

Підтверджено, що вимоги до якості вибухового дроблення визначаються насамперед параметрами гірничого, транспортного та дробильно-сортувального обладнання, тоді як основними критеріями оцінки є вихід негабаритних фракцій, середній розмір уламків і рівномірність гранулометричного розподілу.

У межах цього розділу проведено польові дослідження щодо застосування пінної забійки як альтернативи традиційній піщаній забійці під час дроблення золотоносних кварцитів. Порівняння двох технологічних варіантів показало, що застосування пінної забійки забезпечує помітне покращення показників дроблення.

Зокрема, встановлено, що при використанні пінної забійки вихід негабаритних фракцій знизився до 5%, тоді як при застосуванні традиційної піщаної забійки цей показник становив 9%. Таким чином, застосування пінної забійки дало змогу зменшити відсотковий вихід негабаритного матеріалу на 4%, що підтверджує її вищу технологічну ефективність порівняно з традиційною піщаною забійкою.

Для забезпечення об’єктивності порівняння в розділі застосовано методику цифрового фотоаналізу гранулометричного складу з використанням спеціалізованого програмного забезпечення. На відміну від традиційних методів візіальної або ручного вимірювання, цифровий фотоаналіз дає змогу оперативно отримувати кількісні характеристики дроблення, зокрема середній розмір уламків, частку негабаритного матеріалу та показники рівномірності розподілу, а також розширювати вибірку шляхом аналізу кількох фотографій. Важливо, що така методика є придатною для польових умов, не потребує зупинки виробничого процесу та може використовуватися для формування статистичної бази даних з метою подальшої оптимізації параметрів буро-вибухових робіт.

Ключові слова: буро-вибухові роботи, свердловинний заряд, забійка, піщана забійка, пінна забійка, продукти детонації, динаміка тиску, утримання тиску, напружено-деформований стан, подрібнення порід, гранулометричний склад, негабаритні фракції, чисельне моделювання, ANSYS Explicit Dynamics, WipFrag.

LIST OF THE APPLICANT'S PUBLICATIONS

Scientific works presenting the main scientific results of the dissertation

1. **Shukurlu E.** Estimation of fractionation of minerals using geoinformation systems in engineering and geological prospecting / N. Zuievska, T. Kosenko, E. Shukurlu, V. Korobiichuk // Technical Engineering. - 2024. - № 1 (93). - P. 332-338. https://doi.org/10.26642/ten-2024-1(93)-332-338 **(contribution of co-authors:** Zuievska N. — analysis of recent research and publications, formulation of the research aim; Kosenko T. — application of the geoinformation system; Shukurlu E. — conducting engineering-geological surveys, substantiation of the research problem; Korobiichuk V. — introduction, analysis of recent research).

2. **Shukurlu E.** Integration of GIS and geodetic monitoring for gold deposit modeling and mine planning/ N. Zuievska, T. Kosenko, E. Shukurlu, P. Hajiyev, N. Shukurlu // Geo-Technical Mechanic. - 2025. - № 173. - P.175-185. https://doi.org/10.15407/geotm2025.173.175 **(contribution of co-authors:** Zuievska N. — statement of the problem and its connection with practical tasks, analysis of recent research and publications, formulation of the research aim; Kosenko T. — application of GIS for determining mineral concentrations; Shukurlu E. — formation of the database for modeling, georeferencing of the geoinformation modeling method to the terrain; Hajiyev P. — analysis of mineral distribution by depth; Shukurlu N. — analysis of recent research and literature sources).

3. **Shukurlu E.** Using the WipFrag image analysis system to evaluate the quality of explosive rock fragmentation / V. Berezdetskyi, E. Shukurlu // Coll.res.pap.nat.min.univ. – 2024. - №79. - P.7–14. https://doi.org/10.33271/crpnmu/79.007 **(contribution of co-authors:** Berezdetskyi V. — use of the software for mathematical modeling; Shukurlu E. — statement of the problem, analysis of recent research, formulation of the aim, preparation of input data for modeling, processing of the obtained results).

4. **Shukurlu E.** Prospects for the development of gold deposits based on geodesic monitoring and GIS technologies / T. Kosenko, E.Shukurlu// Coll.res.pap.nat.min.univ. – 2024 - №79. - P.38–48. https://doi.org/10.33271/crpnmu/79.038 **(contribution of co-**

authors: Kosenko T. — use of the Surfer software for modeling; Shukurlu E. — conducting geodetic monitoring, statement of the problem, preparation of input data for modeling, processing of the obtained results).

5. **Shukurlu E.** Numerical simulation of sand and foam stemming for improved rock fragmentation in gold-bearing quartzites / N. Zuievska, V. Berezdetskyi, E. Shukurlu // Coll.res.pap.nat.min.univ. - 2025. - № 82. - P.29-43. https://doi.org/10.33271/crpnmu/82.029 (**contribution of co-authors:** Zuievska N. — statement of the problem and its connection with practical tasks; Berezdetskyi V. — use of the ANSYS software for mathematical modeling; Shukurlu E. — analysis of recent research, formulation of the aim, preparation of input data for modeling, processing of the obtained results).

6. **Shukurlu E.** Features of the construction of a collector network in difficult topographic conditions by microtunnel/ N. Zuievska, O. Vovk, L. Shaidetska, E. Shukurlu // Coll.res.pap.nat.min.univ., 2022. № 70 – P.57-75. https://doi.org/10.33271/crpnmu/70.057 (**contribution of co-authors:** Zuievska N. — modeling and analysis of results; Vovk O. — statement of the problem and its connection with practical tasks; Shaidetska L. — development of initial conditions for soils and concrete structures, analysis of the obtained results; Shukurlu E. — assessment of the complex topographic conditions of the excavation route).

7. **Shukurlu E.** Assessment of mineral resources for Yukon's gold mining district using GIS technologies / T. Hrebeniuk, L. Shaidetska, V. Bronytskyi, E. Shukurlu // Coll.res.pap.nat.min.univ. 2025, 81, p.28–36. https://doi.org/10.33271/crpnmu/81.028 (**contribution of co-authors:** Hrebeniuk T.— modeling and analysis of results; Shaidetska L. — statement of the problem and its connection with practical tasks; Bronytskyi V. — development of initial conditions for soils and concrete structures, analysis of the obtained results; Shukurlu E. — application of a methodology combining satellite imaging of the area, its digitization, and transfer into GIS application software).

8. **Shukurlu E.** Development of mathematical decision-making support tools for effective response to emergencies during the transportation of dangerous substances by road transport/ A.V. Iatsyshyn, L.M. Markina, O.O. Tiutiunyk, V.V. Tiutiunyk, E.

Shukurlu // IOP Conference Series: Earth and Environmental Science, Volume 1254, 4th International Conference on Sustainable Futures: Environmental, Technological, Social and Economic Matters (ICSF-2023). – 2023. https://doi.org/10.1088/1755-1315/1254/1/012110 **(contribution of co-authors:** Andrii V. Iatsyshyn — contributed to the conception and design of the study, analyzed the literature. Liudmyla M. Markina — evaluated the potential chemical risk in the vicinity of the accident and settlement zone. Olha O. Tiutiunyk — determined the main parameters affecting the depth of secondary damage cloud as a result of an accident at a chemically hazardous facility. Vadym V. Tiutiunyk — determined the area and extent of chemical damage in the braking area. Elnur Shukurlu — determined the spill area of chemically hazardous substances).

Scientific works confirming the approbation of the dissertation results

9. **Shukurlu E.** The Use of GIS to Improve the Parameters of Gold-Bearing Quartzite Extraction Technology / N. Zuievska, A. Kryvoruchko, L. Shaidetska, E. Shukurlu // International scientific and technical conference Geomining. Studies in Systems, Decision and Control, Springer, Cham. – 2024. - № 224. – P. 135–146. https://doi.org/10.1007/978-3-031-70725-4_10 **(contribution of co-authors:** Zuievska N. — statement of the problem and its connection with practical tasks; Kryvoruchko A. — analysis of rock mass fracturing; Shaidetska L. — analysis of recent research; Shukurlu E. — conducting geomonitoring and analysis of spatial data for modeling, processing of the obtained results).

10. **Shukurlu E.** Using the wipfrag image analysis system to evaluate the quality of explosive / P. Hajiyev, E. Shukurlu, N. Zuievska. // Proceedings of the International Scientific and Technical Conference "Current State and Prospects for the Development of Geotechnical Engineering. GEO-25" [Electronic resource]. — Kyiv: Igor Sikorsky Kyiv Polytechnic Institute. - 2025. - P.25-28. https://geobud.kpi.ua/wp-content/uploads/Zbirnyk-materialiv-GEO-2025-ISBN-978-617-8324-55-1-.pdf **(contribution of co-authors:** P. Hajiyev — image-based analysis of the obtained photographs to determine the fragment size distribution, E. Shukurlu — assessment of

fragment size distribution of the blasted material, N. Zuievska — statement of the problem and its connection with practical tasks).

11. **Shukurlu E.** Use of GIS technologies for geospatial analysis of gold ore deposits / T. Kosenko, E. Shukurlu. // Proceedings of the International Scientific and Technical Conference "Current State and Prospects for the Development of Geotechnical Engineering. GEO-25" [Electronic resource]. — Kyiv: Igor Sikorsky Kyiv Polytechnic Institute. - 2025. - P. 99-103. https://geobud.kpi.ua/wp-content/uploads/Zbirnyk-materialiv-GEO-2025-ISBN-978-617-8324-55-1-.pdf **(contribution of co-authors:** T. Kosenko — statement of the problem and its connection with practical tasks, E. Shukurlu — application of the developed methodology for analyzing deposit concentration by means of a GIS software package).

PLAN

INTRODUCTION

Actuality of theme. The current stage of development of Azerbaijan's gold mining industry is relatively recent; however, it is already characterized by a steady increase in production, expansion of the mineral resource base, and the opening of new open pits for mining gold-bearing quartzite formations. Under these conditions, the application of modern geoinformation technologies becomes especially important, as they make it possible to substantiate the directions of mining development, refine reserve estimates, and optimize rock mass extraction volumes. At the same time, the large-scale fragmentation of gold-bearing ore creates a need to improve the efficiency of drilling and blasting operations while ensuring the required particle-size distribution of the blasted rock. This is because fragmentation quality directly affects loading, hauling, and subsequent crushing processes, as well as overall production costs.

Given the possible consequences of blasting operations in open pits, one of the main technological challenges in mining gold-bearing quartzites is to ensure the required size distribution of the rock mass while minimizing negative environmental impacts. Where blasting operations cannot be avoided, it is necessary to implement modern, scientifically substantiated organizational and technological measures aimed at achieving the required fragmentation quality and reducing environmental load. Therefore, the scientific substantiation of a technology for blasting-induced fragmentation of gold-bearing quartzites, based on the use of advanced software, mining-direction optimization technologies, and modern stemming materials, constitutes an urgent scientific and technical task.

Relationship of the dissertation with scientific programs, plans, and topics.

The dissertation was carried out within the framework of the scientific activities of the Department of Geoengineering of the National Technical University of Ukraine "Igor Sikorsky Kyiv Polytechnic Institute", including the scientific initiative topic "Scientific Foundations of Resource-Saving Technologies in Mining and Geotechnical Construction" (State Registration No. 0115U005398) and according to Contract

No/Дндч/0201.01/2430.01/162/2022 "Optimization of technological parameters of destruction of gold-bearing quartzites".

Aim and objectives of the research. The aim of the dissertation is to scientifically substantiate an improved drilling-and-blasting technology in gold-bearing quartzite massifs of open-pit mining operations by selecting an effective stemming material to improve fragmentation quality and reduce the yield of oversized fractions.

To achieve this aim, the following research objectives were formulated in the dissertation:

- to develop a methodology for analyzing a gold ore deposit and substantiating promising directions for mining operations based on the integration of geodetic monitoring and GIS technologies;
- to study and analyze the mechanism of fragmentation of gold-bearing quartzites;
- to investigate the influence of stemming material on the formation of toxic post-blast gases;
- to perform numerical modeling of the influence of stemming material on blast energy retention and the efficiency of rock fragmentation during open-pit blasting operations in gold-bearing quartzites;
- to improve the methodology for assessing the particle-size distribution of blasted rock mass in large volumes of rock;
- to investigate the influence of stemming material on the particle-size distribution of the blasted rock mass.

The object of the research is the process of destruction of gold-bearing quartzite massifs during drilling-and-blasting operations under open-pit mining conditions.

The subject of the research is the parameters and elements of drilling-and-blasting technology in gold-bearing quartzites, in particular the properties of stemming that determine the pressure dynamics of detonation products, the nature of the stress–strain state of the massif, and fragmentation indicators.

Research methods. In the course of preparing the dissertation, a set of general scientific and specialized research methods was used to solve the defined scientific tasks, including: review, systematization, generalization, and analysis of previous theoretical developments and practical experience related to the research topic; geological mapping; remote methods for obtaining initial data based on satellite images; methods of mathematical statistics and probability theory; as well as mathematical modeling methods and photo analysis methods.

The dissertation is a completed scientific work containing new scientifically substantiated results, which are as follows:

- polynomial regularities of the change in detonation product pressure of a borehole charge over time when using sand and foam stemming have been established;
- the influence of stemming material on the distribution of harmful post-blast gases within the working zones of the open pit has been identified and verified in practice; it has been shown that adding 5% chalk to the foam stemming composition reduces the average values of harmful gas concentrations by approximately 40%;
- based on numerical modeling, new quantitative and qualitative relationships have been obtained between the ejection time of stemming made of different materials, the nature of the stress–strain state of the rock mass, and the degree of fragmentation of gold-bearing quartzites. These results were confirmed by field data and made it possible to reduce the yield of oversized fractions from 9% to 5%.

Practical significance of the obtained results:

— a digital geospatial model of the Tulallar deposit has been developed, which, based on the obtained data of geospatial analysis of mineral deposits and concentrations, makes it possible to select optimal directions for the development of mining operations;

— the material for borehole stemming has been improved in order to enhance the quality of fragmentation and reduce gas formation;

— the methodology of photographic recording of the fractional composition of the blasted rock mass under the conditions of the Tulallar open-pit mine has been improved.

The personal contribution of the applicant to the scientific works published in co-authorship is as follows: [1] — conducting engineering-geological surveys, substantiation of the research problem; [2] — formation of the database for modeling, georeferencing of the geoinformation modeling method to the terrain; [3] — statement of the problem, analysis of recent research, formulation of the aim, preparation of input data for modeling, processing of the obtained results; [4] — conducting geodetic monitoring, statement of the problem, preparation of input data for modeling, processing of the obtained results; [5] — analysis of recent research, formulation of the aim, preparation of input data for modeling, processing of the obtained results; [6] — conducting geomonitoring and analysis of spatial data for modeling, processing of the obtained results; [7] — development of an algorithm for creating a digital model for transport operations under open-pit mining conditions; [8] — development of an algorithm for photographic recording and comparison of the results with the visual method; [9] — conducting geomonitoring and creation of a database for the digitalization of the deposit; [10] — analysis of complex topographic conditions has been carried out.

Approbation of the results of the dissertation work. The main provisions and results of the dissertation have been presented at the international scientific and technical conference Geomining (2023) and at the International Scientific and Technical Conference "Current State and Prospects for the Development of Geotechnical Engineering (GEO-25)" (Kyiv, 4–5 June 2025), and have been published in the conference proceedings.

Publications. The results of the dissertation have been published in 11 scientific works, including 7 articles in scientific professional journals of Ukraine, 1 article in a journal indexed in the Scopus scientometric database, and 3 in the proceedings of international scientific and practical conferences.

Structure and scope of the dissertation. The dissertation consists of an introduction, 4 chapters, conclusions, a list of references, and an appendix. The total volume of the dissertation amounts to 151 pages of text, including 53 figures, 5 tables, 1 appendix, and a list of references comprising 70 titles on 10 pages; the main text of the dissertation is presented on 141 pages.

CHAPTER 1. GEODETIC MONITORING AND GIS TECHNOLOGIES DEVELOPMENT PROSPECTS OF GOLD DEPOSITS

1.1 Geodetic Monitoring and GIS Systems in Gold Deposit Development

The goal of this research is to create an analytical method applicable to gold ore deposits by combining geodetic monitoring data with GIS technologies, thereby achieving both the accurate determination of the spatial distribution of the valuable components of the gold ore deposit and the greater efficiency in the mining process.

In the study conducted at the Tulallar gold deposit, research methods were applied with a comprehensive analytical approach, considering modern geodetic technology and Geo-Informational Systems (GIS). Moreover, the research techniques entailed geodetic monitoring methodologies, acquiring spatial data (GoogleEarth), entailing combining geodetic monitoring with spatial data collected from GoogleEarth application. Creating a three dimensional model of ore body configuration with Surfer software facilitated the ability to visually analyse the locations and configurations of ore distribution. Because of combining the two methods mentioned above, the study produced quality visual images of ore distribution and Identified areas that have future areas for Mining [1, 2].

The research demonstrates how geodetic monitoring combined with GIS technology can very successfully be used to determine where there are high-prospect areas for mining operations. Both technologies do so, on the one hand, with the provision of accurate mapping data and geological models, and on the other, the dimensional data from Surfer and Google Earth together was used to produce a fully realized three-dimensional model of the ore bodies and that model was used to determine the quantity of resources that could be removed from those locations, maximizing the mining process.

We've developed a new technique to analyse the gold holdings by combining Geodetic Data with GIS Tools in synergy, to create 3D models of gold deposits, which not only demonstrate where the gold is present, but also shows how much of all types of minerals are available at the location. This method provides much more accurate exploration and mining operations as well as a way of governing environmental risks involved in gold mining.

The approach has potential use cases in identifying new mine locations, improving mining operations, and minimising environmental impact. The integrated Geodetic-GIS dataset produces a spatial analysis that can facilitate optimum mine planning. The approach outlined in this study can be adopted at additional deposits for optimum optimisation of the resource and the economic performance of the mine.

Developing gold resources has become a strategic priority in the current mining industry and plays an integral role in supporting both local and national economies. The mining sector finds it increasingly difficult to extract resources in a productive, efficient, and environmentally sound manner. As a consequence, relevancy and optimal exploration and development of mines will require new and advanced spatial technology to further enhance mine planning accuracy and sustainability [3, 4, 5].

Speed, which is achieved through high-precision geodetic measurements, is one of the most effective ways to obtain geodetic monitoring of a site as it provides the ability to not only determine the surface stability of the site, but to estimate the deposit characteristics as well as to monitor the environmental conditions of the site. In all three phases of mining (pre-mining, mining and post-mining), this instrument will provide decision-makers with information needed to make sound decisions regarding the operations through visual representation (map) and analysis of the structure (geometric location).

The use of Geographic Information Systems (GIS) technology allows users to display and present spatial data in multiple ways, such as through a three-dimensional (3D) representation of the area. The user will thereby be able to generate accurate three-dimensional models of the area, calculate the volume of a mineral deposit, or evaluate the impact of mining on a particular area, among other possibilities. When users combine different sources of information (e.g., geodetic and GIS) in their models, they obtain the best possible overall representation of extraction efficiency for a given mineral resource in combination with the least amount of environmental risk [6, 7].

Previous research that uses GIS combined with geodetic monitoring can help find the ideal resource extraction location when assessing geology, topography, ore deposition and work limitations. In the mining industry, GIS enables more accurate and efficient decision making through sustainable use of natural resources while minimizing environmental damages.

This study intends to develop and apply ways to assess the Tulallar Doulevard gold deposit economic and geological potential (Azerbaijan) through the use of principles of geodetic and integrated GIS technology. Two software programs were used, which helped to complement each other. The Google Earth software was used for visualising the spatial distribution of the gold deposit, whereas Surfer was used for modelling and analysing the spatial distribution representation as produced using Google Earth [8, 9, 10].

1.2 Geological and Structural Overview of the Tulallar Deposit

The Tulallar deposit can be found in the north-eastern region of the Lesser Caucasus mountains. The area where it is situated features an array of high-to-medium mountain topography. The absolute elevation measurements for this are approximately 1200 to 2500 meters in height, sometimes up to 3000 meters. In the case of the northern slope, there are several large rock outcroppings that will reach approximately 400 to 500 meters in height. To the southwest of the deposit lie the Kapaz and Murovdag mountain ranges, which further add to the overall complex topography of this deposit.

In light of information from the National Geological Exploration Service of Azerbaijan, there is a significant amount of perennially-renewable material throughout the ores in the Kini Pompalai region. Many of these rocks were separated due to large amounts of movement from natural forces. In addition, the majority of the central portion of this rock are essentially comprised entirely of intermediate-acid tufa deposits, although the outer areas contain primarily andesite/basalt mineral formations. Dykes (or dike formations) exist within this area, as well as being entirely andesite-basaltd mineral formation. The pyrite content within these rocks is very high. There are also many quartz veins and calcite-quartz veins located within these rock formations.

Accurately determining mineral deposits and their spatial geometry are critical factors in developing mining operations sustainably and economically. Traditional geological techniques (2D maps and cross sections) do not adequately represent the real complexity of an ore body geometry in areas that are structurally complex or contain a wide variety of different minerals. Recent technological advances in geodetic monitoring and Geographic Information System (GIS) technology combined with three dimensional (3D) modeling applications provide new ways to visualize and interpret the subsurface in more accurate and reliable visual representations [11, 12].

This research considers the Tulallar deposit of gold in the Gadabay district, western Azerbaijan. Tulallar is developing, relatively new deposit that is located inside the Lesser Caucasus Metallogenic and has an abundance of gold and polymetallic formations. Tulallar has complex geology that comprises volcanic and sedimentary rock sequences (hydrothermal alteration) and faulted rocks too. The presence of these 3 geologic characteristics controls where (location) and the amount (quantity) of occurrence of gold hosting quartz vein deposits and ore bodies in this area, (see Figure 1.1).

Figure 1.1. Panoramic view of the Tulallar gold deposit open-pit mine located in the Lesser Cauca-sus region, showcasing terraced excavation levels and surrounding forested landscape

The initial exploration of the Tulallar project has identified epithermal gold mineralization that are predominantly contained within Quartzite units which display high degrees of variation in gold concentration on both lateral and vertical scales. Over 150 exploration drill holes were completed for purposes of defining the mineralized zones as well as determining their potential to provide economic returns. The data collected forms the foundation for developing an accurate geodetic and geological 3-dimensional model to support the necessary tools for effective mine planning and mine resource management. The research aims to produce a high-resolution 3D model of a gold deposit, showing how gold varies in different locations within the deposit. Borehole and topographic data are combined, along with modern interpolation techniques, to get an even greater understanding of the distribution of ore and it's zonation. This model is not only able to improve predictions about the amount of gold left to be mined but it will also help decide the best ways to mine the ore efficiently and in an environmentally friendly manner [13, 14].

Figure 1.2. Engineering-geological investigations of the Tullallar deposit

The mineralization of the Tulullar gold deposit is gold–quartz and contains relatively few different minerals. The main sulfide minerals in this deposit range from pyrite to chalcopyrite, bornite, sphalerite, galena, tetrahedrite, and pyrrhotite. Oxide minerals include goethite, hematite and limonite, which may be present along with native gold. The associated gangue minerals consist of quartz, barite, chalcedony, chlorite, sericite and epidote. As the main ore mineral, pyrite unfortunately occurs in large quantities (up to 20%) in the ore zones, and up to about 0.02–0.5 mm in aggregate sizes. The gold mineralization is of the high sulfide type, and is characterized by strong silicification, kaolinization, and brecciation. The mineralized zone contains intermediate to acid volcanic rocks (andesite, dacite, rhyolite), which show a continuum of metasomatic alteration, in some cases partial, between the contacts of different lithological units. The upper-most levels of the mineralized zone are dominated by oxidized ore, usually accompanied by strong silicification. Below this lie a transition zone of both oxidized ore and sulfide minerals such as Pyrite. This transition forms the mixed oxide–sulfide transitional Zone.

Geochemical analysis of ore samples detected 0.1170% lead (Pb), 0.048% manganese (Mn), 0.0105% titanium (Ti), 0.0042% chromium (Cr), 0.0046% vanadium (V), 0.0019% molybdenum (Mo), 0.0112% zirconium (Zr), 0.1225% copper (Cu), 0.000017% gold (Au), 0.00386% silver (Ag) and; 0.006671% cobalt (Co) as trace elements. This information helps to identify the spatial distribution patterns of occurrences of gold bearing zones. (4)

The area under study is located in the north-western part of the Geygel uplift between the Dashkesan and Agdzhakand depressions. A network of control points for geodetic control has been established within the boundaries of the Tulallar deposit, with the coordinates of the reference stations shown in Table 1.1.

Table 1.1. Coordinates of Exploration Site Points

Hole ID	X	Y	Hole ID	X	Y
W1	605220	4476400	W10	605190	4478680
W2	605760	4476480	W11	605050	4478400
W3	605750	4476910	W12	604990	4478200
W4	605700	4476980	W13	604985	4478000
W5	605750	4477600	W14	605060	4477820
W6	605725	4477800	W15	605010	4477480
W7	605815	4478000	W16	605080	4477000
W8	605800	4478080	W17	604900	4476870
W9	605710	4478680			

The UTM Zone 38 coordinate system and Baltic Height System were used to specify the station positions. Their coordinates were tied to the fourth order of the national geodetic network. The station coordinates were then ported to Google Earth so that they could be used for additional spatial analysis [15, 16, 17].

The accuracy and efficiency of spatial analysis of the deposit were improved by exporting data from Google Earth and importing it into Surfer software. The data from Google Earth Pro was used to construct an accurate contour map of the relief of the study area. To produce the contour map of relief, a number of surface points were selected in Google Earth Pro using the WGS-84 coordinate system, and the absolute elevation of each point was determined by using the GPS Visualizer conversion tool. The dataset generated was then loaded into Surfer [18,19].

A digital elevation model (DEM) was made with a Kriging interpolation type because it's good for analyzing uneven land. The DEM was made to show contour lines of the extraction area so that it would show the boundaries of the extraction area in the study area. In Figure 3, you can see a contour map of the study area.

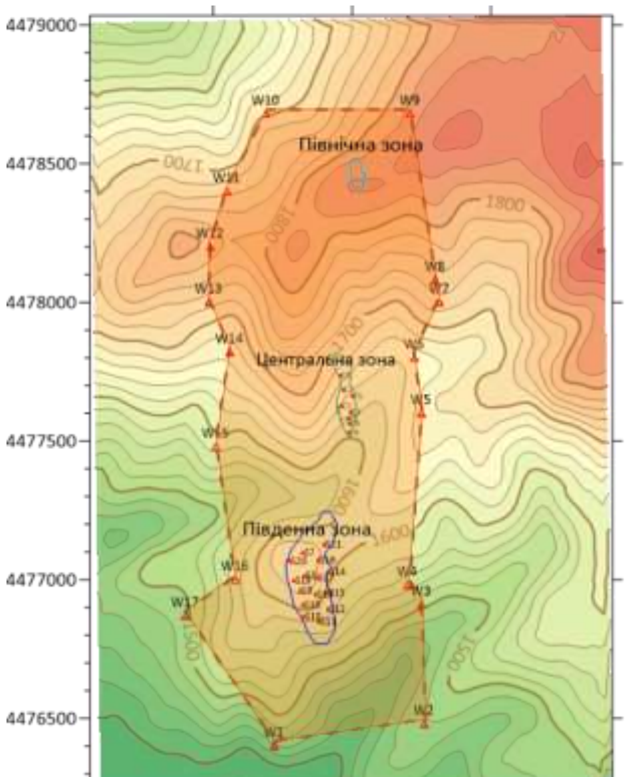

Figure 1.3. Terrain contour map of the Tulallar extraction area generated using Kriging interpolation in Surfer.

Moreover, exporting data out of Google Earth will aid to utilise geospatial data to a greater degree of precision in map making, constructing 3D Models and performing spatial analysis. The format for the aerial images exported from Google Earth is .KML. The real world coordinates are established using Control Points that match the important points of interest on ground.

When done, the georeferenced map is included in the set coordinates of that system (most likely, UTM). With Surfer, additional maps (i.e., a Contour map with surface isolines - see the earlier Figure 1.3), can be overlaid on the georeferenced base map, or a Drillhole map that shows where all boreholes were drilled (Figure 1.4).

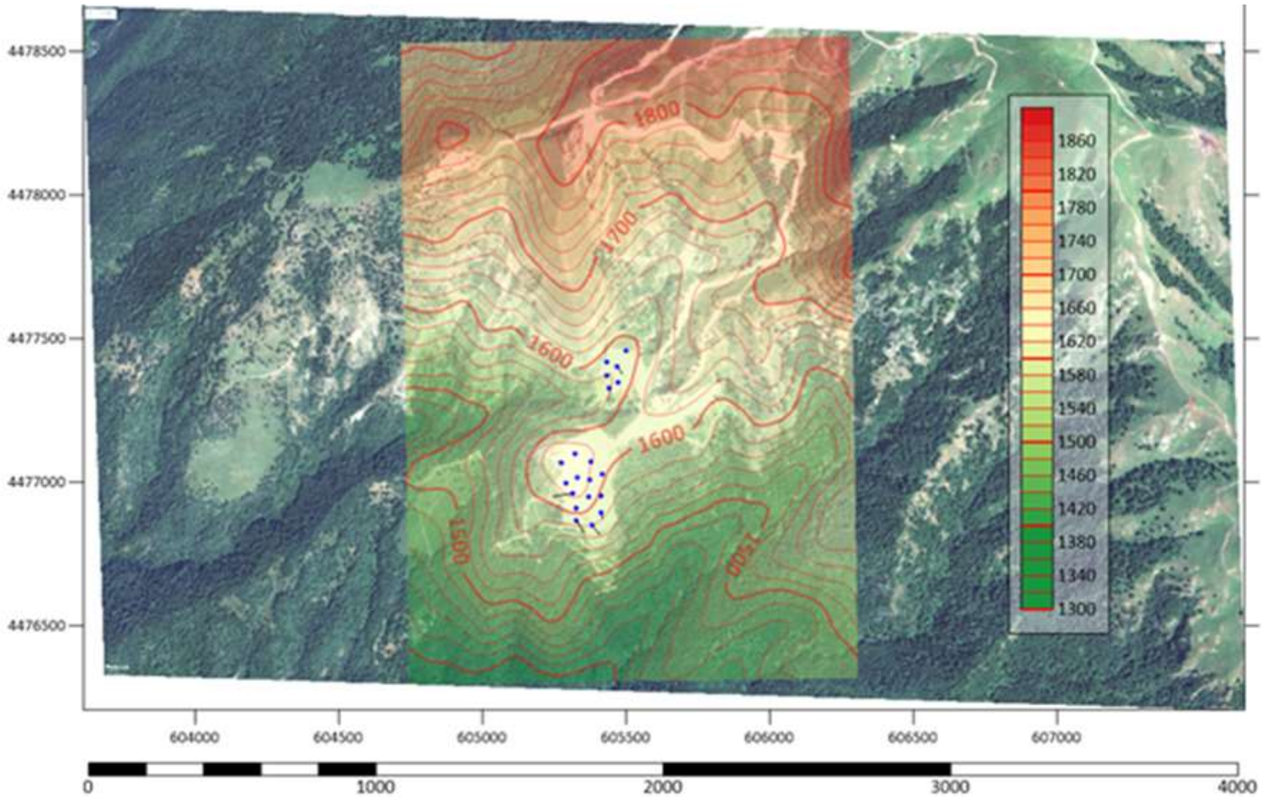

Figure 1.4. Integration of georeferenced aerial imagery and borehole map in Surfer software

With this combined approach to mapping, you can see how surface features relate to geological structures, like how topography relates to the mining area. You can also make detailed models of the land. You have the ability to change how you see things, like choosing different colors or line styles, so that you can see the different things you are analyzing clearly. This allows you to provide a lot of information in a way that makes sense visually.

When it comes to research about mineral deposits and mining operation plans, topography is very significant. Creating digital elevation models is also made possible using GIS technologies and various ways to create digital maps of minerals using different types of interpolation methods. Among the most commonly used interpolation techniques are Natural Neighbor, IDW and Kriging [20, 21, 22].

The Natural Neighbor Method applies the principle of weighing averages of values of surrounding points to create a uniform surfaces. This creates an interpolated surface that is basically smooth. Therefore we can use the method when we have unevenly spaced data, but it will probably not provide entirely accurate results if we were to use it to interpolate data that has large differences in altitude between the locations of each point.

The IDW method gets its point values by dividing those numbers by how far apart they are from each other. The more closely two points are together, the more alike they are, leading to one influencing the other much greater. While this is a great method for data that is evenly spread out over a large flat area, it can fail when used in mountainous areas because spatial trends are not taken into account.

Natural Neighbor interpolation is a geometric method of interpolation that uses Voronoi tessellations of a discrete sample point set for its calculations. When adding a ‘query’ point to the Voronoi diagram of the sample set, the query automatically creates its own Voronoi polygon in the sample set. The creation of the polygon for the ‘query’ point will create a new cell (Voronoi) for that point, but some of the cell is overlapped by other cells (from other nearby points). Sibson coordinates are used as the interpolation weights, which are the ratios of the sub-cell area "stolen" from the other nearby natural neighbor cells divided by the total area of the entire Voronoi region for the 'query' point. The interpolated value is obtained by using a weighted average of the values at those natural neighbors to the 'query' point. The weight for a natural neighbor point, i, to the query point, q, is mathematically if $A_i(q)$ denotes the area stolen from the Voronoi cell of point p_i, and $A(q)$ denotes the total area of the Voronoi cell of the query point q, then the Natural Neighbor weight is $\lambda_i(q) = \frac{A_i(q)}{A(q)}$ and the interpolated value is: $\hat{z}(q) = \sum_{i \in N(q)} \lambda_i(q) z_i$.

This method meets all requirements for partition of unity and barycenter; thus, the weights will be nonnegative with sum equal to unity and will recreate linear fields exactly.

Geometric representation of the Natural Neighbor Method (figure 1.5). The illustration shows the initial sample points along with their respective Voronoi cells and the newly created query point q, along with areas of $A_i(q)$, which were extracted from the Voronoi cell of the natural neighbours. In doing so, this clearly demonstrates how the weighting coefficients are determined.

Graph of change in weight of $\lambda_i(q)$. The graph can be an example for analysis of weight variation of neighboring points of q while it changes position along a line. The weights are determined by both the position of i with respect to q and by the spatial distribution of the points [23].

Blue circles, representing "known points", are locations where data, such as concentration measurements, have been obtained. A red star, representing "estimation point" is the point where the value will be predicted by combining measurements from all the "known points". The gray arrows show that the predicted value at the "estimation point" will be derived from a weighted sum of the values at all the "known points"[24].

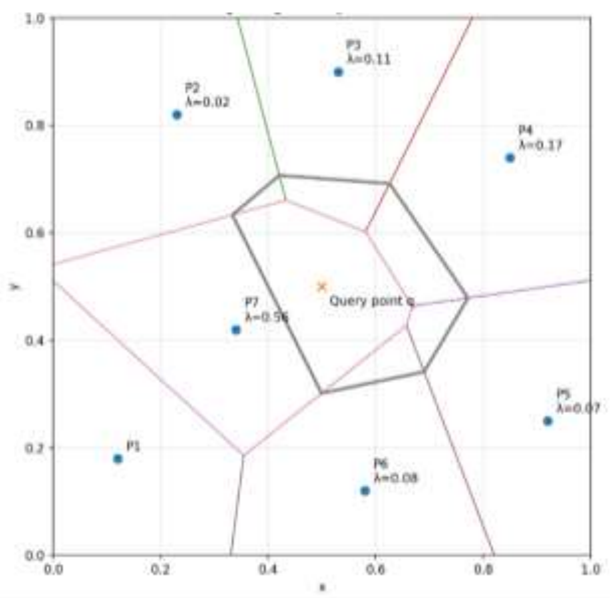

Figure 1.5. Schematic illustration of Natural Neighbor geometry

Figure 1.6, the diagram illustrates the fundamental principle of Kriging:

$$\hat{Z}(x_0) = \sum_{i=1}^{n} \lambda_i \cdot Z(x_i) \qquad (1.1)$$

where $\hat{Z}(x_0)$ – the estimated value at location x_0, $Z(x_i)$ – the measured value at sample location i, λ_i – the kriging weight assigned to sample i, n – the number of neighboring samples used.

The weights λ_i are determined by taking into account the spatial correlation of the data (through the variogram), rather than distance alone [25].

Among its many advantages, the primary advantage of the kriging method is the ability to analyze data based on several different aspects of spatial distribution, including point clustering, spatial scale of variability, anisotropy and the confidence level associated with the measurements. According to the Surfer help documentation, the algorithm considers the relative position of points, length of spatial change, confidence in the observations, and inherent anisotropy of the process. Therefore, Kriging is highly suitable for modeling complicated mountainous and mining regions, which have a distinct spatial pattern of elevation change.

The disadvantages of kriging, on the other hand, include higher computational complexity and the requirement to develop and calibrate a semivariogram; also, higher researcher qualifications are required when choosing a model.

Consequently, the Natural Neighbor technique can be considered a locally based geometric interpolator that operates effectively with data that is irregularly spaced and produces an even surface inside the convex boundary created by the point set. The method has one advantage of providing "stability" with no "extreme points" (artificial extremes) but it does not extrapolate the data boundary and has no explicit consideration of spatial trend.

The Inverse Distance Weighting (IDW) method is essentially the most basic of the interpolation algorithms, and it's also one of the fastest as well. It's a good method for use in preliminary analysis or with point distributions that are relatively consistent and continuous. While the method uses distance as the primary criteria for determining interpolation, it does not use the autocorrelation of the data points, and the result is that there may be some local "bulls eye" artifacts in the finished product along with a less accurate depiction of complex areas.

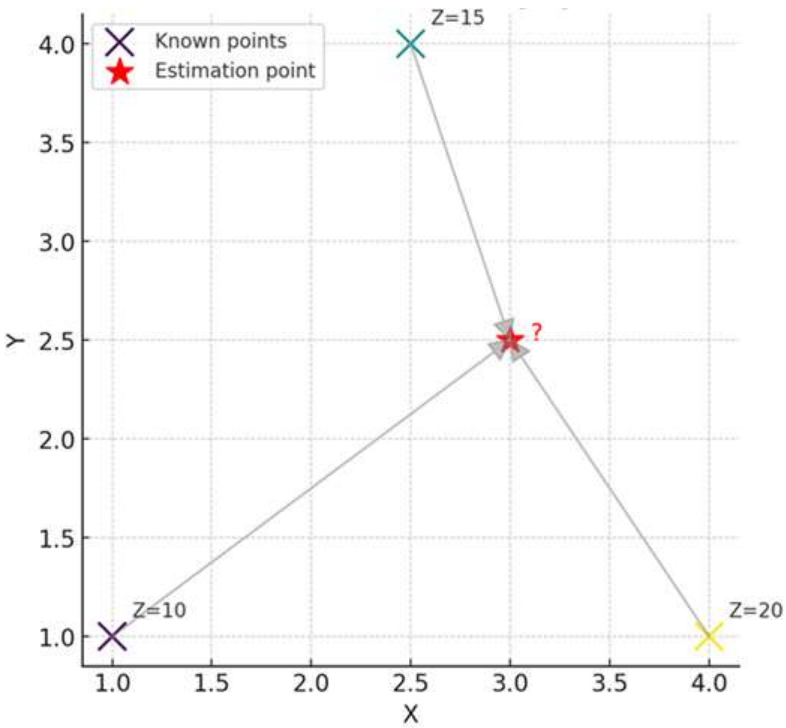

Figure 1.6. Schematic illustration of Kriging method

The Kriging method, as shown in Fig. 1.6, is the most analytically backed approach. The analysis is supported by both interpolation and spatial variability, done through a semivariogram. That is why it is more preferable to use compared to others for areas with very complex surface morphology and distinct local features and uneven spatial distribution of points and the presence of structural trends. Surfer has this method set as the default to use with XYZ data, which continues to show how useful the method is there.

Kriging was selected as the method to use in the gold deposit relief study based on four different interpolation methods used to develop the surface of the mining terrain; these include Natural Neighbor, IDW, Kringing and Nearest Neighbor. Based on the results of the comparative analysis, the kriging method is most appropriate and provided the most realistic depiction of the relief's spatial structure. Unlike IDW, kriging does not produce intense local anomalies near singular points of observation, but unlike Natural

Neighbor, kriging considers both the overall spatial correlation and the trend in the change of elevations, as well as the local geometry of the distribution of the point elevations. For a gold deposit mining terrain where the structure of the relief is complex and exhibits sharp differences in elevation with ordered patterns of spatial variance in elevation, kriging provides a distinct benefit [26, 27].

So, the Kriging method is basically the best one to use when designing a digital terrain model because it takes into account how your data is distributed and gives you the most accurate results when showing the surface of the gold deposit.

Kriging is a geostatistical method for Interpolating spatial data sets by providing statistically optimal surface estimates. Kriging uses both distance and spatial correlation among points. In modeling complex topographic structures, Kriging can achieve accurate results by utilizing variograms, which describe the variability or spatial dependence between points separated by differing distances. For mountain landscapes, where elevation can rapidly change over a very short distance, kriging can provide an accurate and smooth surface elevation model [28,29].

Therefore, the best method to represent a mountainous area using many measured elevation points in a digital elevation model would be the kriging method.

Figure 1.7 illustrates how the digital elevation models produced using the Natural Neighbor, IDW and Kriging methods varied, respectively, in Surfer. The elevation at the Tulallar site, which varies between 1400 meters and 1800 meters above sea level is used to define the site as mountainous, and Kriging produced the best representation of that surface.

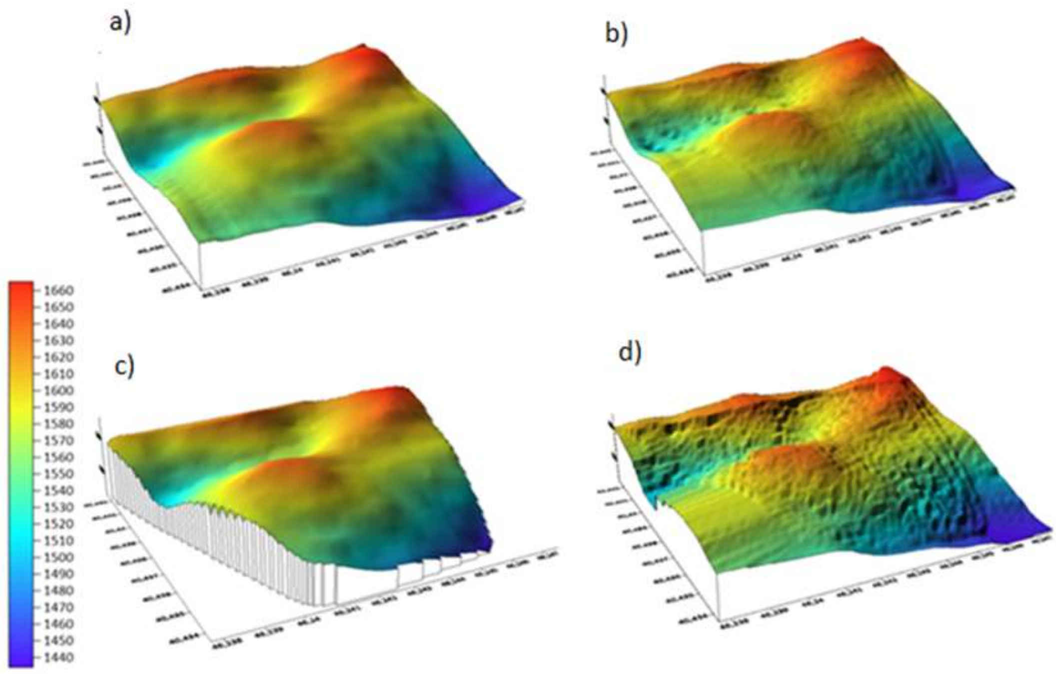

Figure 1.7. Digital elevation models of the Tulallar site using different interpolation methods: (a) Kriging, (b) Inverse Distance Weighting, (c) Natural Neighbor, (d) Nearest Neighbor

The formation of the primary ore-bearing structures at the Tulallar deposit was due to the influence of tectonic activity. It is generally agreed by geologists that three separate zones containing gold-bearing ore exist at this site. Two of these zones are located in the northern and southern portions of this deposit and they have similar rock compositions. However, there is a significant difference in the way gold is distributed between these zones. The northern area contains low-grade ore with a maximum concentration of gold of up to 50 grams per tonne; while in contrast, the southern area contains high-grade ore with concentrations of gold up to 1000 grams per tonne. The two areas of deposit probably formed at different times and under different geodynamic conditions.

Gold-quartz ores in the north have a low percentage of sulphides (less than 5%). In contrast, gold-quartz ores in the south contain native gold either as grains or associated with sulphides. Grains of native gold from the southern zone vary in size from about 0.004 mm to about 0.05 mm (a significant size range). Rare occurrences of high concentrations of gold are observed at locations within the southern zones, which are believed to have the most significant future potential for exploitation.

This study looks at and compares the middle and southern parts of the Tulallar deposit.

Exploratory drilling was conducted in order to estimate the amount of mineable ore present in the Tulallar Gold Deposit. A total of 152 boreholes were drilled, which together represent a drilling length of 17,705.55m, with drill angles ranging from 50 to 90 degrees. The drill hole database from boreholes in the central and southern areas is presented in Table 1.2.

Table 1.2. Borehole data for the southern and central zones of the Tulallar deposit

Hole ID	X	Y	Elevation	Au (g/t)
C1	605434	4477421	1589	1,90
C2	605434	4477372	1579	1,70
C3	605469	4477403	1585	3,15
C4	605473	4477349	1585	1,03
C5	605501	4477457	1590	2,00
C6	605442	4477328	1578	1,80
C7	605468	4477684	1655	2,23
C8	605458	4477735	1669	1,42
S7	605322	4477098	1632	5,45
S8	605331	4477016	1633	3,00
S9	605314	4476962	1627	3,70
S10	605324	4476911	1607	2,10
S11	605382	4476849	1579	1,00
S12	605414	4476894	1586	1,80
S13	605370	4476948	1611	1,30
S14	605415	4477029	1605	0,70
S15	605413	4476953	1597	1,70
S16	605378	4477071	1621	0,64
S17	605375	4477007	1618	5,00
S18	605327	4476868	1590	0,90
S19	605290	4476998	1631	3,40
S20	605275	4477068	1638	3,05

Exploratory drilling techniques helped determine the direction of gold distribution along the strike and depth and identified the limits of ore bodies that have commercial value.

A 3D model was prepared using the Golden Software Surfer program to display the spatial relation of the gold bearing ores according to the value of the constituent element. It allows mineral resources to be studied subsurface thoroughly and with higher precision.

3D modeling was done with Drillhole, in which you input the coordinates, elevations, and gold concentrations found at different depths of each borehole. We used two important parameters (Sizing Method and Color Method) to make this drilling information more informative in terms of visualization. When you select the data-driven option, the Sizing Method and Color Method will automatically change the diameter and color of each segment of the borehole based on the gold concentration at that depth. (as seen in Figure 1.8).

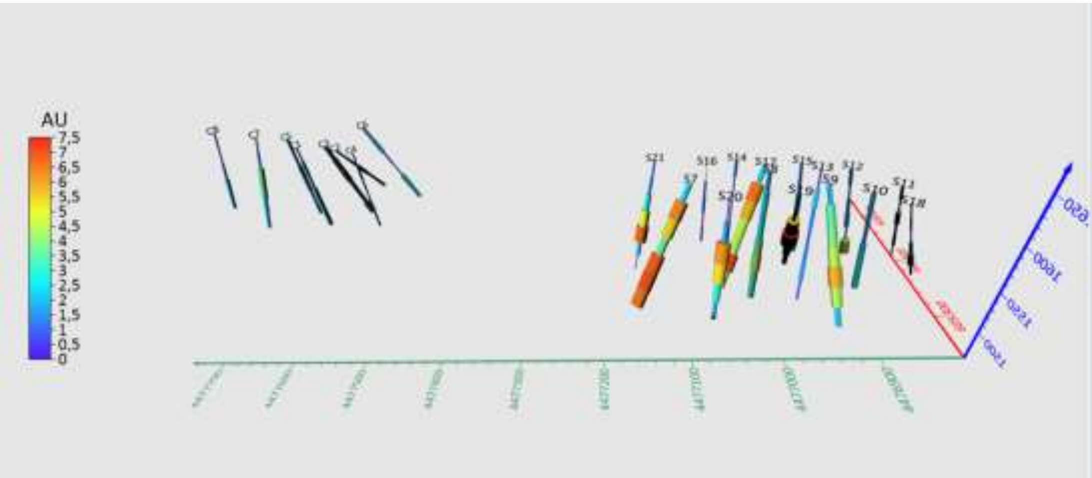

Figure 1.8. 3D visualization of gold concentration along borehole lengths using the Drillhole tool in Surfer

The comprehensive and accurate representation of the boreholes' locations in three-dimensional space has been accomplished by adding the surface terrain to the three dimensional model provided in Figure 1.4. In addition, this will create a more dynamic, flexible model and increase its ability to be interpreted; thus, the area of highest concentration of gold will be easier to be identified within their lateral extent and depth (see Figure 1.9)

The completed 3D model incorporates data on the spatial distribution of the areas studied, along with the changes in concentration of the valuable component across these zones, plus variations in concentration at different depths.

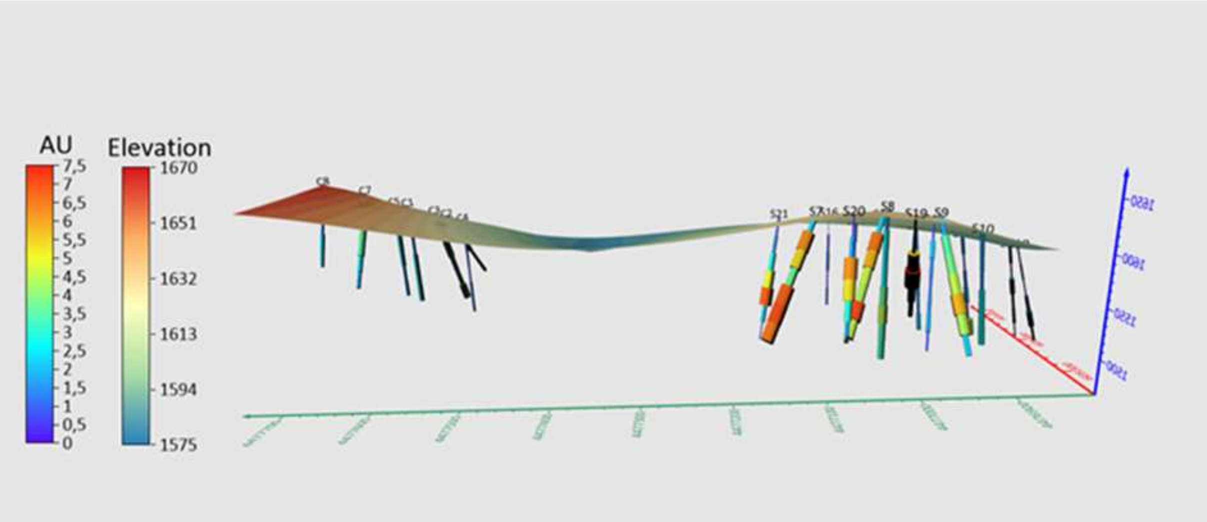

Figure 1.9. 3D model of gold concentration zones with surface topography added

Based on the findings from the modeling, numerous boreholes in the southern region contained the largest concentrations of gold, which ranged from 2.5g/t to 7.0g/t. In particular, S7, S9, S17, and S19 were four of the boreholes exhibiting the highest concentrations of gold. There was one borehole (i.e., S16) where the lowest observed gold concentration was 0.8g/t. Gold concentrations vary along the length of the boreholes due to numerous factors. The locations of the gold within the boreholes can be attributed to geological heterogeneity, variations in the mineralogy of the rocks containing the gold, and variations in the hydrothermal systems.

In addition, in the southern zone, the northwestern end contains higher gold grades boreholes, while the further away from the northwestern end you go, the lower the grade of gold becomes. The average grade of gold throughout the southern section of the property is 2.41 grams per tonne.

In the central zone, gold content appears to be generally low. The maximum gold content of 3.0 - 3.5 g/t exist in borehole C3 and borehole C7, while the minimum content of 0.7 g/t was found in borehole C4 and borehole C8. Average gold content in central zone has been found to be 1.9 g/t. You can also see how the high-grade areas are distributed spatially on the gold concentration isoline map in Figure 1.10.

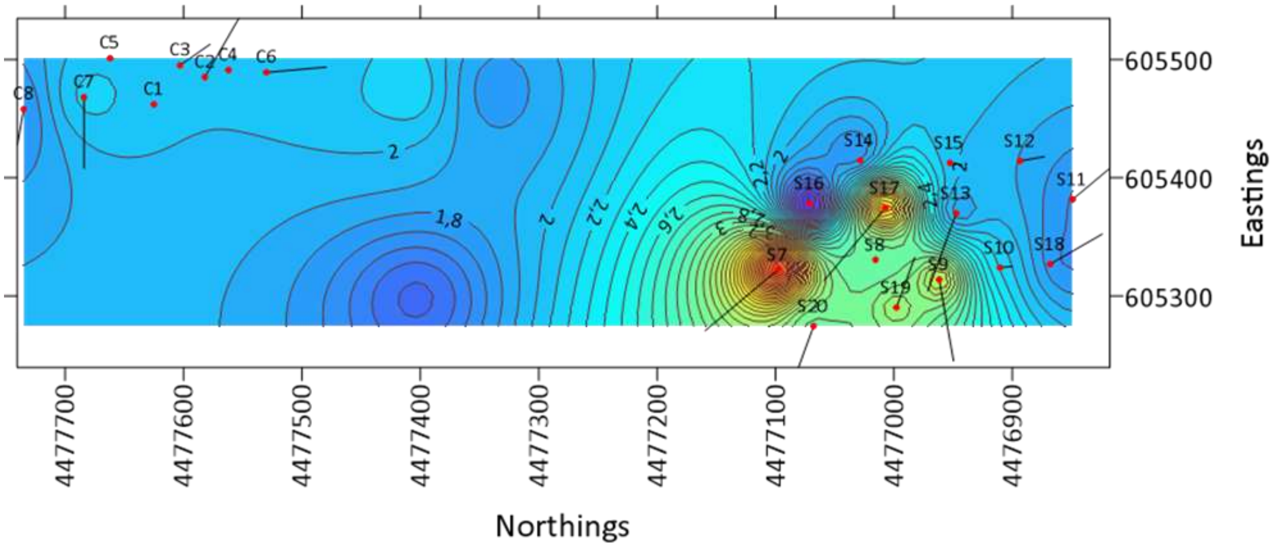

Figure 1.10. Isoline map showing the spatial distribution of gold concentration across the central and southern zones

While the average concentration difference between both zones is minor, there are specific locations within the southern zone where the gold concentration is much greater than the average value. According to a comparative study, gold concentrations within the southern zone exceed the central zone levels. This demonstrates that the southern zone provides the best potential for additional development.

Nearly all areas with high prospectivity for mining have been accurately identified through the innovative utilization of geodetic monitoring technology in addition to GIS in the analysis of gold mines. An all-encompassing method of mapping together with geodetic data produces an accurate geological map and model that can assist management in making informed decisions.

Creation of a three-dimensional model representing the distribution of ore in the Tulallar deposit and the patterns of gold concentration within the deposit became achievable through the combination of the Surfer and Google Earth programs. The importance of this model was resource estimation and optimisation mining operations.

According to the modelling results, the southern region of the Tulallar deposit was characterized by higher concentration of gold (average 2.41 grams per tonne) as compared to the central region (average 1.9 grams per tonne). Localized areas of high gold content (approximately 7 grams per tonne) are present in the southern region which makes it one of the most promising regions for further development. On the contrary, the central region produced a maximum of 3.5 g/t and had a more varied spatial distribution of ore bodies.

Therefore, the combination of geodetic and GIS methods provides a qualitative breakthrough in mineral deposit studies. They help to enhance economic performance of mining activities, as well as reduce environmental risks. This highlights the need to use these types of technology within today's mining industry for the sound and sustainable development of natural resources.

1.3 Comparative Spatial Analysis of Gold Concentration Zones

Develop 3D models of subsurface mineral distributions (SMDs) convert and combine all previously unconnected pieces of geological data to create a single, consolidated 3D representation of the SMD. The resulting 3D digital model of the ore body (and its spatial attributes) provides a means to visually examine, analyze and predict where the ore body is located with the host rock, as well as develop and implement more efficient and effective means of extracting the ore. Because of the depth of information that is provided by a 3D SMD model, geologists and miners now have an entirely new perspective on the morphology of the ore body in your host rock, (compared to two-dimensional maps and cross-sections).

In software platforms used for these applications, Surfer is an important platform for developing grid-based surfaces as well as viewing geospatial datasets.

It is critical to obtain as much data on the target deposit as possible prior to commencing the modeling work. This is the results of the geological exploration drilling programme and the geochemical and geophysical surveys. Additionally, the concentration of the “Value” contained within the borehole is also critical to the modeling process along with the identification of the structural components and surface outcrops. All of the information must be referenced to a single coordinate system for accurate 3D modeling.

In this study, UTM zone 38 was used as the primary coordinate system along with the Baltic height system to identify the locations of borehole collars and all depth-related points inside boreholes. The coordinates of the stations were referenced to the fourth-order national geodetic network. To obtain geological data from the Tulallar deposit, a total of 152 boreholes were drilled and had a total drilled length of 17,705.55 meters. The geological and geodetic data from these boreholes are summarized in Table 1.3.

Table 1.3. The geological and geodetic data for these boreholes are summarized of the Tulallar deposit

Hole ID	X	Y	Elevation	Depth	Concentr
C1	605462	4477625	1639	90,00	1,90
C2	605485	4477582	1621	85,00	1,70
C3	605495	4477603	1624	100,00	3,15
C4	605491	4477562	1614	105,00	1,03
C5	605501	4477662	1636	120,00	2,00
C6	605489	4477530	1648	120,00	1,80
C7	605468	4477684	1655	105,00	2,23
C8	605458	4477735	1669	140,00	1,42
S7	605322	4477098	1632	145,00	5,45
S8	605331	4477016	1633	145,00	3,00
S9	605314	4476962	1627	125,00	3,70
S10	605324	4476911	1607	115,00	2,10
S11	605382	4476849	1579	105,00	1,00
S12	605414	4476894	1586	105,00	1,80
S13	605370	4476948	1611	140,00	1,30
S14	605415	4477029	1605	130,00	0,70
S15	605413	4476953	1597	130,00	1,70
S16	605378	4477071	1621	95,00	0,64
S17	605375	4477007	1618	145,00	5,00
S18	605327	4476868	1590	120,00	0,90
S19	605290	4476998	1631	106,00	3,40
S20	605275	4477068	1638	120,00	3,05
T1	605434	4477421	1629	85,00	0,85
T2	605434	4477372	1619	105,00	0,57
T3	605469	4477403	1625	90,00	0,30
T4	605473	4477349	1625	95,00	1,70
T5	605501	4477457	1630	110,00	1,50
T6	605305	4477400	1618	60,00	0,80

The development of the 3D model in Surfer will involve creating a base surface as the first step to represent the topography of the area you are studying. At this point, you create grid files by interpolating the discrete elevation values that are available from the borehole collar locations. The individual measurements are used to produce a continuous surface that shows how the selected parameter is distributed throughout the area.

The geostatistical Kriging method was used for interpolation because it is recognized as the most scientifically validated method for deposit modeling.The surface output is an accurate depiction of terrain morphology in the data collection area. Thouh Integration of borehole data in Surfer allowed for the generation of 2D contour maps and 3D models to display the spatial heterogeneity of gold distribution across the central and southern zones.

In the southern area gold concentrations ranging from 2.5 g/t to 7.5 g/t with an average concentration of 2.41 g/t. High- grade gold concentrations were concentrated in the southwestern area. The central area recorded a lower range and a more diverse range of gold concentration (0.7 g/t to 3.5 g/t; 1.9 g/t average).

The 3Dd isosurfaces indicated that the deposit had vertical zoning; the southwestern zones achieved maximum gold values of the available samples at 1500 m. The samples obtained from the same area at 1550 m were only slight decreased in value, while the samples collected at 1600 m were greatly diminished in value.

The results of the 3D modelling indicate that the highest concentrations are at various levels, but the highest and most continuous concentrations are in the southwestern part of the deposit.

There are many variances in geology within this deposit. This will have an effect on how to get the material out based on the vertical elevation.

The first step that needs to be completed prior to the commencement of the model building process will involve the gathering of all available information concerning the targeted deposit. The key will be to review the results of the exploration work and geophysics and geochemistry collected during the exploration stages; the information that will need to be provided to support this project primarily will be the borehole data, historical and current concentrations of the precious metal, structural features, and the surface outcrops. It will also be important to ensure that all information provided will be in reference to the same coordinate system so that an accurate 3D model will be produced.

For the purpose of determining both the position of the borehole collars and every point on the borehole that is associated with a given depth, both the UTM Zone 38 coordinate system and the Baltic Height System were used. The UTM (Universal Transverse Mercator) system uses 60 cartographic zones that cover the entire Earth's surface. Each of these cartographic zones is 6° in longitude. The UTM Zone 38 covers all areas located between the longitude lines of 42° east to 48° east (i.e., portions of the Caucasus, Azerbaijan, eastern Turkey, and northern Iran). The coordinates in this system are given in meters.

The easting (X) describes the interval in metres between the centre-line of the defined zone and the measurement point; a "false easting" of 500,000m is applied to all points to eliminate the presentation of negative numbers. The northing (Y) is the distance in metres north of the equator (in the northern hemisphere), because the metre is the basic distance depicted in the UTM-38, which is very useful when utilizing UTM-38 for purposes such as geodetic surveying, the mining industry, and the monitoring of any other aspect of an infrastructure.

Station coordinates referred to the fourth-order national geodetic network. Exploration activities to obtain the geological information needed on the Tulallar deposit, included drilling of a total 152 boreholes totaling 17,705.55 meters.

At the beginning of the 3D construction modelling process within the Surfer program it is necessary to first establish a Base Surface (the terrain of the area of interest). It is then very important to create Grid Files by interpolating the individual elevation data from borehole collars, and this is accomplished by converting the measurements taken at specific locations into a continuous surface representing the selected parameter's spatial distribution.

Kriging is a geo-statistical technique used for interpolation and because it is generally acknowledged as the best scientific method for deposit modellng. The produced surface is a good indication of what the landform looks like within the area of data collection.

The Drillhole tool in Surfer (Fig. 1.11) is utilized to input coordinates, collar elevations, and the concentration of components according to depth in each borehole. The creation of a borehole layer over the base surface is made possible and the generation of an initial 3D visual display of the distribution of components along borehole routes (Fig. 1.12). The point based-data shown in the model represent the concentration of a specific component in the individual boreholes.

The Surfer software is designed to provide sophisticated visualization of volumetric objects, including isometric zones that reflect a certain concentration of valuable components. This is an essential feature to produce complete geological models.

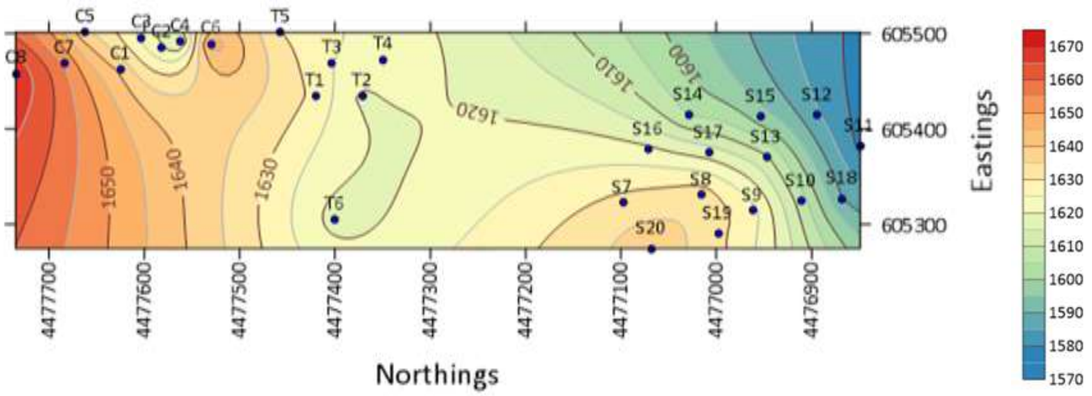

Figure 1.11. Input of borehole data using the Drillhole tool in Surfer (UTM Zone 38 coordinate system in meters)

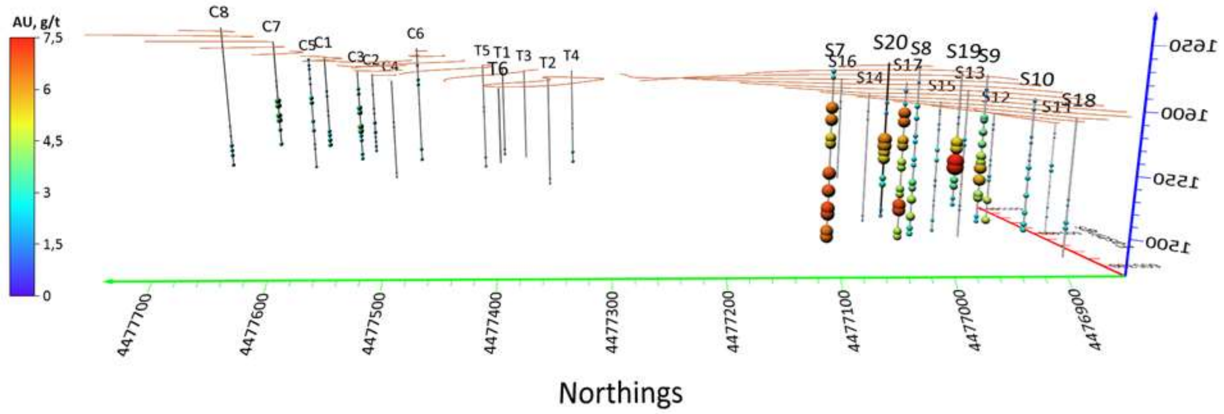

Figure 1.12. Initial 3D visualization of component concentration along borehole depth (UTM Zone 38 coordi-nate system in meters)

To build 3D objects like these, you need to do a lot of work upfront and make sure you bring in the right data. See Table 4 for an example. A major part of creating the models is assigning coordinates to each point measured. You assign two coordinates (*x* & *y*) in the plane and a third coordinate (*z*) representing their true elevation values. The elevation value was determined from the depth at which the core samples were collected from each borehole. By doing this, you'll know where all the points of your model are located in 3D.

A spatial location associated with concentration of valuable components at that location is tracked along the borehole. The entire database supports development of highly accurate grid surface models to show the volume of the ore body and its attributes as a quality measure.

Table 1.4 – Sample dataset of borehole drilling results with spatial coordinates and corresponding gold concentration values (C Value) for 3D modeling.

Hole ID	X	Y	Z	C Value
S7	605322	4477098	1632	0.00
S7	605322	4477098	1630	2.40
S7	605322	4477098	1625	2.40
S7	605322	4477098	1600	6.30
S7	605322	4477098	1590	6.30
S7	605322	4477098	1575	5.40
S7	605322	4477098	1570	5.40
S7	605322	4477098	1545	6.80
S7	605322	4477098	1530	6.80
S7	605322	4477098	1515	7.00
S7	605322	4477098	1510	7.00
S7	605322	4477098	1495	6.50
S7	605322	4477098	1490	6.50
S8	605331	4477016	1633	1.70
S8	605331	4477016	1620	1.70
S8	605331	4477016	1600	2.60

Surfer generates a 2D contour plot of gold locations by importing the processed input dataset. Contour lines indicate the amount of gold at the same point so, viewing the concentration of gold across the surface.

A main benefit of this method is that it allows vertical variations in gold distribution to be analysed dynamically (i.e., through the changing location of the Slicing Plane, see Figure 1.13). Changing the Slicing Elevation produces a series of Contour maps at two or more depths that allow you to observe how an ore body changes (location, shape, and size) with depth over time. You are also able to observe the internal heterogeneity of the gold distribution throughout the deposit.

The technique is very effective in visualising the morphology of the ore deposit and in identifying the zones of high mineral concentration.

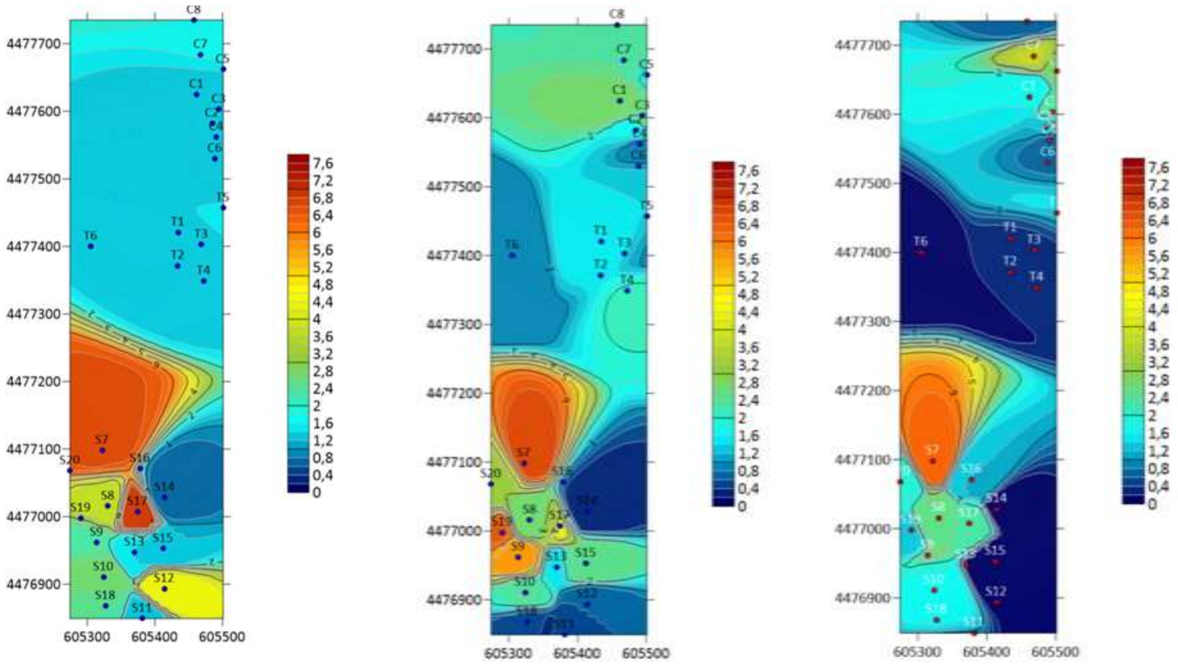

Z=1500 м Z=1550 м Z=1600 м

Figure 1.13. Gold concentration distribution at different depth slices, illustrating the spatial variability and internal structure of the ore body within the Tulallar deposit

The subsequent phase of the modeling process is to design a spatial depiction of the distribution of the value element, and this is accomplished through Surfer's innovative 3D View feature. The 3D View tool basically takes an interpolated grid, produces a volumetric model based on it, in the form of isosurface. Isosurface, in three-dimensional, function as the contour lines, joining all the points of the space that have the same concentration of the value element.

This tool can assist in generating a three-dimensional rendering of an industrial or cutoff concentration specified by a user in the subsurface as a solid form. In this case, the minimum economically viable concentration of gold can be represented by an isosurface that defines the limits of the industrial ore body.

At this location, 2.5g/t of gold is regarded as the minimum concentration at which it can be mined economically. From this concentration level, a three dimensional model was built to depict where the three dimensional area had gold at or above the economically mineable concentration. The model is shown in Figure 1.14.

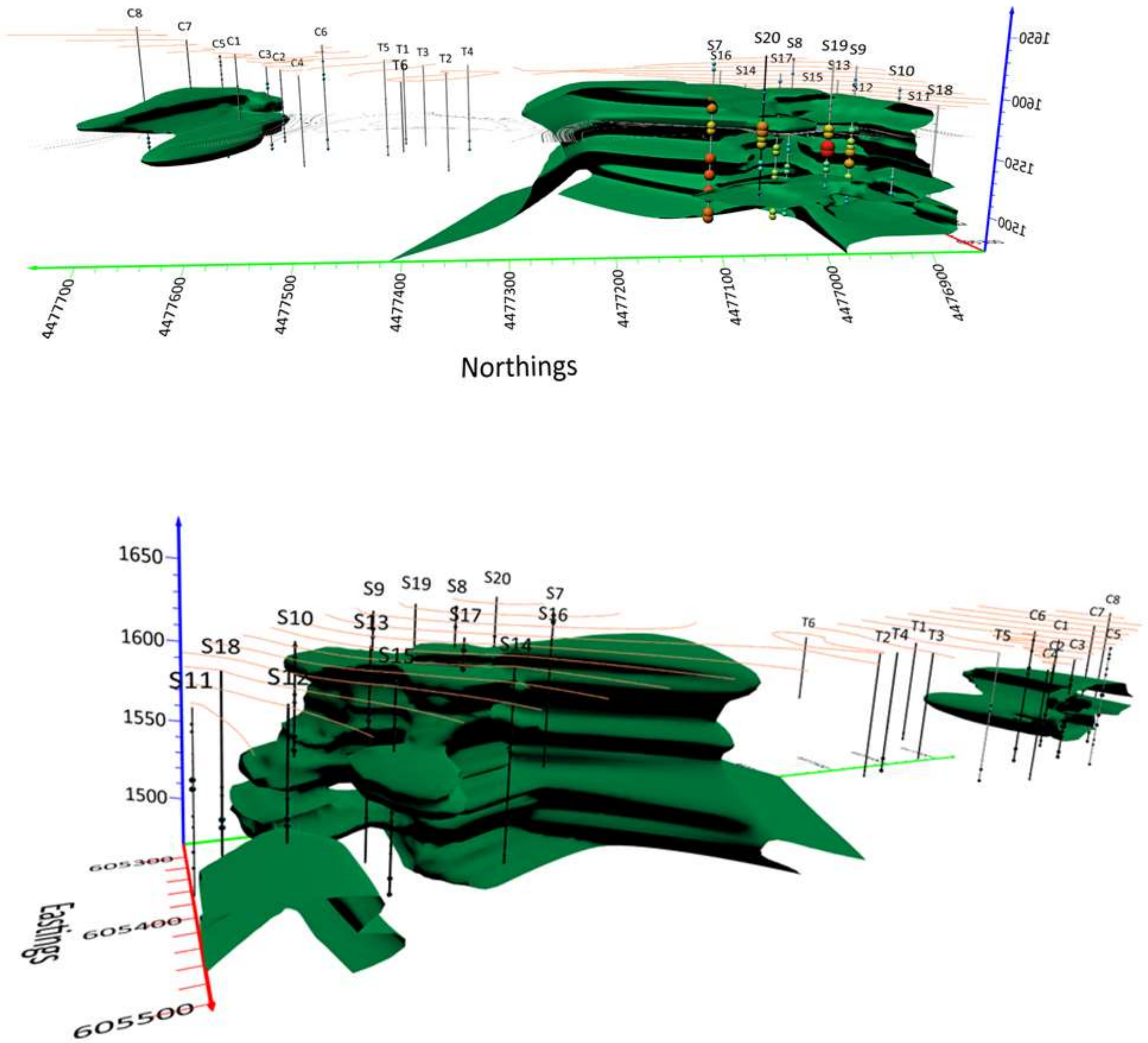

Figure 1.14. 3D model of the spatial distribution of areas with a gold concentration of 2.5 g/t from different perspectives (m)

The 3D View Tool contains multiple interactive features like rotation, scaling, or translation as well as the ability to adjust the view angles; so that you can see some of the morphological non-obvious characteristics of a deposit and how they spatially relate to each other.

Additionally, Surfer allows you to overlay more than one isosurface at a time, each representing a different concentration of gold. For the purpose of illustration and further analysis, I have selected three different concentration values: green will represent 2.5 g/t, yellow will represent 4.5 g/t, and red will represent 6.5 g/t (refer to figure 1.15).

With the help of this methodology, visual distribution dynamics of spatially distributed gold concentrations within a certain volume are evaluated. Consequently, the users are enabled to develop clearer concept of high grade zones and their association with the surrounding geological formation.

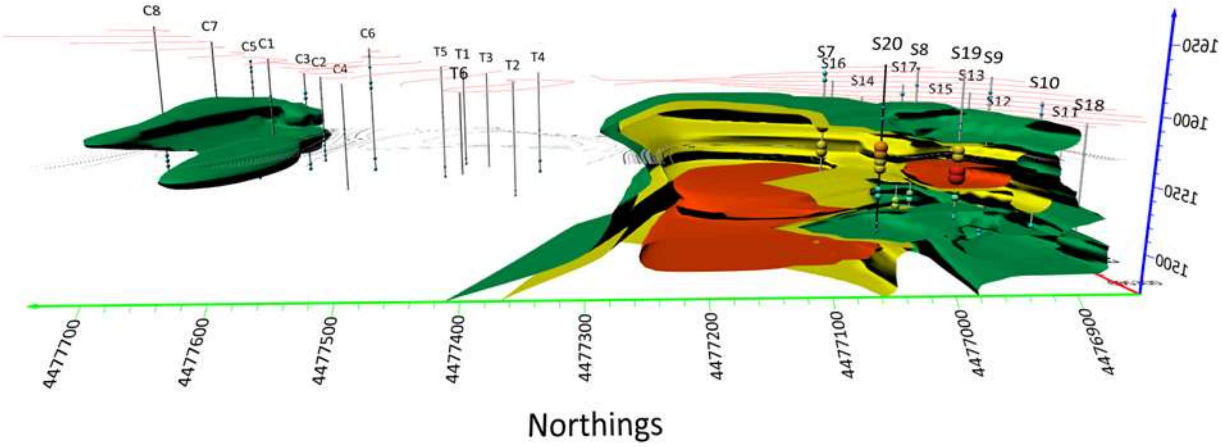

Figure 1.15. Three-dimensional model of the subsurface distribution of gold at varying concentrations: 2.5 g/t (green), 4.5 g/t (yellow), and 6.5 g/t (red), (m)

Analysis of the data and the 3D figure (Figure 1.13) shows that gold concentration varies by elevation. The concentration of gold is between 1and1.5 gt in the central and northern areas of the study area at 1500 m in elevation, while the concentration in the southwestern part of the area is as high as 6.5 gt.

With an elevation of 1550 m above sea level, the distribution patterns are somewhat different than before. The central part still has stable concentrations of gold, the central region to the north has a higher concentration 2.5g/t of gold, whereas there is a continued occurrence of high concentration of gold in the southwestern region but it has shortened in the west extension axis by a small amount. The southeastern zone has low gold concentration overall at this elevation.

Across the whole Survey Area, the gold concentration is declining at the 1600m level, which is closer to the surface than the other levels. However, the Southwest section of the Survey Area continues to be the most productive, with gold concentrations between 4.5 and 5.5 g/t.

Moreover, there were also some extreme values within the sample dataset itself; Gold Concentration is at the lowest end of the range or 0.5 grams per tonne (g/t) but most of it is located primarily within the central area of sample dataset. The highest Gold Concentration is at 7.5 g/t and has a record in the southwestern section of the project, borehole S19 sample, at an elevation of 1560 meters, as shown in Figure 1.16.

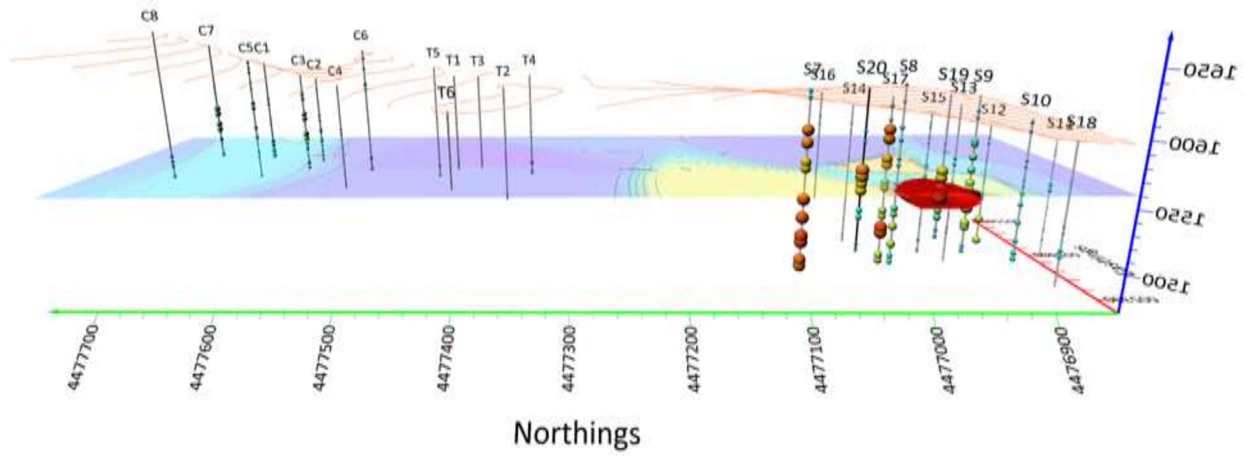

Figure 1.16. Area with the highest concentration (m)

According to the analysis, the concentration of gold in the southwestern part of the study area is much higher than in the centre and north, and therefore the results support the conclusion that the southern part of the area is the most promising for future development, with potential for further development to the northwest.

By manipulating data relating to both Elevation and Concentration, it will be possible to analyze the Deposit in its entirety and do so with the greatest degree of accuracy possible. Through this analysis, Depths that can be mined at Optimum efficiencies can be determined as well as Extraction Technology Selection Criteria that are based on sound logic. The Data that results from this type of analysis provides a solid, Reliable foundation to use for estimating Resources and creating a strategy to exploit the Deposit.

1.4 Conclusions to Chapter 1

In this chapter we are going to talk about how we analyzed the Tulallar gold deposit by using the most up-to-date geodetic monitoring techniques as well as GIS-based spatial modeling methods. We used topographical data, geologic data, and gold concentration data to develop detailed contour maps and models of three dimensional morphology and mineralization of the deposit.

The research showed that the combination of data from Google Earth and Surfer software produced effective 3D models of mine ore bodies, helped in determining gold concentration across various mine depths, and identified high-potential zones for mining. The use of several methods of interpolation (with Kriging being one of the most important methods) was crucial in generating a digital elevation model of a mountainous area.

The spatial assessment revealed the existence of zoning patterns within the deposit, substantially with the higher gold concentrations in the southwest and lesser in the central and northern portions. The gold concentrations in the southwestern portion are as high as 7.5 g/t and therefore are considered by the researcher to be the most prospective areas for future development. The spatial distribution of gold concentrations have a large change with respect to the elevation; therefore, vertical zoning of gold concentrations will be a major factor in how mining operations are properly conducted.

The method presented enables visualizing ore bodies accurately, and the discovery of usable ore bodies has allowed for the use of the most statistically viable process for ore extraction. The combined findings provide a sound basis to guide different extractive processes like exploration, reserves estimation, and mine planning.

The findings have verified that the combination of Geodetic monitoring and GIS technologies improve the precision of mineral resource assessment. They have also provided an optimal way to utilize the resources to ensure environmentally sustainable mining activities.

CHAPTER 2. INFLUENCE OF THE STEMMING DESIGN ON THE MECHANICAL EFFECT OF A COLUMN CHARGE EXPLOSION

One of the most effective and practical ways to improve the efficiency of blasting operations is the use of reliable stemming (tamping), because stemming directly controls the confinement of detonation products and, therefore, the share of explosive energy that is transformed into useful mechanical work in the rock mass (fracturing, crack growth, and displacement) rather than being lost through premature venting to the atmosphere.

A comprehensive literature review confirms that stemming is strongly linked to reduced fly rock, reduced air-blast/overpressure, lower fume emissions, and improved fragmentation and muck pile movement due to enhanced confinement and longer pressure retention inside the blasthole. Proper stemming should thus be treated as a primary design variable in production blasting, comparable in importance to burden, spacing, charge diameter, and explosive type.

Figure 2.1. Schematic diagram of the borehole configuration used at the Tullallar deposit

It is well established that the performance of elongated borehole charges in breaking rock masses is largely governed by the stemming system (length, material properties, and geometry) on Figure 2.1. Laboratory-scale and field-scale studies demonstrate that insufficient confinement causes early crater formation and rapid gas escape, leading to reduced fragmentation efficiency and increased adverse effects, whereas adequate confinement prolongs the action time of high-pressure gases and stress waves in the near-field region, thereby enhancing crack initiation and propagation in the collar zone and surrounding rock.

Modern research also emphasizes that the stemming effect cannot be explained by stemming length alone. Material properties (density, stiffness, grain-size distribution, compressibility, permeability, cohesion, and wetting behavior) strongly affect the magnitude of the initial pressure peak, the rate of pressure decay, the onset of stemming movement, and the probability of premature ejection/blowout. For example, controlled laboratory experiments on high-explosive blasts showed that stemming conditions measurably influence fragmentation outcomes even when the explosive and geometry are kept constant, confirming that stemming modifies the overall energy partitioning between shock-driven breakage and gas-driven crack growth.

In modern open-pit mining, drilling-and-blasting operations play a key role in productivity, because fragmentation quality governs the efficiency of loading, hauling, and crushing/milling. Reliable stemming is one of the most effective levers for improving blast outcomes while simultaneously reducing safety and environmental risks. Although debates sometimes arise about stemming necessity in special cases (e.g., reactive ground, hot holes, presplit blasting), the broad body of evidence supports stemming as a critical tool for controlling blast performance and mitigating adverse effects when properly engineered.

Blasting with sufficient stemming generally allows for the following:

- Decreased explosive consumption per unit due to more efficient use of the energy from the explosives,

- Enhanced quality of fragmented materials including the collar region and fewer oversized materials,

- Decreased operational expenses for further processing of materials due to less variability in crushing processes and reduced occurrence of secondary breakage, and

- Reduced occurrence of detrimental effects caused by blasting (e.g., fly rock, air blast, toxic fumes, etc.) [29,30].

One of the most important indication are drilling stems material change. This results in improved containment as well as improved fragmentation because crushed aggregate has almost entirely replaced the use of drill cuttings as a stemming material in the recent period. Field bench blasting studies have shown that when crushed aggregate replaced the drill cuttings as stemming material, there was a significant reduction in the distribution of the resulting fragments, as well as improvements to the size and shape of the muck piles, which were associated with improvements in the loading and hauling operations. Mine-to-Mill studies have found that using aggregate stemming reduces the variation in the ROM, decreases the variation in the mill feed and therefore lowers the cost of processing and equipment wear.

At the same time, “optimal” stemming is not universal: it depends on explosive type, hole diameter, burden/spacing, rock mass structure, and desired fragmentation targets. Recent experimental and analytical studies demonstrate that stemming length and material interact: increasing stemming length can improve fragmentation and reduce recoil/ejection risk, but the same length may behave differently depending on whether the material is clay-like, granular aggregate, water-based, or hybrid (e.g., sand + clay). This reinforces the need to treat stemming as a coupled design problem rather than a fixed rule-of-thumb. A large-scale analysis using actual production results also showed that stemming-to-burden ratio can be optimized to balance fragmentation and safety by limiting explosive gas escape; the reported optimum in that study (for the investigated conditions) was around $St/B \approx 0.67$ [31, 32]

Key requirements for stemming systems generally include: simplicity and low cost, rapid installation, stable confinement during the critical detonation and gas-expansion period, and predictable behavior against premature ejection.

There are four stages of physical activity, as relates to stemming (conceptual model):

- Shock Compression Stage: the shock wave slams through the stemming, making the stemming very dense or stressed.
- Rarefaction Stage: unloading shockwaves cause even distribution of pressure throughout the length of the stemming column.
- Free Movement Stage: The stemming begins to move as one object, based on how compressible it is and what frictional resistance it has;

Ejection Stage: The stemming is expelled or broken into pieces. One of the main factors that will determine when this stage begins is the time it takes for the high-pressure gases to be released after the stemming has been removed. The longer they are confined, the more energy they will be able to transfer into the rock mass.

Stemming affects the length of time the detonation products are confined in the blasthole (and their pressure–time history). A proper stemming will provide a longer duration of high pressure applied to the borehole wall; also, the effective impulse transferred to the nearby rock is higher resulting in better crack growth, rock fragmentation and throw. Also, it will reduce the portion of the energy released as overpressure and fly rock in the air.

The contemporary literature review demonstrates that the length of the stem and the material or system used to stem a blast hole significantly impact the performance of a stem. More efficient stemming materials provide an equivalent amount of confinement to the blast hole with a shorter length of stem; the improved performance results in either better collar breakage or better use of the available collar length by extending the explosive column length while still fulfilling the safety requirements. This observation is consistent with the results of the tests performed, in which hybrid or engineered stemming materials produced better results compared to drill cuttings, mainly in the drilling zone where the venting began too quickly [33, 34].

Material impacts (i.e.: crushed stone stemming and hybrid Systems). Research shows that crushed aggregate stemming generally achieves more effective results compared to drill cuttings because the crushed aggregate develops an enhanced interlocking, reduced permeability pathways, and offers greater resistance to gas-driven acceleration. Furthermore, recent studies broadened the scope of research by identifying size distribution of aggregates as a key factor in terms of size distribution of aggregates and how they produce gas ejection when partially stemmed and their effect on the overall production of a system during full-scale tests.

Mechanistic validation from empirical tests conducted under strictly regulated test procedures provides laboratory experiment evidence that chemical explosives and controls (the mechanic effects) are largely responsible for altering the nature of the breakage resulting from the application of either a stop or free charge. Laboratory results are consistent with an interpretation which indicates that, through the application of stemming, not only do stress waves interact differently with each other; but also, when gas pressures are present, their effect on combating rock is altered. In model testing, stemming length and a variety of stemming materials were measured to determine how they affected the appearance of blowout holes, how the fragments formed in the dust cloud looked, and the strain that was created on the stone surface. Through the test results, stemming was found to be an adjustable means of obtaining the maximum amount of productive energy while protecting people from harm, such as stemming blasting.

The environmental aspect refers to dust/fumes control. In addition to rock fragmentation, stemming selection is now focused more and more on reducing both dust and hazardous fumes. One paper presents an overview of modern methods for reducing the levels of dust produced during the blasting process in construction projects, and establishes that both dust levels from blasting operations and their control are impacted by the combinations of stemming materials and techniques. The paper further discusses the use of various engineering solutions (including those related directly to stemming) to reduce or eliminate the generation of dust during blasting operations. In particular, Recent laboratory investigations of water based stemming systems have examined the ability of chemicals that improve the wetting properties of water (such as surfactants and/or inorganic salts) to improve the amount of dust that can be controlled with water based stemming systems. These studies show that, in addition to their traditional purpose of providing confinement, stemming systems can also be used to provide an additional level of protection to the environment [35, 36, 37].

Another technology-based approach is the use of chemical additives in stemming designs for the purpose of lowering post-blast fume levels. Laboratory studies have shown that carbonate-based fillers can reduce nitrogen oxide emissions through neutralizing reactions at the same time the stemming helps "trap" the detonation gases for a longer period of time within the cavity; this has given rise to the general idea that environmentally-focused stemming formulations (i.e., those that incorporate CaCO3-based additives) can be included in blast designs along with the traditional mechanical performance criteria.

In general, the most recent research indicates that designers should treat stemming as one of the primary variables available to them in designing production blasts. By optimizing the stemming, particularly through the right selection of stemming material and, when applicable, engineered or hybrid stemming systems, the fragmentation of rock (including the collar zone) will be optimized; the occurrences of negative incidents such as blowouts, flyrock, air-blast and fumes will be reduced; and the efficiency of downstream operations will be increased through a more uniform run-of-mine (ROM) feed.

One of the most effective ways to increase the efficiency of blasting operations is the use of effective stemming. Many theoretical and experimental studies are performed on the use of stemming in blasting because blasting serves many purposes (i.e., rock fragmentation, creating cavities, creating a profile, etc.) in diverse types of rock with diverse physical and mechanical properties. There has been limited theoretical research into the effect of stemming on blasting efficiency; however, such research has only recently begun to appear [38, 39].

The effectiveness of long borehole/explosive charges in breaking rock masses depends largely on the features of the stemming material. Stemming performs the major function of containing explosive products during the time when the products are undergoing secondary detonation reaction and secondary decomposition reaction to develop mechanical energy from the expanding gases.

Stemming – Fragmentation controlling Stemming also controls the exit of gases from borehole. Premature escape of gases due to Stemming would cause incomplete detonation, more toxicity of gases produced after detonation, uncontrolled ejection of rock fragments from the collar and intensified air shock waves. Since stemming plays an important role in the explosive energy derived from that blast, new studies focus on the material properties in addition to the charge parameters that would be optimal for a given charge geometry.

2.1 Analysis of the Role of Stemming in Borehole Charges

In the current development of open-pit mining, drilling and blasting operations play a key role in increasing production efficiency. Ensuring the availability of adequately fragmented rock mass allows for the optimal use of loading and transportation equipment. One of the main ways to enhance blast efficiency is the use of reliable stemming. A large number of theoretical and mostly experimental studies have been conducted due to the varying objectives of blasting operations, such as rock loosening, cavity formation, and profiling, as well as the diversity of rock structures and their physical-mechanical properties.

There is ongoing debate regarding the necessity of using stemming in explosive boreholes during blasting operations in mining. However, scientific research clearly confirms the effectiveness and feasibility of using stemming.

Blasting operations with stemming allow for a reduction in the specific consumption of explosives, improved rock fragmentation quality, reduced costs of blasting operations, and minimized environmental impact.

The key requirements for stemming include: simplicity and low cost of fabrication, ease and speed of installation, and an optimal duration for containing the detonation products. Stemming significantly affects both the efficiency and safety of rock blasting by increasing the initial pressure and duration of explosive gas action on the rock, reducing the initial velocity of gas escape from the borehole, limiting ejection into the collar zone, minimizing air shock wave intensity, and improving the detonation process.

Besides controlling fragmentation intensity, stemming must prevent the premature escape of gases from the borehole, which is associated with incomplete detonation and an increased concentration of toxic components in the gas mixture. It also prevents the destruction of the borehole collar and uncontrolled scattering of rock fragments, as well as the generation of an intensified air shock wave. Thus, modern studies pay special attention to both the parameters of the elongated charge and the properties and geometry of the stemming material [40, 41, 42].

Stemming is widely recognized as a key element of borehole charge design because it governs the degree of confinement of detonation products and, consequently, how effectively explosive energy is converted into useful mechanical work in the rock mass. The literature review “Stemming and best practice in the mining industry” summarizes that proper stemming reduces adverse blasting phenomena (flyrock, air-blast, fumes) and is directly associated with improved fragmentation and movement due to enhanced confinement and reduced premature venting of energy. This conclusion is consistent with the general understanding that insufficient confinement leads to early crater formation and energy losses, whereas adequate confinement increases gas retention and improves fragmentation in the relevant portions of the blast hole.

Research also indicates that stemming performance depends not only on stemming length but substantially on stemming material and stemming systems (contrivances). The review notes that while studies on stemming length are relatively limited, evidence on the influence of stemming materials and stemming devices is well documented, and the required stemming length is partly material-dependent: the more efficient the material is at containing explosive energy, the shorter the length needed to achieve the same confining effect.

In this context, [43] highlight that the use of a proper stemming material can reduce the total amount of stemming required by more than 40%, which can allow more explosive to be loaded while maintaining confinement and improving collar fragmentation.

A frequently reported finding is that replacing drill cuttings (drill chippings) with crushed aggregate improves fragmentation and downstream productivity. Multiple sources cited in the review agree that crushed aggregate stemming results in better fragmentation than drill cuttings.

In [44] reported lower characteristic fragment sizes (K50) and improved muckpile throw when crushed aggregate was used; they also observed loading and hauling productivity improvements (reported on the order of ~18%)

In [45] documented mine-to-mill benefits at an operating mine, including improved ROM uniformity and reduced SAG mill feed variability, which enabled measurable energy savings and reduced crusher wear.

Besides fragmentation, stemming is repeatedly linked to the control of blowouts, dilution, and flyrock. In [46] found that adjusting stemming length reduced stemming blowouts and horizontal movement, which is desirable for dilution control; fewer blowouts are associated with reduced flyrock and improved fragmentation.

The review further reports that adequate stemming can reduce air-blast (overpressure), thereby increasing the fraction of explosive energy available for useful rock breakage and movement.

Overall, modern evidence supports the view that stemming should be treated as a primary design variable in production blasting. Its optimization—especially through appropriate stemming material selection and, where applicable, stemming systems—can improve fragmentation quality (including collar fragmentation), reduce adverse outcomes such as blowouts, flyrock and air-blast, and contribute to downstream operational efficiency through more uniform ROM feed [43–46].

In [47] emphasized that stemming increases the effective use of explosive energy. He defined useful explosive work as the energy consumed in rock fragmentation, while non-useful forms include the scattering of fragments, air shock waves, excessive crushing of rock in direct contact with the charge (brisant action), and other effects which may even be detrimental to further processing of mineral resources.

Such excessive crushing leads to increased thermal energy loss, as finely fragmented rock mixed with detonation products can absorb significant heat during gas expansion. Additional thermal losses occur when gaseous detonation products escape from the borehole before completing their expansion to atmospheric pressure. The effective energy output of the explosive is also diminished by chemical losses from incomplete detonation reactions.

The optimal parameters of stemming depend on multiple factors, including the properties of the explosive and stemming material, the charge design, and the surrounding geological environment.

Stemming helps to minimize energy loss during detonation by ensuring both complete detonation of the explosive and maximal release of its potential energy [46, 47].

In experiments involving oversized rock fragmentation with surface-applied charges of varying detonation velocities, the criterion for effectiveness was the relative degree of fragmentation, evaluated by the total newly formed rock surface area. For surface charges, blast work is governed primarily by the impulse, which is proportional to the explosive’s density and the square of its detonation velocity, and occurs solely via the shock wave.

Although it might seem stemming is unnecessary in such cases, experiments showed that stemming significantly increases fragmentation. For instance, an explosive with a detonation velocity of 4.5 km/s and stemming produced the same degree of fragmentation as a 7.0 km/s explosive without stemming (Figure 2.2). This can be explained by the increased completeness of detonation and the higher detonation pressure achieved when stemming is used.

Stemming increases the effective length of the shock wave and the initial pressure of explosive gases. According to rock failure theory via reflected waves, the line of least resistance (LLR) that is overcome by the explosion is proportional to the effective wave length. Stemming ensures the retention of high pressure in the borehole long enough for fracturing to occur throughout the entire zone from the free surface to the charge cavity.

The analysis of scientific research indicates that the improvement of borehole charge design to enhance rock fragmentation and reduce the production of oversized fragments remains an open and insufficiently studied area. Various approaches yield differing outcomes, highlighting the need for further investigation.

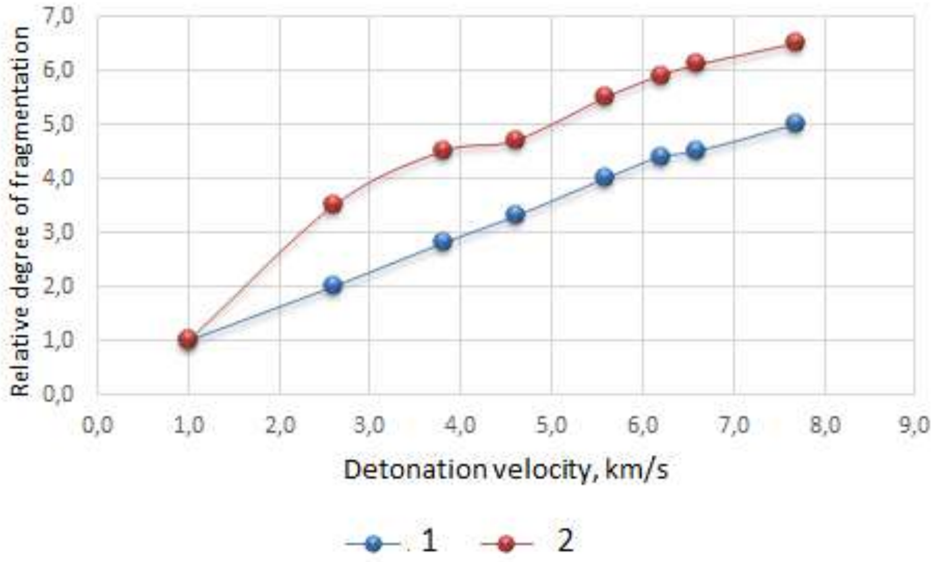

Figure 2.2. Influence of stemming on the efficiency of rock fragmentation by surface charges (curve 1 — without stemming, curve 2 — with stemming) [47]

The efficiency of surface mining operations largely depends on the quality of rock mass preparation for excavation. This quality is assessed by such parameters as the uniformity of the particle-size distribution of blasted rock, the average fragment size, the loosening factor, and the characteristics of the blasted rock pile.

Modern approaches to controlling the quality of blast-induced rock fragmentation are primarily focused on the zone of controlled fragmentation. It is within this zone that all major blasting factors exert their influence, including shock waves, stresses generated by direct and reflected waves, and the expansion of gaseous detonation products.

The upper part of the bench belongs to the zone of uncontrolled fragmentation. In this area, only partial rock breakage occurs during blasting, since wave processes have little influence here due to their rapid attenuation. The dominant factor in this zone is the blasting action of gaseous detonation products. Its effect on the overall quality of rock fragmentation is significant: the loosening factor in this zone is lower than in the controlled fragmentation zone, and it is also the principal source of oversized fragments.

The secondary crushing of oversized fragments requires additional costs and significantly increases the environmental burden.

The only way to improve the quality of rock mass preparation in the uncontrolled fragmentation zone without increasing explosive consumption is to enhance the blasting action of detonation products by extending the duration of their effect on the rock mass. The retention of detonation products within the borehole is achieved by stemming the upper part of the hole, where no explosive charge is placed. In blasting practice, drill cuttings are most commonly used as stemming material.

The purpose of stemming is to create resistance to the explosive products and to prevent the rapid escape of explosive gases from the borehole, thereby ensuring more efficient use of explosive energy. The resistance provided by stemming depends on its length and on the properties of the stemming material.

Previous studies [47, 48] have shown that the blasting effect produced by detonating a concentrated charge in a borehole without stemming is reduced by 3.0–3.5 times.

Stemming materials may be granular, liquid, plastic, solid, or foamed. Granular stemming materials, most commonly sand, have a bulk density of 1.2–1.5 t/m^3. Liquid stemming materials include water and foam gels, with a density of 1.0–1.1 t/m^3. Plastic stemming materials, the most common of which is a sand-clay mixture, have a density of 1.5–2.0 t/m^3. However, density alone is not the determining factor. High adhesion to the borehole walls is also of great importance, and this can be achieved by incorporating cementing fillers into the stemming material.

Figure 2.3 presents the results of studies on the stemming ejection duration for different stemming materials and varying stemming lengths. The results indicate that a foam-gel-type stemming material with a density of 1.1 t/m^3 (1120 kg/m^3) provides a longer retention time of detonation products compared with sand stemming and, consequently, ensures higher pressure. The rational stemming length was determined under the following conditions: rock type — sandstone with a hardness coefficient of f = 10 and a density of 2.8 t/m^3; borehole geometry — 12 m in length and 250 mm in diameter; explosive type — emulsion explosives of the Emulgit brand and ANFO 30, 50,

60. As a result of the study, the optimal stemming length was determined, which effectively accounts for the pressure decay time in the borehole (Fig. 2.4). In this case, the length ranges from 4.3 to 5.0 m.

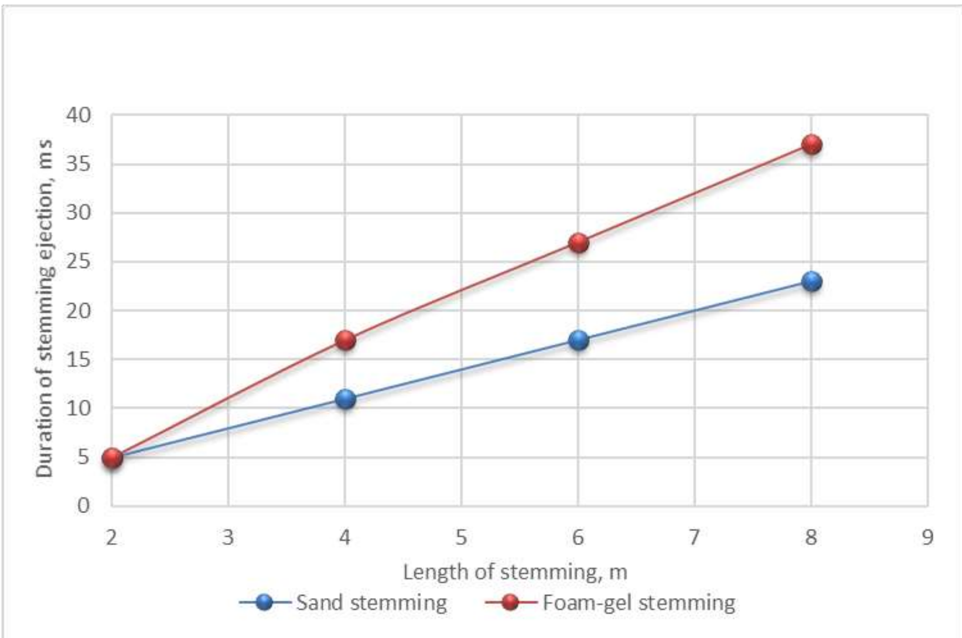

Figure 2.3. Dependence of the stemming ejection duration on the stemming material type and stemming length

In the conducted studies, the time corresponding to the pressure decay at the borehole collar under the free outflow of detonation products is equal to $5t_p$ (where t_p is the travel time of the elastic wave along the borehole). The outflow process of detonation products from a borehole 12 m long and 250 mm in diameter occurs within 4–22 ms, depending on the stemming length.

The investigation of the physical processes governing pressure variation caused by detonation products under borehole blasting conditions demonstrated that stemming made of an absorbing mixture provides higher pressure and a longer confinement time of explosive products compared with sand stemming. As a result, the optimal stemming length for a borehole explosive charge was determined, allowing the rock fragmentation process to be optimized. It was established that the stemming length of the explosive charge is a key parameter affecting the efficiency of rock blasting. Determination of the optimal stemming length in a borehole explosive charge requires consideration of the type of stemming material and its physical properties, the properties of the explosive, and the geometric parameters of the borehole.

2.2. Assessment of the Influence of Stemming Material and Geometry on Ejection Parameters

Studies and mining practice confirm that stemming material should ensure both ease of application and delayed deformation under the pressure of expanding gases, thereby prolonging the retention of detonation products within the borehole. In practice, clay-sand mixtures are preferred because of their plasticity and good adhesion to the borehole walls during deformation.

Whereas, in small-diameter blast-hole charges, stemming improvement is often limited to the selection of material or the use of special locking devices, in borehole charges the stemming design—its geometry and dimensions—provides much broader opportunities for improvement.

From the standpoint of interaction with the detonation wave, the initial stage includes the propagation of the shock wave through the stemming body to its upper end, the formation of a reflected rarefaction wave, and the weakening of the material’s structural integrity. This is followed by deformation, radial expansion of the stemming, and an increase in frictional forces along the borehole walls. At this stage, the role of the stemming material is less significant compared with the forces and deformations developing within it.

When determining blasting parameters, special attention is given to substantiating the rational stemming length. Various methodological approaches exist for its determination, based on the condition that the stemming ejection time must exceed either the time required for rock mass breakage or the time of complete charge detonation. Since rock mass destruction occurs under the combined effect of gaseous explosion-product pressure and stress-wave energy, the optimal stemming length is the one that ensures retention of the explosion products in the charge cavity for a period sufficient for effective rock breakage. Changing the composition of the stemming makes it possible to regulate the parameters of the explosive impulse and its time characteristics. Based on experimental data, a calculation scheme has been developed that makes it possible to quantitatively assess the influence of stemming material properties on the specific pressure impulse, taking into account the compressibility of individual stemming layers and friction forces.

To determine the influence of the physical and mechanical properties of the stemming material on the retention behavior of detonation products in the borehole and on the conditions of stemming ejection, two variants of the borehole charge model were considered: one with sand stemming and the other with foam stemming. In both cases, the geometric parameters of the model remained identical, and the only difference was in the properties of the stemming material.

The borehole had a diameter of 110 mm and a depth of 5.0 m, extending to the ground surface. The lower part of the borehole, 3.3 m in length, was filled with ANFO explosive, while the upper part, 1.7 m in length, was filled with stemming material.

For sand stemming, the density was taken as ρ_{sand}=1500 kg/m^3, while for foam stemming it was assumed to be ρ_{foam}=680 kg/m^3. In addition, the following parameters were used for foam stemming: Young’s modulus E = 7.5 × 10^5 Pa, Poisson’s ratio ν = 0.2, and maximum tensile stress σ_t=800 Pa. The geometric parameters of the borehole and stemming were as follows: borehole diameter d = 0.11 m, stemming length L_s=1.7 m, and explosive charge length L_e=3.3 m

The cross-sectional area of the borehole is determined from the geometric relationship:

$$A = \frac{\pi d^2}{4} = \frac{\pi \cdot 0.11^2}{4} = 9.503 \cdot 10^{-3}$$

where A is the cross-sectional area of the borehole, m^2, and d is the borehole diameter, m.

The volume of the stemming is determined as the product of the borehole cross-sectional area and the stemming length:

$$V_s = A \cdot L_s = 9.503 \cdot 10^{-3} \cdot 1.7 = 1.62 \cdot 10^{-2}, \text{ m}^3$$

The lateral contact surface area between the stemming and the borehole walls is calculated using the following formula:

$$S_{lat} = \pi d L_s = \pi \cdot 0.11 \cdot 1.7 = 0.59 \text{ m}^2$$

where V_s — the stemming volume, m³; S_{lat} — the area of the lateral contact surface of the stemming, m²; L_s — the stemming length, m.

The mass of the stemming is determined using the general relationship:

$$m = \rho V_s \qquad (2.1)$$

where m is the mass of the stemming, kg; ρ is the density of the stemming material, kg/m³; and V_s is the stemming volume, m³.

For sand stemming:

$$m_{sand} = \rho_{sand} V_s = 1500 \cdot 1.616 \cdot 10^{-2} = 24.23 \text{ kg}$$

For foam stemming:

$$m_{foam} = \rho_{foam} V_s = 680 \cdot 1.616 \cdot 10^{-2} = 10.99 \text{ kg}$$

The mass ratio of sand stemming to foam stemming is equal to:

$$\frac{m_{sand}}{m_{foam}} = \frac{24.23}{10.99} \approx 2.2$$

Thus, the mass of sand stemming is around 2.2 times that of the foam stemming. The mass of the sand alone is not enough to create a seal that traps the detonation products within the borehole.

Evaluating the force produced by detonation products. The amount of force exerted on the stem by the detonation products is calculated using the formula below.

$$F(t) = AP(t) \qquad (2.2)$$

The peak pressure value is the same in both cases and is assumed to be: $P_{max} \approx 2.4 \cdot 10^9$ Pa. Accordingly, the maximum force exerted by the detonation products on the stemming is: $F_{max} = AP_{max} = 9.503 \cdot 10^{-3} \cdot 2.4 \cdot 10^9 \approx 2.28 \cdot 10^7$ N

Thus, the peak force exerted by the gases on the stemming is approximately 22.8 MN.

Assessment of the equivalent resistance to stemming ejection. For the quantitative comparison of the confinement capacity of the two stemming materials, the equivalent contact stress corresponding to the resistance to stemming ejection from the borehole was evaluated. In this case, the following relationship was used:

$$\tau_{eff} = \frac{F}{S_{lat}} \qquad (2.3)$$

where τ_{eff} — the equivalent shear resistance stress, Pa; F is the force exerted by the detonation products pressure, N; S_{lat} — the contact surface area, m².

n the calculations, the following values were used: for sand stemming at the final stage of the process, $P_{sand} \approx 0.8 \cdot 10^9$ Pa, for foam stemming $P_{foam} \approx 1.2 \cdot 10^9$ Pa.

Then $F_{sand,end} = AP_{sand,end} = 9.503 \cdot 10^{-3} \cdot 0.8 \cdot 10^9 \approx 7.6 \cdot 10^6$ N

and the equivalent resistance stress is: $\tau_{sand} = \frac{7.6 \cdot 10^6}{0.59} \approx 12.94$ MPa

Similarly, for foam stemming:

$F_{foam,end} = AP_{foam,end} = 9.503 \cdot 10^{-3} \cdot 1.2 \cdot 10^9 \approx 1.14 \cdot 10^7$ N

$\tau_{foam} = \frac{1.14 \cdot 10^7}{0.59} \approx 19.41$ MPa

The ratio of the equivalent resistances is equal to:

$$\frac{\tau_{foam}}{\tau_{sand}} = \frac{19.41}{12.94} \approx 1.5$$

Thus, the effective resistance to ejection for foam stemming is approximately 1.5 times higher than that for sand stemming.

The obtained results indicate that the effectiveness of stemming is determined not only by its mass, but primarily by the nature of its contact with the borehole walls, its ability to compact and seal the channel, and the conditions governing the confinement of detonation products within the charge zone. Although the mass of foam stemming is lower than that of sand stemming, the analytical estimates performed show that foam stemming creates a more effective barrier to gas escape.

This can be explained by the fact that, under loading, the foam deforms, compacts, and adapts better to the irregularities of the borehole walls, thereby forming a denser contact layer. In the case of sand stemming, despite its greater mass, the intergranular void space and the less continuous nature of the contact may promote faster gas breakthrough and, accordingly, a more intensive pressure decay within the borehole.

From the standpoint of interaction with the detonation wave, the initial stage includes the propagation of the shock wave through the stemming body to its upper end, the formation of a reflected rarefaction wave, and the weakening of the structural integrity of the material. This is followed by deformation, radial expansion of the stemming, and an increase in frictional forces along the borehole walls. At this stage, the role of the stemming material itself becomes less significant compared with the forces and deformations developing within it.

The velocity of stemming movement in the borehole is best described by the equation of motion of the stemming treated as a piston subjected to gas pressure, friction against the borehole walls, and its own weight. This approach is used in modern studies: the stemming motion is considered one-dimensional, the stemming is treated as a body moving along the borehole axis, and the gas pressure is taken as the main driving force. The literature also emphasizes that such modeling is closely related to the problem of internal ballistics.

The basic equation takes the following form:

$$ma = F_1 - F_2 - G, \qquad (2.4)$$

where m – mass of the stemming , kg; a — its acceleration, m/s^2; F_1 — force og gas pressure acting on the stemming, N; F_2 — friction force of the stemming against the borehole walls, N; G — weight of the stemming, N.

For a cylindrical borehole: $F_1 = \frac{\pi d^2}{4} p_x$ та $m = \frac{\pi d^2}{4} L_s \rho_s$ where d — the borehole diameter, m; p_x — is the gas pressure in the borehole, Pa; L_s — is the stemming length, m; ρ_s — is the density of the stemming material, kg/m^3.

The relationship describing the pressure variation as the stemming moves is as follows: pV^3 =const.

Then, for engineering calculations, a formula can be used in which the average pressure and the average friction force are already applied.

$$v \approx \sqrt{\frac{2(\overline{P}A - \overline{F_2})x}{m}} \qquad (2.5)$$

where the following quantities are taken into account: the average gas pressure $\overline{P}$, the borehole cross-sectional area A, the average resistance force $\overline{F_2}$, the displacement path x, and the stemming mass m. Taking equation (2.1) into account, we obtain:

$$v \approx \sqrt{\frac{2(\overline{P}A-\overline{F_2})x}{\rho_s A l_s}} = \sqrt{\frac{2\overline{P}x}{\rho_s l_s}\left(1-\frac{\overline{F_2}}{\overline{P}A}\right)} \qquad (2.6)$$

Now, if the resistance to motion is expressed not as a separate force $\overline{F_2}$, but through the equivalent attenuation coefficient $1-\frac{\overline{F_2}}{\overline{P}A} \approx e^{-\beta l_s}$, then we obtain:

$$v = \sqrt{\frac{2\overline{P}x}{\rho_s l_s} e^{-\beta l_s}} \qquad (2.7)$$

The time of complete stemming ejection from the borehole was determined from the relation $t = \frac{x}{v}$.

The obtained results indicate that foam stemming, despite its lower density, provides significantly longer confinement of detonation products within the borehole than sand stemming. This is explained by the fact that its effective resistance coefficient to motion is higher.

Thus, foam performs more effectively not because of its greater mass, but due to its better sealing properties, deformability, and greater overall resistance to gas breakthrough.

If it is assumed that $\beta_{sand} \approx 2.36\, m^{-1}$, then the velocity can be calculated as follows: $v_{sand} = \sqrt{\frac{2\cdot 1.17\cdot 10^9\cdot 1.7}{1500\cdot 1.7}\cdot e^{-2.36\cdot 1.7}} \approx 168.3$ m/s. Accordingly, the ejection time of sand stemming can be determined as follows: $t_{sand} = \frac{1.7}{168.3} \approx 0.0101\, s = 10.1\, ms.$

For foam stemming, we assume: $\beta_{foam} \approx 3.83\, m^{-1}$. $v_{foam} = \sqrt{\frac{2\cdot 1.65\cdot 10^9\cdot 1.7}{680\cdot 1.7}\cdot e^{-3.83\cdot 1.7}} \approx 85.0$ m/s. Accordingly, the ejection time of foam stemming can be determined as follows: $t_{foam} = \frac{1.7}{85.0} \approx 0.0200\, s = 20.0\, ms.$

As a result of the calculations, it was established that, for the same borehole geometry and the same stemming length, the mass of sand stemming is 24.23 kg, whereas the mass of foam stemming is 10.99 kg. Thus, sand stemming is approximately 2.2 times heavier. However, the greater mass does not ensure better confinement of detonation products within the borehole.

Based on the analysis of the pressure curves, it was found that the average pressure in the case of foam stemming is approximately 40% higher than that for sand stemming, while the potential work of the detonation products is about 40.5% greater. The assessment of the equivalent contact resistance showed that, for foam stemming, it is approximately 1.5 times higher than for sand stemming.

Therefore, the use of foam stemming is more effective than sand stemming, since it provides better borehole sealing, prolongs the retention time of detonation products in the charge zone, and promotes a more complete utilization of the explosive energy for rock mass fragmentation.

2.3. Analysis of the Effectiveness of Foam Stemming in Reducing Harmful Gas Emissions

Another area of stemming improvement was aimed at reducing the negative environmental impact of blasting operations, which manifests itself in the formation and dispersion of dust-and-gas clouds and the emission of harmful gases. Mass blasts carried out in open-pit mines are accompanied by the formation of intense dust-and-gas clouds that pollute both the pit atmosphere and the surrounding adjacent areas. Such clouds can spread over considerable distances from the blast site. At the same time, the emitted gases are characterized by high concentrations of toxic substances, including oxides of carbon, sulfur, nitrogen, and others.

The main sources of dust and gas generation in open-pit mines are drilling and blasting operations, which account for up to 35% of total emissions [1]. The intensity of dust-and-gas formation during blasting in open pits depends on many factors, the most important of which include the physical and mechanical properties of the rock mass and its water content, the methods used for drilling blast holes, the range of explosives applied, the types of stemming materials used, blasting techniques, the timing of blasting operations, and the meteorological conditions at the time of the mass blast, among others.

At present, technological, organizational, and engineering measures aimed at reducing dust and gas emissions during mass blasts in open-pit mines are well known [49–53]. Technological measures include the use of explosives with a zero or near-zero oxygen balance. Organizational measures include accounting for the natural wind flow and shifting the blasting time to the period of its maximum activity, as well as replacing the stemming material. Engineering measures include irrigation of the blasting zone with water or dust-suppressing solutions, as well as the use of hydrostemming. At one time, an improvement of the method for reducing dust and gas emissions into the quarry atmosphere during mass explosions was proposed, developed by the M.S. Polyakov Institute of Geotechnical Mechanics of the National Academy of Sciences of Ukraine [50].

Its essence is as follows. During mass explosions in quarries, detonation products are released into the atmosphere. Small dust particles and gases form a gas and dust cloud. Therefore, under adverse meteorological conditions, part of the gas-dust aerosol can leave the boundaries of the quarry space and is carried by the air flow. The concentration of dust in the upper part of the gas and dust cloud can reach 2000 mg/m3 (up to 34% of the total amount of dust), CO – 0.04%, NO2 – 0.007%. Reduction of dust emissions is achieved by reducing the mass of the substantive (explosive) in wells on the surface of the rock block, reducing the number of wells and reducing the diameter of their mouths, the use of combined hydraulic packing, the use of hydraulic dust sup-pression systems, etc.

Experimental studies [50] have shown that spraying fine water mist over the surface of an explosive rock block leads to a more effective reduction in dust concentration than with standard spraying of liquid droplets. This is due to the fact that water fog in the district lasts longer and is transported over long distances. Consequently, the processes of interaction of moisture with dust particles are longer. It is also possible to propose a method to reduce dust formation and gas emissions during explosive rock breakage on the pit ledge. Blast wells are drilled on the surface of the ledge of the rock block. Explosive wells are used to place explosives and initiators. After that, the inactive part of the wells is sealed with a combined packing.

The lower inactive part of the well is filled with fine gravel, and in the upper part a sealed hose made of elastic polymer material filled with hydrogel is in-stalled. At the same time, the walls of the hose fit snugly to the inner surface of the drill bit. The upper part of the sealed sleeve has a mushroom-like shape, the diameter of which is larger than the diameter of the zone of active cracking (Fig.2.4, 2.5).

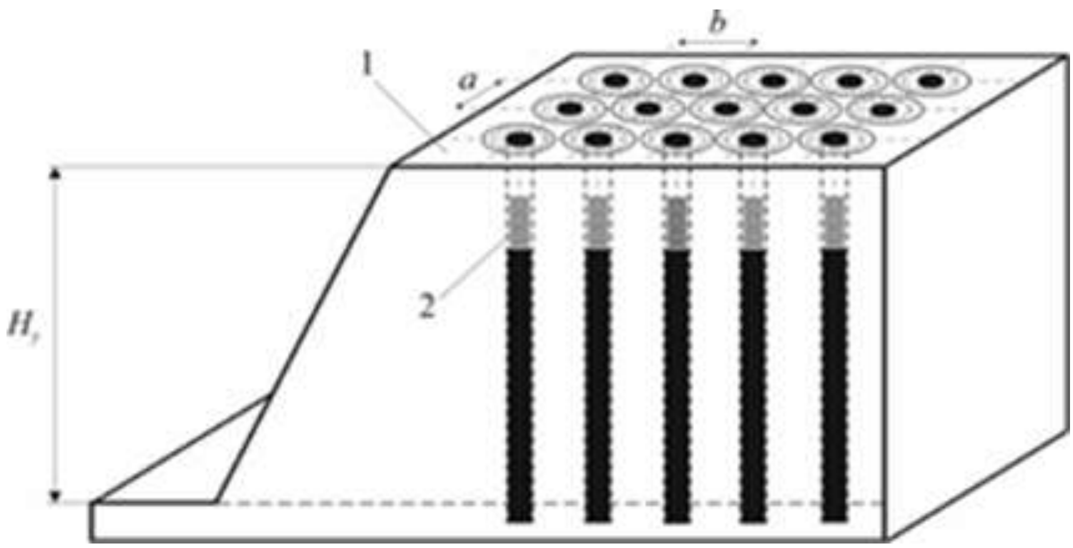

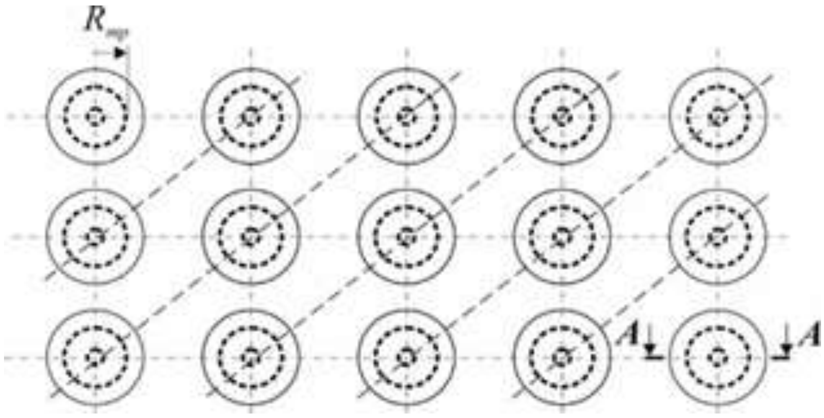

Fig.2.4: The appearance of the ledge of the rock block and the scheme of drilling explosive wells. 1 – the surface of the ledge of a rock block; 2 – explosive well; Hy – height of the cornice. Rтр - the radius of the zone of active cracking, m

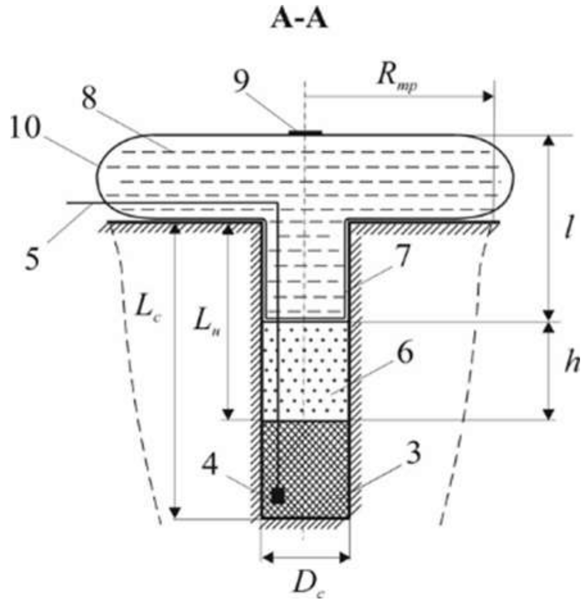

Fig.2.5: A-A section of the blast wellhead. 3 – explosive charge; 4 – initiator of the explosive charge; 5 – waveguide of the initiation system; 6 – stemming that is made of crushed stone; 7 – hermetic hose; 8 – hydrogel; 9 – check valve; 10 – mushroom-shaped protective layer; Dc - borehole diameter, m; Lc - length of the well, m; Lн - the length of the inactive part of the well, m; l – length of the sealed sleeve, m; h - the height of the crushed stone pack, m

At the moment of charge detonation, the shell of the hermetic hose is destroyed and solid detonation products interact with the hydrogel. Detonation products moving

During mass explosions in quarries, detonation products are released into the atmosphere. Fine particles of dust and gases form a gas-dust cloud. Reducing dust emission is achieved by reducing the mass of explosives in wells, reducing the number of wells and reducing the diameter of their mouths, using combined hydraulic clogging, using hydraulic dust suppression systems, etc. A method for effectively reducing dust-gas emission with the installation of sealed sleeves made of polymer material filled with hydrogel in the upper part of the well is presented.

All types of stemming currently in use are divided into two groups: those made of granular materials and liquid-based stemming. The main drawback of the listed methods is the labor-intensive nature of the process.

Thus, despite the achievement of certain positive results, the possibilities for improving the quality of rock mass preparation by blasting and reducing its environmental hazard have not yet been fully realized. A promising approach is the use of readily available components for the preparation of stemming material from solutions based on quarry water removed from blast holes during dewatering. Reducing the labor intensity of stemming operations through the mechanization of the blasting complex, which enables the preparation of stemming material directly at the blasting site, is also considered a means of improving blasting quality. Recently, the method of stemming blast holes with low-density stemming materials in the form of foam has been actively used.

For the neutralization of toxic gases, it is advisable to use inexpensive and widely available substances such as slaked lime, soda ash, and chalk. In our study, chalk is proposed because it is sufficiently widespread and is often present in overburden rocks. The use of chalk with a particle size of 40 μm increases its total surface area and, accordingly, enhances the rate and completeness of the chemical reaction for the neutralization of nitrogen oxides.

$$CaCO_3 + 2NO_2 + 0{,}5O_2 \rightarrow Ca(NO_3)_2 + CO_2 \tag{2.8}$$

The resulting particles of calcium nitrate agglomerate and settle onto the surface of the blasted rock mass.

In order to increase the foam volume, reduce its cost, and improve its environmental performance, studies were carried out on the use of chalk $CaCO_3$ as an additional additive.

Foam production is recommended to be carried out by the hydrate-foaming method [9, 10]. Its essence lies in mixing naturally occurring amorphous silicon oxide (in this case, the rock diatomite is considered) with an alkali to form alkaline hydrosilicates. During the treatment of diatomite with sodium hydroxide in the presence of water, the following reaction takes place:

$$mSiO_2 + 2nNaOH + (p-n)H_2O \rightarrow nH_2O \cdot mSiO_2 \cdot pH_2O \qquad (2.9)$$

Diatomite is considered as the main raw material component, the chemical composition of which is presented in Table 2.1. Sodium hydroxide powder is proposed as the pore-forming agent, while chalk is used as an additive. The material is produced using standard powder technology [9, 10]. As a result, a porous structure with a uniform pore distribution is obtained.

Table 2.1.Chemical composition of diatomite

	Parameter, %					
	SiO_2	Al_2O_3	Fe_2O_3	CaO	MgO	Loss on ignition
Diatomite	76,2	6,8	3,5	1,0	0,9	11,6

The addition of 5% chalk increases the density from 300 kg/m^3 to 680 kg/m^3. The porosity decreases from 80% to 67–69%. During the interaction of chalk with alkali, the foaming activity decreases according to the following equation:

$$CaCO_3 + 2NaOH \rightarrow Ca(OH)_2 \downarrow + Na_2CO_3 \qquad (2.10)$$

The decrease in the porosity of the finished material can be explained by the fact that the interaction of these components results in the release of an insufficient amount of gas (fig. 2.6 and fig.2.7).

Fig. 2.6. The internal structure of the samples without the addition of chalk.

Fig. 2.7. The internal structure of the samples with 5% chalk content.

Despite the decrease in the porosity of the foam stemming, nitrogen oxide emissions are reduced by 10%. The proposed dust-control method increases the dust suppression efficiency by 20% compared with the water-emulsion methods currently in use.

During field investigations at the quarry, an instrumental environmental monitoring system was organized using automatic air quality monitoring stations. Monitoring was carried out at five control points, which made it possible to assess the spatial distribution of gaseous and particulate pollutant concentrations within the zone affected by mass blasting. The layout of the monitoring stations is shown in Fig. 2.8. This observation arrangement makes it possible to record both the immediate post-blast impact and the subsequent dynamics of pollutant dispersion within the quarry and in the adjacent surrounding areas [51, 52, 53].

As a result of using foam stemming in blasting operations, excavator productivity increases by 18%, while the dispersion zone of fine dust and the dust-and-gas cloud is reduced by 1.8–2 times. The assessment of the environmental consequences of blasting during pilot-scale testing showed that the height of the dust-and-gas cloud in areas blasted using foam-gel stemming was more than two times lower than in areas where drill cuttings were used as stemming material.

When assessing the gas factor, particular attention was paid to nitrogen dioxide (NO_2), which is one of the hazardous components of the post-blast gas cloud. In analyzing the results, it is advisable to distinguish between air quality standards for ambient air in populated areas and those for workplace air. For ambient air, the key parameter is the maximum one-time permissible concentration, which is used to assess the impact within the sanitary protection zone of the quarry and at the boundary of residential development. For workplace air, separate occupational safety standards are applied, which determine the conditions under which personnel may be allowed to enter the blast site after natural or forced ventilation.

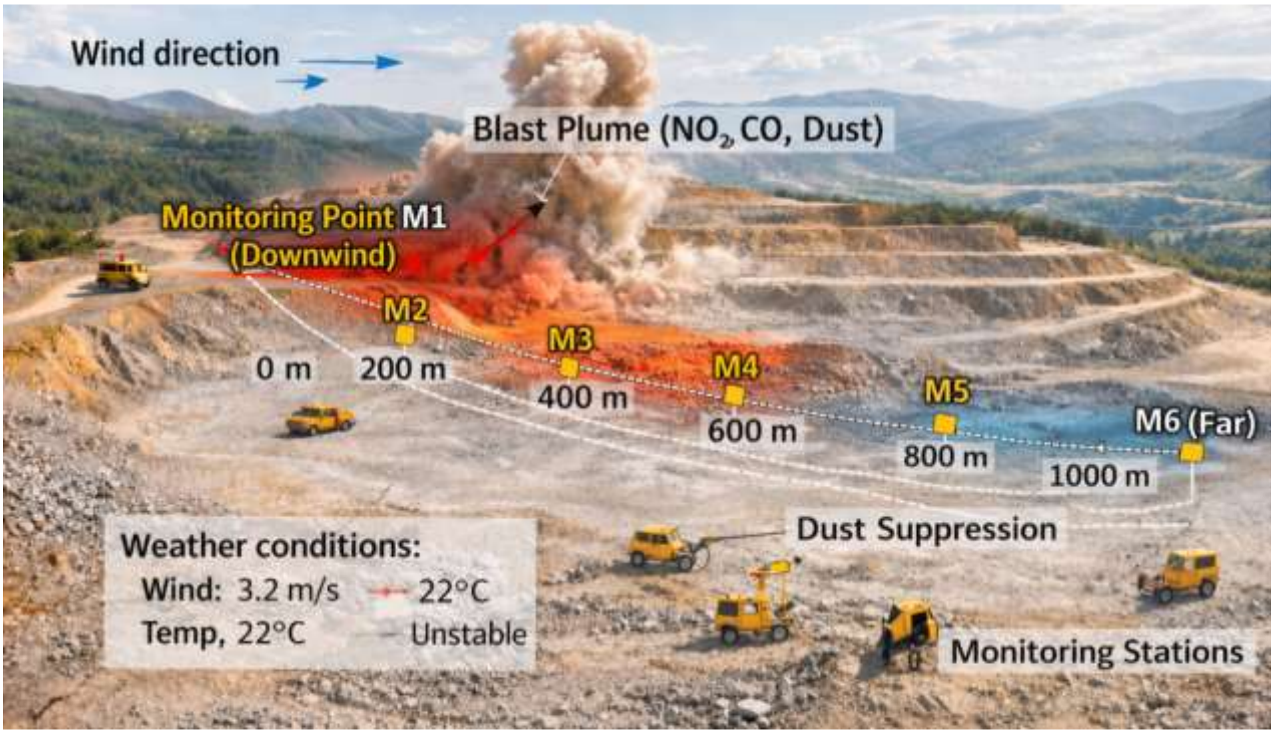

Fig. 2.8. Layout of monitoring stations: 1, 2, ..., 5, 6 — station numbers.

Thus, during mass blasting, monitoring of NO_2 concentrations has a dual significance: on the one hand, it is necessary to prevent exceedances of environmental standards beyond the boundaries of the enterprise, and on the other hand, it is essential for ensuring safe working conditions within the quarry itself (fig. 2.9). The analysis was carried out in accordance with the current Ukrainian standards for ambient air in populated areas, approved by Order of the Ministry of Health of Ukraine No. 813 dated May 10, 2024, and the standards for workplace air, approved by Order of the Ministry of Health of Ukraine No. 1192 dated July 9, 2024.

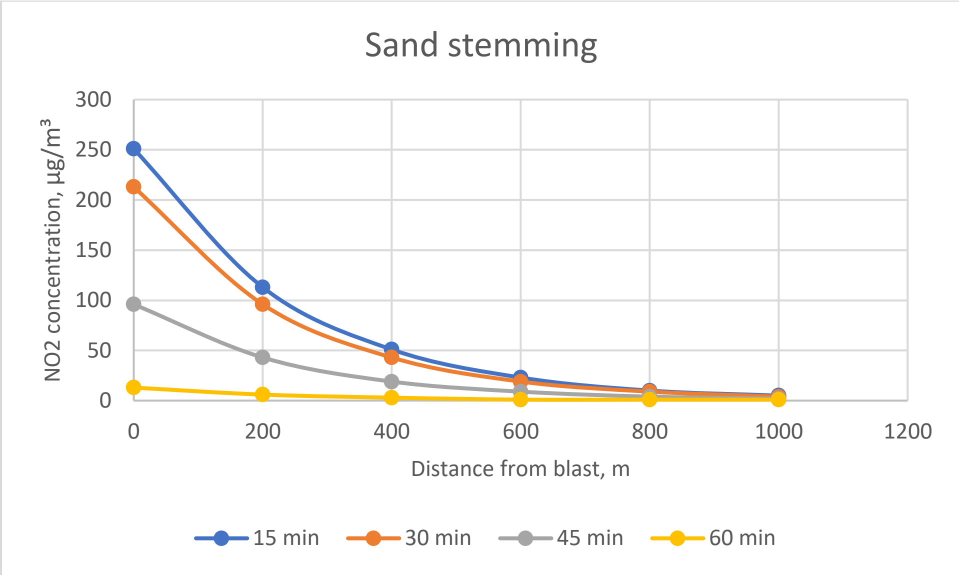

a)

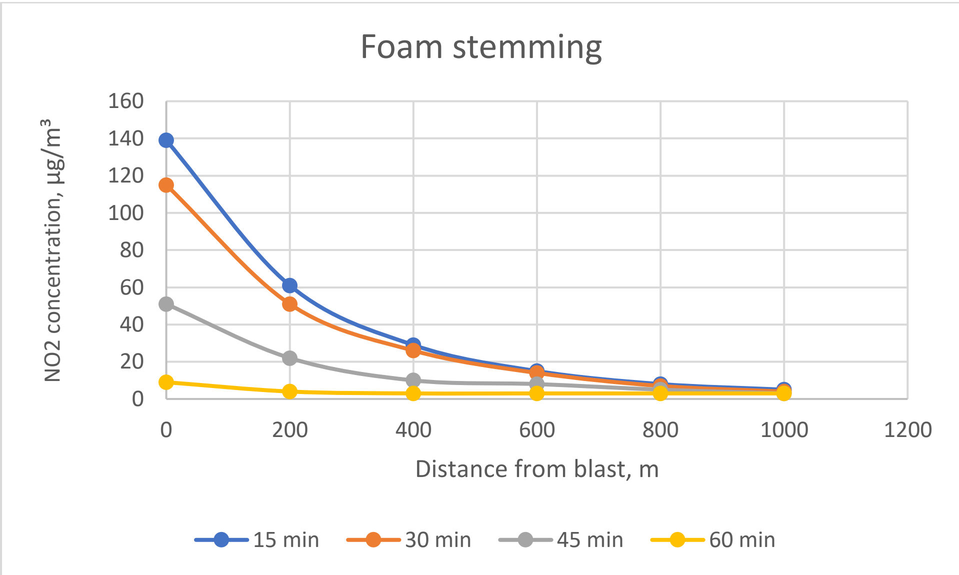

b)

Fig. 2.9. NO_2 concentration values at every 200 m from the blast epicenter for mass blasts using sand borehole stemming (a) and foam borehole stemming (b).

Carbon monoxide (CO) was also assessed separately, as it is one of the principal toxic components of gaseous detonation products (fig. 2.10). For ambient air at the boundary of the sanitary protection zone, the maximum one-time CO concentration is monitored, and the assessment is performed for the most unfavorable meteorological conditions, which makes it possible to conservatively estimate the risk of gas cloud propagation toward adjacent areas. The intensity of CO formation depends significantly on the type of explosive and its oxygen balance: the use of modern explosives with a zero or near-zero oxygen balance contributes to reducing the proportion of toxic components in post-blast gases. In the workplace air, CO monitoring has direct operational significance, since personnel may be allowed to enter the blast area only after the concentration has decreased to the permissible level and this has been confirmed by instrumental measurements. For ambient air in populated areas, the current Ukrainian maximum one-time standard for CO is 5.0 mg/m^3, while separate state medical and sanitary standards apply to workplace air; in Ukrainian practice, post-blast control is carried out on the basis of gas analysis results before personnel are admitted to the hazardous zone.

According to the obtained experimental and calculated data, the use of different types of stemming has a significant effect on post-blast carbon monoxide concentrations. When solid stemming was used, the CO concentration increased from 0.7 mg/m^3 to 3.50 mg/m^3, whereas with foam-gel stemming it increased from 0.8 mg/m^3 to 1.218 mg/m^3. This indicates a substantial reduction in the intensity of gas formation or, more precisely, a lower CO concentration in the monitored air environment after blasting. The calculated relative efficiency of CO concentration reduction for foam-gel stemming was $\eta=0.652$, which confirms its advantage over conventional solid stemming. Therefore, the use of foam-gel materials can be considered not only as a technological measure for controlling blasting parameters, but also as an effective means of reducing the gas load on both the environment and the workplace air.

Another important area of research is the assessment of air dustiness after mass blasting, since dust, especially when it contains a high proportion of free silicon dioxide, poses a significant hazard both to quarry workers and to the population of adjacent areas.

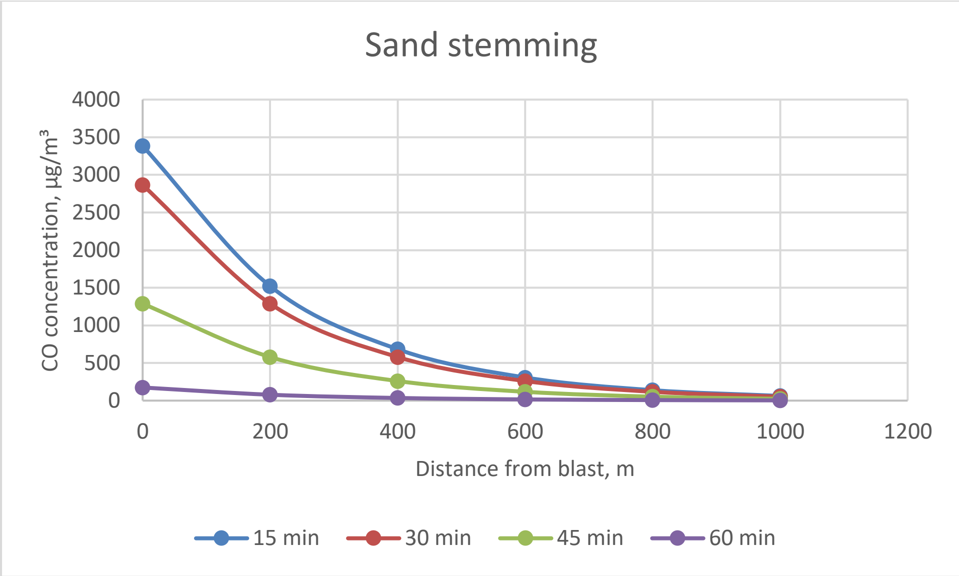

a)

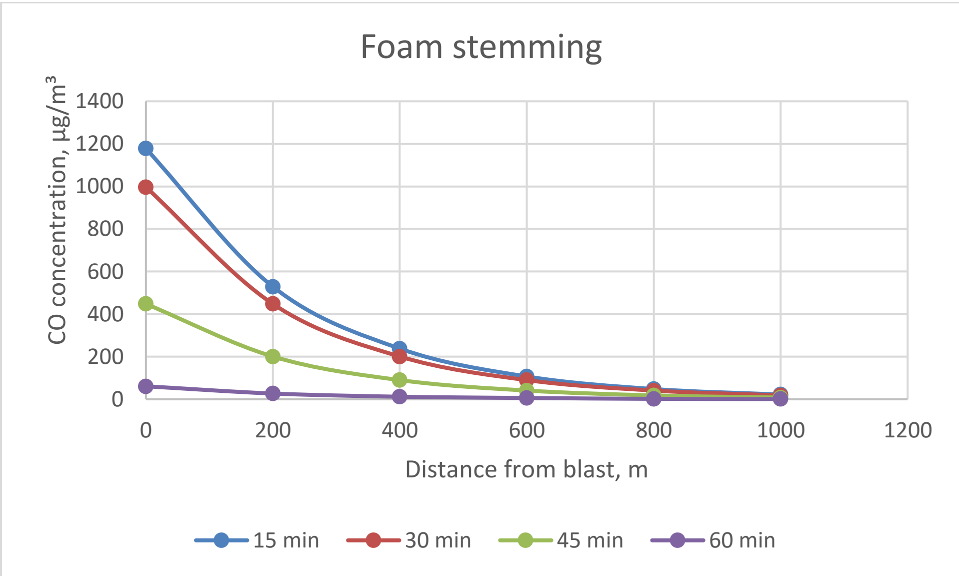

b)

Fig. 2.10. Carbon monoxide (CO) concentration values at every 200 m from the blast epicenter for mass blasts using sand borehole stemming (a) and foam borehole stemming (b).

For quartzite-bearing rocks, this issue is particularly relevant due to their high SiO_2 content, which results in increased fibrogenic activity of the dust and a higher risk of occupational diseases, particularly silicosis (fig. 2.11). Therefore, when analyzing dust pollution, it is necessary to consider not only the total mass concentration of dust, but also its mineralogical composition, particle-size distribution, and dispersion conditions after blasting. Different assessment criteria are applied to ambient air in populated areas and to workplace air, while for the workplace environment the standards are differentiated depending on the content of free silicon dioxide in the dust. In the case of quartzites and other siliceous rocks, dust control is one of the key components of the environmental and occupational safety system. In Ukraine, workplace air standards are indeed established separately for chemical substances in the working environment, and admission to the hazardous zone after a mass blast is determined on the basis of air analysis results and the decision of the blasting supervisor.

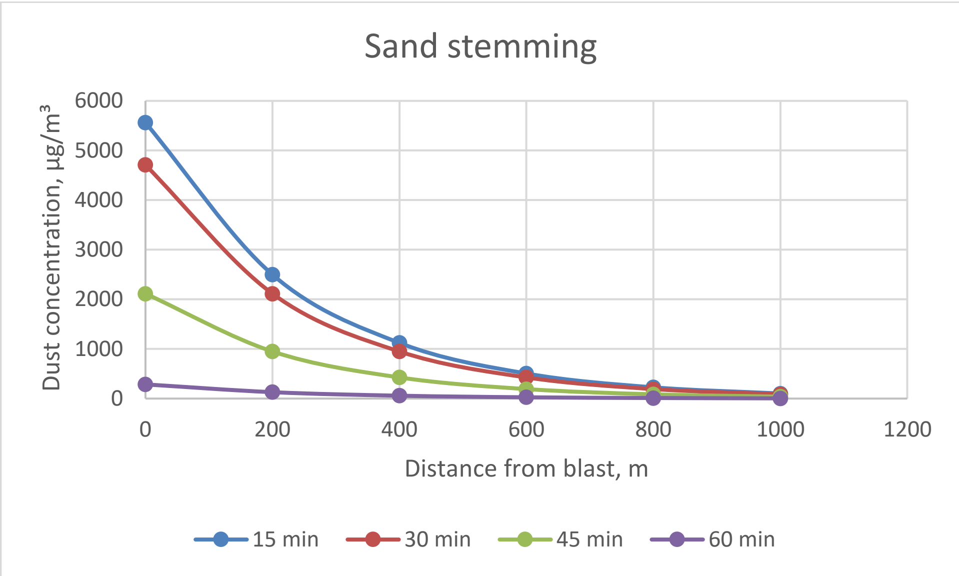

a)

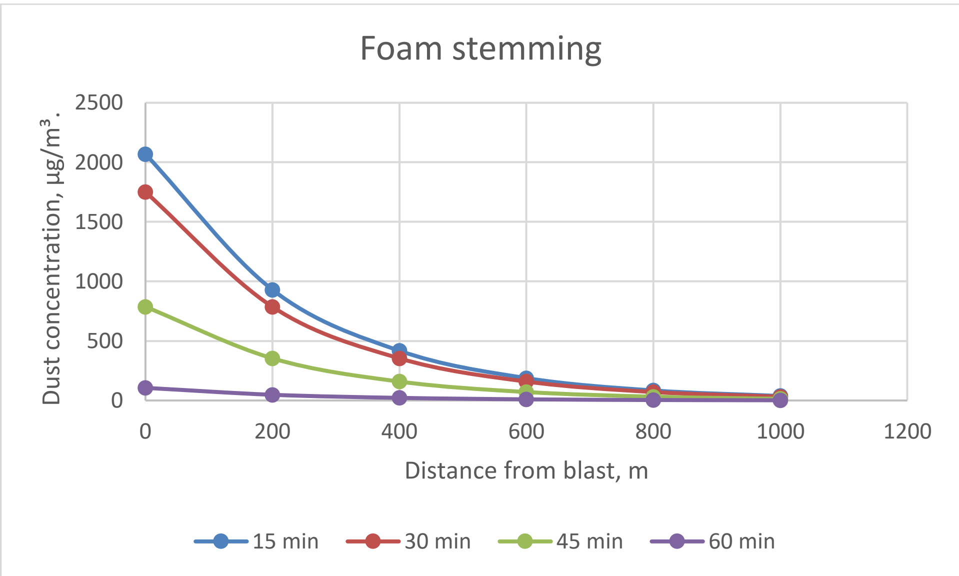

b)

Fig. 2.11. Air dust concentration after mass blasting at 200 m intervals from the blast epicenter for blasts using sand borehole stemming (a) and foam borehole stemming (b).

Analysis of the graphical relationships showed that when sand stemming was used, the maximum dust concentration after blasting reached 5.75 mg/m³, whereas with foam stemming it was 2.139 mg/m³. Thus, the use of foam stemming provides a reduction in the maximum dust concentration of approximately 63%. This result indicates a significant positive effect of foam stemming materials on the intensity of dust-and-gas emissions during mass blasting. This is important not only from a sanitary and hygienic perspective, but also from a technological one, since lower dust levels improve visibility in the quarry, increase operational safety, reduce waiting time before subsequent production operations can begin, and decrease the environmental burden on adjacent areas.

According to safety regulations, gas concentrations (instrumental) and atmospheric (environmental) conditions (measurements) should not be measured until the dust/gas cloud has initially dispersed and the blasted rock mass has stabilized (settled) after the completion of a large blast event. Current Ukrainian safety standards for industrial explosives use state that rescue personnel may be allowed entry into the quarry after 15 minutes have elapsed from the time of the explosion event; all other personnel may be allowed entry based upon the results of the air analysis. In reality, a considerably longer pause is often used in order to assess both gaseous and particulate/dusty states; that interval may be as long as 30–60 minutes depending upon weather conditions, the size of the blasting area (quarry), the size of the blasting event, and the amount of natural aeration.

Thus, the research results confirm that the problem of suppressing dust-and-gas emissions during mass blasting in open-pit mines remains relevant from both environmental and production-technological perspectives. Traditional methods based on the use of water jets and curtains are often labor-intensive and do not always provide sufficient efficiency under large-scale blasting conditions. In this regard, a promising direction is the development and implementation of new multifunctional stemming materials and technologies capable of simultaneously ensuring the required quality of explosive rock fragmentation and reducing the level of dust-and-gas load on atmospheric air. The obtained results on the use of foam stemming indicate the feasibility of further research in this area and the potential for practical application of such solutions under quarry conditions.

2.4 Conclusions to Chapter 2

Reliable stemming is a critically important element of a borehole charge design, since it directly determines the efficiency with which detonation energy is converted into mechanical work within the rock mass. By confining the detonation products within the borehole during the most important phase of gas expansion, stemming increases both the initial pressure and the duration of explosive gas action, thereby improving crack formation and rock displacement while reducing non-productive energy losses to the atmosphere. In addition, proper stemming prevents premature gas escape, which could otherwise result in incomplete detonation, increased toxicity of post-blast gases, uncontrolled flyrock ejection from the collar zone, and intensified airblast effects. Therefore, stemming should be regarded not as an auxiliary component, but as a determining factor in fragmentation quality, blasting safety, and the environmental impact of blasting operations.

Stemming effectiveness depends on more than just length; it’s also determined by the mechanical attributes of the stemming and the shape of the stemming system. Several phases of stemming physical reaction occur during the detonation, and that includes shock compression, rarefaction, free movement, and ejection. All the phases determine how long the borehole remains sealed so that pressure can act outward towards the surrounding rock mass.

From an engineering perspective, the optimal stem material should be simple to apply in practice, and exhibit delayed deformation when subjected to the forces of expanding gases, thus maximizing the length of time that the detonation products are kept confined. The use of clay and sand mixtures is very common in this capacity as they exhibit excellent plasticity, and adhere strongly to the borehole wall.

Analytical and numerical studies demonstrated that any small change in confinement time of detonation products can lead to a great increase in blasting efficiency.

In addition to fragmentation performance, the choice of stemming material is becoming increasingly important due to environmental constraints, primarily those related to dust-and-gas emissions during mass blasting. Under quarry conditions, drilling and blasting operations are among the principal sources of dust and gas generation, and under unfavorable meteorological conditions the dust-and-gas cloud may spread beyond the quarry boundaries, creating safety risks and compliance issues. Therefore, improvement of stemming technology is increasingly focused on achieving two objectives:

1) prolonging the confinement time of detonation products in order to improve fragmentation, especially in the upper, less controllable part of the bench;

2) reducing dust-and-gas emissions through the use of materials and systems capable of trapping dust particles and neutralizing harmful gases.

In this context, foam stemming is a promising approach, since it can provide longer pressure retention while simultaneously limiting dust propagation. Field assessments reported in the analyzed materials indicate that the use of foam stemming can increase excavator productivity by up to about 18% and reduce the dispersion zone of fine dust and the dust-and-gas cloud by approximately 1.8–2 times. In addition, the height of the dust-and-gas cloud in blasts with foam stemming was more than twice lower than that observed with conventional drill-cuttings-based stemming.

These results indicate that foam-based stemming can improve both production efficiency — through a more favorable particle-size distribution of the blasted rock mass and better muckpile characteristics — and environmental performance, owing to reduced aerosol pollution near the boundaries of sanitary protection zones.

Further development of foam stemming is also associated with its chemical and microstructural modification aimed at enhancing dust capture and gas neutralization. As a practical approach, the use of inexpensive and readily available additives such as chalk has been proposed: fine chalk particles (about 40 μm) increase the reactive surface area, thereby promoting more complete neutralization reactions of nitrogen oxides and enhancing the overall environmental effect of blasting.

The use of a hydrate foaming method involving natural siliceous raw materials such as diatomite has been proposed for the formation of porous structures. It has been established that increasing the chalk content in the foam increases density and decreases porosity; however, the overall yield of the dust fraction may be significantly reduced — according to some data, by 2.5–3 times.

In general, stemming optimization — through the selection of material, geometry, and the use of multifunctional foam systems — should be considered one of the most effective means of improving fragmentation quality, reducing oversize yield, lowering the specific consumption of explosives, and decreasing dust-and-gas emissions. Therefore, further improvement of foam stemming compositions with enhanced dust-absorbing capacity and gas-neutralizing ability is scientifically and practically justified, especially for large-scale quarry blasting, where both productivity and compliance with environmental requirements are of decisive importance.

CHAPTER 3. PROBLEM STATEMENT AND ITS CONNECTION TO RELEVANT PRACTICAL CHALLENGES: NUMERICAL MODELING OF EXPLOSIVE EFFECTS IN ROCK MASSES

In modern mining industry, more than 80% of rock volumes in open-pit mines are broken by drilling-and-blasting operations, the effectiveness of which largely determines the performance of all subsequent mineral extraction and processing stages. Costs for drilling-and-blasting operations amount to approximately 25% of the unit production cost of the blasted rock mass.

Elongated charges of explosive materials are widely used in blasting practice. Their detonation produces complex gas-dynamic processes, as a result of which about 90% of the detonation-wave energy is directed at an angle of 70–80° to the longitudinal axis of the borehole, and only 10% is directed into the surrounding rock mass. Such an energy distribution does not ensure maximal conversion of the wave into work for creating a system of fractures in the borehole walls, which explains the rather low level of useful effect of the explosion [54, 55].

One of the key factors determining the efficiency of charge energy use is the quality of the stemming. It is the stemming that retains the gaseous products of the explosion in the borehole during the first milliseconds after detonation, promoting the development of fractures in the surrounding massif and increasing the degree of fragmentation. Insufficient or poor-quality stemming leads to premature gas escape, energy loss, and an increase in oversized fragments. Conversely, an appropriately selected stemming material and design can significantly improve fragmentation efficiency and reduce explosive consumption.

The detonation of an elongated cylindrical charge in a borehole generates transient processes that depend on the type of explosive, charge design, initiation method, as well as the physico-mechanical properties of the stemming. The process of crack formation in the rock mass between adjacent boreholes is a consequence of the dynamic effect of the explosive load, and the effectiveness of this effect is directly determined by how well the gases are retained by the stemming [56].

Mathematical modelling of these processes reduces to a gas-dynamic problem: determining the distributions of pressure and velocity of the gaseous explosion products in the charge cavity and calculating the impulse of the wave along the inner surface of the borehole. This requires consideration of two interrelated problems: the motion of the gaseous explosion products in the charge cavity and the motion of the rock mass under the action of the explosive load [56].

It is important to account for the coupled motion of both media — the explosion gases and the rock mass — since this coupling governs the development of through-going fractures between adjacent charges.

Thus, the study of the effect of stemming on the efficiency of explosive breakage is an exceedingly relevant task. The application of computer modelling makes it possible to analyze these processes in detail, assess stemming quality, and select optimal materials and design solutions to increase the efficiency of drilling-and-blasting operations.

The optimization of stemming parameters represents one of the most effective approaches to enhancing the efficiency of blasting operations in hard rock mining, particularly in the extraction of gold-bearing quartzites. Reliable stemming ensures controlled utilization of the explosive energy, directly influencing the quality of rock fragmentation and the overall performance of subsequent mineral processing stages.

Extensive theoretical and experimental research [57] has demonstrated that the efficiency of elongated borehole or blast-hole charges in hard, heterogeneous rock masses is significantly determined by the physical and mechanical characteristics of the stemming. Its primary function is to securely confine the explosion products during the period of secondary detonation decomposition reactions, ensuring the effective conversion of expanding gas energy into mechanical work. This process enables the fracturing and displacement of the quartzite mass while minimizing energy losses.

Stemming plays a vital role in processing gold bearing quartzites due to their relatively high compressive strength, anisotropic nature and variable structural regime. The proper application of optimal stemming can provide not only better control over fragmentation but also limit the creation of fines that would adversely affect the subsequent processes and lower rates of gold recovery. In addition, stemming reduces the chances of premature venting of gases from the blast hole which, in case if occurred, can produce toxic gases, unhealthy air, and excessive dislodging of rocks as well as incomplete detonation.

We have identified many ways to improve blasting efficiency on quartzites containing gold by optimizing stemming material, along with the charge geometry and blasting parameters using an integrated approach. There are several key areas which should be considered when making the selection of a stemming material, these include granule size, density, moisture resistance capabilities and the ability to retain its structural strength when exposed to dynamic loading. The improvement of the physical properties-related characteristics of a Stemming, will allow energy to be used efficiently in the breaking of rocks as well as ensure that there are minimal damages caused to the environment, and other technological and financial operations standards of Mining organizations.

3.1. Problem Statement and its Implementational Importance

The stemming material chosen and designed is critical to the overall efficiency of the blasting operation. The stemming must provide both workability and resistance to deformation during the expansion of the explosive gas; this will keep the explosive gases confined in the hole for as long as possible. In mining operations, plastic clays and sands are used extensively in combination because of their plastic nature and providing a good bond to the hole wall during expansion.

From the perspective of detonation wave interaction, the process begins with the propagation of a shock wave through the stemming body to its upper face, followed by the formation of a reflected rarefaction wave, which weakens the structural integrity of the stemming. This is succeeded by material deformation, radial expansion, and an increase in frictional resistance along the borehole walls, enhancing the confinement effect.

This study included an evaluation of common stemming types, such as sand, which is the most widely used in practice. Based on the geological and operational conditions at the Tulallar site, an improved stemming material was proposed, namely the use of a specific foam stemming composition to enhance blast efficiency.

The detonation of an explosive charge in any medium is a complex dynamic process involving high-strain-rate deformation, shock wave propagation, and material failure. Due to the extreme physical and mechanical conditions involved, many aspects of this process cannot be fully studied through experimental means. As a consequence of this, numerical modelling has become a fourth means for understanding explosive impact in hard rock. The use of modern computational simulation tools enables researchers to study the mechanisms of rock failure and crack propagation, and thus, the optimal drilling and blasting parameters for a specific application. Advanced modeling techniques, in particular, are used to measure the extent and size of fractures in rock caused by blasting.

To solve the problems due to high dynamic velocity, including impact and explosion, which are identified by deformation and nonlinear nature rate, finite element software with explicit solution of continuum mechanics equations have widespread use.

ANSYS Explicit Dynamics is essentially the best simulation programme for this type of modelling; and when used in conjunction with other ANSYS programs, provides a means for creating and running realistic high strain rate simulations (i.e., blast waves acting on a structure). The application can also be used to simulate the loads that occur in the multiple phases of a blast event.

3.2. Explicit Dynamics Modeling in ANSYS

ANSYS Explicit Dynamics was made for simulating tricky, fast-paced events like explosions that shatter solid stuff. Around the world, ANSYS Explicit Dynamics is recognized as one of the premier numerical modeling tools for simulating blasting breakage of rocks [58 - 60].

There are four main solver formulations available to use in ANSYS Explicit Dynamics:

Lagrangian - primarily used for modeling solid materials (rock).

Eulerian - primarily used for modeling fluids/gases (detonation products etc.).

Arbitrary Lagrangian-Eulerian (ALE) combines the Lagrange and the Euler approach to model materials.

The Smoothed Particle Hydrodynamics method (SPH) allows for a meshless approach for modelling large distorted shapes.

The solver selection is determined by the optimal balance between computation precision and speed [60].

Physical and mechanical processes in ANSYS can be mathematically represented by a set of partial differential equations which are the conservation equations for mass, momentum, and energy. The materials are modeled using:

Equations of State (EOS): Relate the Stress/Strain/ Internal Energy or Temperature.

Strength Models: Describe how a material will respond to an applied load.

Failure models – determining the initiation and development of fractures;

Erosion models – used to handle large mesh distortions in Lagrangian simulations by deleting overstretched elements and redistributing forces to neighboring nodes.

For the accurate simulation of explosive interactions with rock, it is essential to select proper material models. ANSYS provides both built-in and user-defined material libraries. Among the most relevant material models for rock mechanics are:

RHT (Riedel–Hiermaier–Thoma brittle material model) – used for simulating fracture density, fragmentation, and stress thresholds in brittle solids;

Drucker–Prager model – appropriate for elasto-plastic behavior in soils and rocks; Johnson–Cook and Cooper–Symonds models – used for metals and high-strain materials.

RHT Concrete Strength Model. The RHT (Riedel–Hiermaier–Thoma) model is a physically-based strength model designed for brittle materials such as concrete, stone, and rock. It accounts for elastic, plastic, and residual behavior, incorporating cumulative damage mechanisms. The model includes strain rate effects, hydrostatic pressure sensitivity, and fatigue damage from repeated loading cycles [61,62]

The RHT (Riedel–Hiermaier–Thoma) Concrete Strength Model. RHT (Riedel–Hiermaier–Thoma) is a *constitutive model for concrete and other brittle geomaterials* (rocks, ceramics, stone). It is used under dynamic loading conditions: explosions, impacts, ballistic penetration, seismic effects. Implemented in ANSYS to simulate material response at high strain rates.

Key features of the model. The RHT model combines: Strength surface – defines elastic–plastic yield depending on stress state. Damage model – accounts for microcrack accumulation, stiffness and strength degradation. Failure surface – describes the complete loss of load-bearing capacity. Porous medium mechanics – distinguishes behavior under compression vs. tension (concrete is strong in compression, weak in tension).

Main equations. Strength surface (simplified form):

$$\left(\frac{\sigma_{eq}}{f_c(p)}\right)^2 + \left(\frac{\sigma_m}{f_t(p)}\right)^2 = 1 \qquad (3.1)$$

where: σ_{eq} - equivalent deviatoric stress, σ_m - mean hydrostatic stress, $f_c(p)$ - compressive strength as a function of pressure p, $f_t(p)$ - tensile strength as a function of pressure p.

Strain-rate effect (dynamic increase factor):

$$\sigma_{dyn} = \sigma_{stat} \cdot \left(\frac{\dot{\varepsilon}}{\dot{\varepsilon}_0}\right)^k \qquad (3.2)$$

where: σ_{dyn} - dynamic strength, σ_{stat} - static strength, $\dot{\varepsilon}$ - strain rate, $\dot{\varepsilon}_0$ - reference strain rate, k - material constant (≈0.02–0.06 for concrete).

Damage evolution:

$$D = \sum \frac{\Delta\varepsilon_p}{\varepsilon_f} \qquad (3.3)$$

where: D - damage variable ($0 \le D \le 1$), $\Delta\varepsilon_p$ - increment of plastic strain, ε_f - critical fracture strain. When D =1, the material is fully failed.

Quartzite, characterized by its high compressive strength and low tensile strength, fits ideally within the assumptions of the RHT model, which is particularly suited for dynamic loading scenarios like blasting or impact. The model allows for gradual accumulation of damage up to complete failure, enabling accurate reproduction of wave propagation and fracture behavior in rock media [63,64].

We selected the Solid Lagrangian Solver to analyze the solid phase (rock mass) material because the Solid Lagrangian Solver allows mesh nodes to move as the rock material deforms. Accurately determining the full extent of deformation and damage to the quartzite rock immediately prior to and after blasting requires using a mesh that deforms with the rock. For analysis purposes, the Solid Lagrangian Solver also provides very precise calculations tracking of the stress wave through the rock/rock fractures and the movement of the rock material because the velocity is calculated at the mesh nodes.

The RHT model is widely believed to be the best model to be used in simulating how a rock mass responds and behaves. The RHT model utilizes an incredible amount of data such as the shockwave pressure and elastic and residual strength parameters and hardening by deformation to construct failure surfaces. The RHT model allows the build-up of damage due to both tensile and compressive loading conditions to accurately predict the amount of cracking as well as the fragmentation of the material resulting from explosive loading conditions.

As noted in multiple studies [65], the combined use of Eulerian and Lagrangian reference frames in ANSYS Explicit Dynamics provides optimal results when simulating explosions in solid media:

The Eulerian formulation is best suited for modeling explosive detonation, as it enables the material to flow through a fixed mesh and effectively handles large gas flow deformations.

The Lagrangian formulation is preferred for solid rock modeling, where the mesh moves with the material, capturing the deformation and fracturing processes with high fidelity.

Manufacturers can easily tie both solvers in ANSYS together for accurate detonation gas and rock energy transfer models as hybrid systems. The combined approach allows for an excellent simulation of rock breakage under actual detonation blast conditions.

You'll find many applications that you can use the hybrid approach of the Explicit Solver in conjunction with the Explicit Dynamics solver to simulate and model:

• Crack initiation and propagation in rock
• Energy transfer from explosive gas to the rock
• Development of fracture networks and fragmentation zones
• Stress wave interaction/reflection patterns
• Stemming optimization of charges, charge shape, and rock geometry

The simulations provide information about the influence of different charge types, confinement techniques, and geological conditions on blast performance. the utilization of RHT and other related modeling techniques support the similar representation of the complex physical properties of rocks under explosive loads.

3.3. Simulation Setup: Modeling of Explosive Charges in Rock Mass

The computational model simulates the detonation of an explosive charge placed within a borehole in a rock mass. The borehole is assumed to be filled to two-thirds of its length with explosive material and one-third with stemming. The primary objective of this simulation is to evaluate how the material type of stemming influences the efficiency of the explosion in terms of energy confinement and rock breakage.

The rock mass is modeled as quartzite, a typical hard and brittle rock often encountered in blasting operations. The explosive used in the simulation is ANFO (Ammonium Nitrate Fuel Oil), a common bulk industrial explosive.

Two stemming materials are considered for comparison:

Case 1: Sand stemming;

Case 2: Foam gel stemming.

These two configurations allow for a comparative analysis of gas confinement, stemming displacement, and subsequent energy transfer into the surrounding rock mass.

The material model for ANFO was selected from the standard ANSYS material library (see Figure 2 for properties). This predefined model includes all necessary parameters for detonation behavior, including detonation velocity, Chapman-Jouguet pressure, and energy release characteristics.

The Jones–Wilkins–Lee (JWL) equation of state is an empirical thermodynamic model widely used to describe the pressure of detonation products as an explosive expands after detonation. Unlike the ideal gas law, the JWL EOS is specifically formulated for the high-pressure, high-temperature expansion regime of explosive gases, so it can represent both the very high pressures near the detonation front and the later pressure decay during expansion. In blast and rock-fracture simulations, it is used to convert the chemical energy released by the explosive into a time-dependent pressure load acting on the borehole wall and the surrounding rock mass [66, 67].

In its standard form, the JWL equation is commonly expressed as:

$$P = A\left(1 - \frac{\omega}{R_1 V}\right)e^{-R_1 V} + B\left(1 - \frac{\omega}{R_2 V}\right)e^{-R_2 V} + \frac{\omega E}{V}, \quad (3.4)$$

where P - Pressure; the specific volume is (V); E - Specific Internal Energy; and A, B, R1, R2, and ω are material constants determined through experimental calibration of a particular explosive. The two exponential terms represent the very fast pressure drop that occurs as the volume of the explosive increases. The energy term describes how the internal energy contributes to the pressure of the detonation products.

Through a physical lens, the JWL EOS doesn't model the chemical reaction mechanism fully in detail.

Instead, it provides a calibrated pressure–volume–energy relationship for the fully reacted detonation products, which makes it especially suitable for hydrocode and explicit-dynamics calculations where the main interest is the mechanical action of the explosive on surrounding materials. For this reason, JWL is commonly combined with a burn model or detonation initiation rule, while the JWL equation itself governs the subsequent expansion of detonation products.

In engineering applications, the JWL EOS is valued because it gives a practical and sufficiently accurate representation of explosive loading for problems such as borehole blasting, crater formation, structural response, and rock fragmentation**.** Its parameters are usually fitted from dynamic experimental data, and they must be treated as an interdependent set, since changing one coefficient independently can distort the predicted pressure history. Figure 3.1

The Eulerian solver was used for the explosive region to model the way that the explosive and its detonation products behave. The Eulerian approach is best suited to model fluid-like materials, such as the explosion gases, which can move through a fixed grid and can exhibit very high deformation rates and expand rapidly due to the detonation shockwave.

Density	931,00 kg/m³
Other	
Explosive JWL	
Parameter A	4,946e+10 Pa
Parameter B	1,891e+09 Pa
Parameter R1	3,9070
Parameter R2	1,1180
Parameter W	0,33333
Initial Relative Volume, V0	0
C-J Detonation Velocity	4160,0 m/s
C-J Energy / unit mass	2,668e+06 J/kg
C-J Pressure	5,15e+09 Pa
Burn on compression fraction	0
Pre-burn bulk modulus	0 Pa
Adiabatic Constant	0
Additional specific energy / unit mass	0 J/kg
Begin Time	0 s
End Time	0 s

Figure 3.1: Material model parameters for explosive material “ANFO”

The Lagrangian solver was used to model the rock mass and stemming in both solvers. It tracks the deformation of the mesh along with the material. By doing so, it provides a comprehensive means for examining the stress, strain, and fracturing in the solid portion of the domain.

With the two solvers, an accurate method of representing the transfer of energy from the detonation gases to the rock mass and stemming has been achieved with a realistic method of simulating the way explosives fracture rock.

The material model for the rock mass represents the physical and mechanical behavior of quartzite, a dense and brittle metamorphic rock. The model parameters are presented in Figure 3.2.

The following components were employed to accurately simulate the response of quartzite under explosive loading:

RHT Concrete Strength Model. The RHT (Riedel–Hiermaier–Thoma) model is a physically-based strength model designed for brittle materials such as concrete, stone, and rock. It accounts for elastic, plastic, and residual behavior, incorporating cumulative damage mechanisms. The model includes strain rate effects, hydrostatic pressure sensitivity, and fatigue damage from repeated loading cycles. Quartzite, characterized by its high compressive strength and low tensile strength, fits ideally within the assumptions of the RHT model, which is particularly suited for dynamic loading scenarios like blasting or impact. The model allows for gradual accumulation of damage up to complete failure, enabling accurate reproduction of wave propagation and fracture behavior in rock media.

P-alpha Equation of State (EOS). This EOS is suitable for porous solid materials and describes volume change under pressure due to pore collapse. It captures the transition of material behavior from a porous to a compacted state. In the context of quartzite, this model accounts for compression, pore closure, and the nonlinear mechanical response of the rock under high-pressure conditions. It is particularly useful for simulating how the rock behaves when subjected to the shock compression typical of blasting [67].

Polynomial Equation of State. This is a general-purpose EOS that expresses pressure as a function of density and internal energy using a polynomial form. It enables the modeling of material response across a wide range of pressure, temperature, and deformation states. For quartzite, this EOS provides a flexible framework for capturing thermomechanical effects under blast loading.

The Lagrangian solver was chosen for the solid domain (rock mass), as it allows the mesh to deform with the material. This is essential for capturing the full deformation and failure behavior of the quartzite during and after detonation. The solver ensures accurate tracking of stress wave propagation, fracturing, and material displacement under high-strain-rate loading.

Density	2660,0	kg/m³
Other		
P-alpha EOS		
Solid Density	2314,0	kg/m³
Porous Soundspeed	2920,0	m/s
Initial Compaction Pressure Pe	2,33e+07	Pa
Solid Compaction Pressure Ps	6e+09	Pa
Compaction Exponent n	3,0000	
Polynomial EOS		
Parameter A1	4,387e+10	Pa
Parameter A2	4,94e+10	Pa
Parameter A3	1,16e+09	Pa
Parameter B0	1,2200	
Parameter B1	1,2200	
Parameter T1	4,387e+10	Pa
Parameter T2	0	Pa
RHT Concrete Strength		
Use cap on Elastic Surface	Yes	
Compressive Strength fc	1,6e+08	Pa
Tensile Strength ft/fc	0,100000	
Shear Strength fs/fc	0,19000	
Intact Failure Surface Constant A	1,6000	
Intact Failure Surface Exponent n	0,61000	
Tension/Compression Meridian Ratio Q2.0	0,68050	
Brittle to Ductile Transition BQ	0,010500	
Hardening Slope	1,1000	
Elastic Strength/ft	0,40000	
Elastic Strength/fc	0,85000	
Fracture Strength Constant B	1,6000	
Fracture Strength Exponent m	0,61000	
Compressive Strain Rate Exponent α	0,025000	
Tensile Strain Rate Exponent δ	0,045000	
Maximum Fracture Strength Ratio SFMAX	1e+20	
Damage Constant D1	0,040000	
Damage Constant D2	1,0000	
Minimum Strain to Failure	0,0100000	
Residual Shear Modulus Fraction	0,13000	
Shear Modulus	1,7e+10	Pa

Figure 3.2 – Physical and Mechanical Properties of the Quartzite Material Model
Stemming Configuration 1: Sand as a Granular Stemming Material.

In the first simulation scenario, sand was used as the stemming material. To model its physical and mechanical behavior under explosive loading, the built-in “SAND” material model from the ANSYS material library was applied, with modifications to the material density to meet the specific requirements of the simulation (see Figure 3.3).

For the numerical modelling of sand stemming, the material can be represented by the Modified Drucker–Prager (MO Granular) constitutive model, which is intended for granular media such as soil, sand, and powders. In this approach, the initial density of the stemming material is set to 1500 kg/m³, corresponding to medium-dense dry sand. The MO Granular model extends the classical Drucker–Prager formulation by accounting not only for pressure-dependent yielding, but also for density hardening and for the variation of shear modulus with density, which makes it suitable for simulating the compressive and inelastic response of sand under blast loading.

The yield strength in the MO Granular model is defined as the sum of two components: a pressure-dependent yield stress and a density-dependent yield stress, which can be written in simplified form as:

$$\sigma_y = \sigma_p + \sigma_\rho \qquad (3.5)$$

where σ_y is the total yield stress, σ_p is the pressure-related contribution, and σ_ρ is the density-related contribution. In ANSYS Explicit Dynamics, this behaviour is introduced through three mandatory tabular input functions: Yield Stress vs Pressure, Yield Stress vs Density, and Shear Modulus vs Density. The unloading and reloading slope is governed by the shear modulus, which is defined as a function of the zero-pressure density of the material.

In practical terms, the pressure hardening component is specified through a tabulated relationship between pressure and plastic yield stress, allowing the model to reproduce the increase in shear resistance of sand under compressive confinement. This is especially important for stemming simulations, because during detonation the sand plug is subjected to rapidly increasing pressure, compaction, and shear deformation. As a result, the MO Granular model enables a more realistic description of sand behaviour during the stages of compression, confinement, and ejection of the stemming column, and therefore provides a suitable constitutive framework for analysing the mechanical performance of sand stemming in borehole blasting.

This material model is tailored for granular media subjected to large deformations, compaction, and partial failure under dynamic loading. It combines features of granular plasticity, volumetric compaction, and tensile failure, which enables a realistic simulation of unconsolidated materials under explosive effects.

Key Components of the Sand Material Model: Density: Initial material density was set to 1500 kg/m^3, corresponding to a medium-dense dry sand. Modified Drucker–Prager Model (MO Granular): This model accounts for pressure-dependent plasticity, incorporating the following effects:

Pressure Hardening: Defined through a tabular relationship between pressure and plastic strain, this component reflects the strengthening of sand under compressive loading.

Density Hardening: Expressed as a table of ultimate strength versus density, this is essential for capturing the behavior of sand during compaction as pore spaces collapse.

Variable Shear Modulus: The shear modulus changes with density according to a defined table, allowing accurate simulation of the material's stiffness at varying levels of compaction.

Initial Shear Modulus: Set to 7.69×10^7 Pa, this value defines the stiffness of the sand before plastic deformation begins. It is typical for medium-density dry sands.

Tensile Failure Model: A maximum tensile pressure value of –0.001 Pa is used to define a technical tensile failure threshold. This prevents unrealistic elongation of elements and triggers element erosion when tensile limits are reached.

Compaction Equation of State – Linear (Compaction EOS Linear):
This EOS describes how sand responds to volumetric changes under compression. Key parameters include:

Solid Density: 2641 kg/m^3 – representing the density of the solid mineral skeleton of the soil without pores.

Compaction Path: A table defining pressure as a function of density, used to simulate the gradual collapse of pores under high pressure.

Linear Unloading: A relationship that defines the speed of sound as a function of density, used for modeling material unloading behavior after the pressure peak.

This combination of physical models provides a detailed representation of sand’s compressibility, shear resistance, and failure behavior under the transient loading conditions typical of blasting.

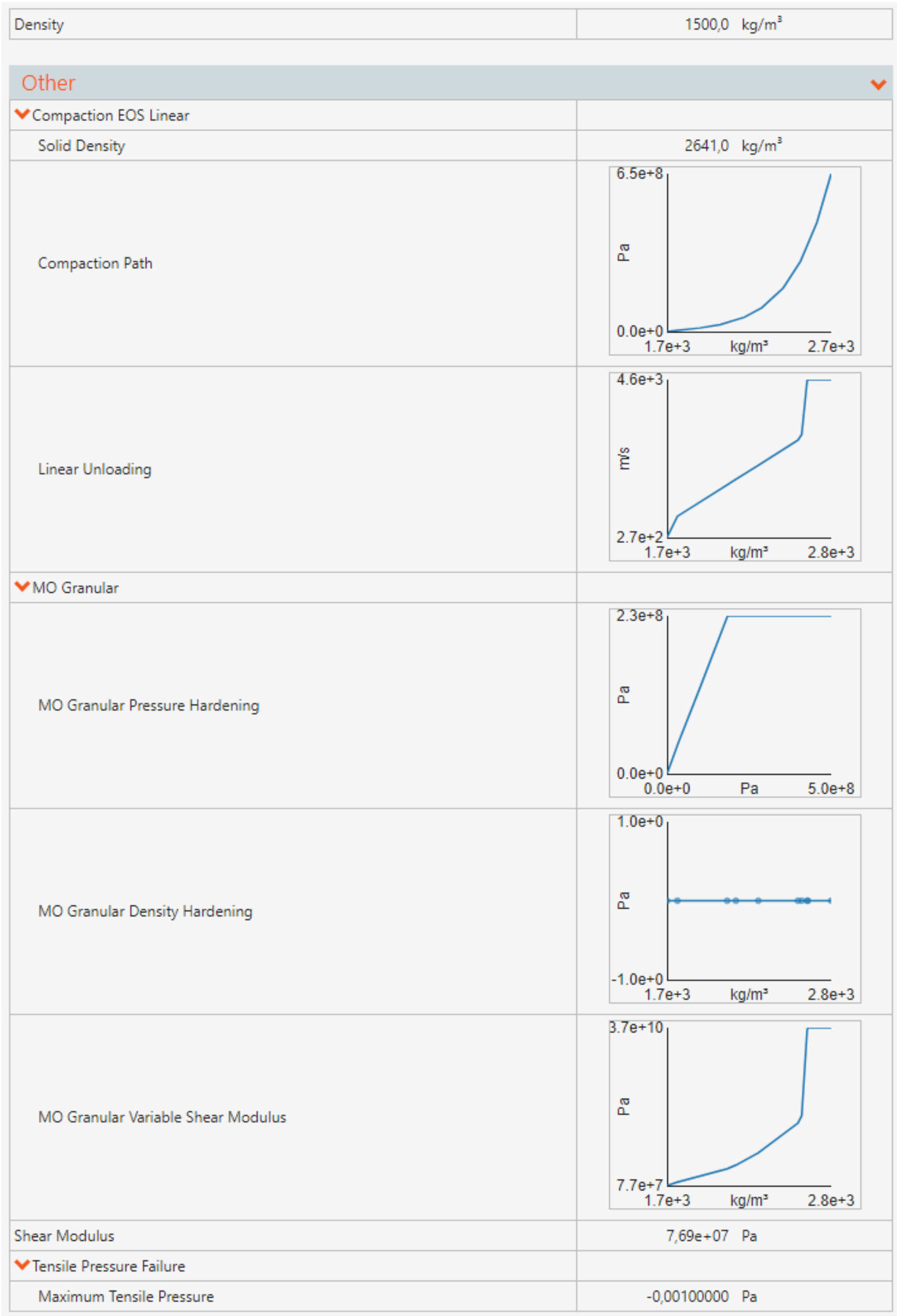

Figure 3.3 – Material Model Parameters for “SAND” in ANSYS Stemming Configuration 2: Foam as a Compressible Energy-Absorbing Material

A foam gel has been introduced as the stemming material for the second simulation scenario. The ANSYS Crushable Foam material model was chosen because it can be used to replicate the physical and mechanical properties of the material under dynamic loads.

It provides a solution for modeling materials that are porous and energy absorbing like engineered fillers, polymeric foams, and porous stemmings.

The Crushable Foam model efficiently represents compressible materials with a large volumetric deformation under pressure and a low tensile strength. Therefore, it is a suitable model to use in designing materials for absorbing blasting energies and delaying gas escaping from boreholes. The Crushable Foam model can be used to describe compaction, energy absorption, and pressure-dependent/ related plasticity of compressible materials.

The model has several characteristics and including: Volumetric compression-type of response to pressure, Negligible tensile resistance (i.e. experiencing realistic crushing type of fracture under tension)

Pore collapse and density behaviour. The materials model assumes a pressure-sensitive yield surface and volumetric hardening due to the collapse of the pores as the foam densifies. This model is commonly used for blast mitigation or shock absorption applications, both of which relate directly to stemming dynamics.

The detailed parameters of the foam gel material used in the simulation are presented in Figure 3.4.

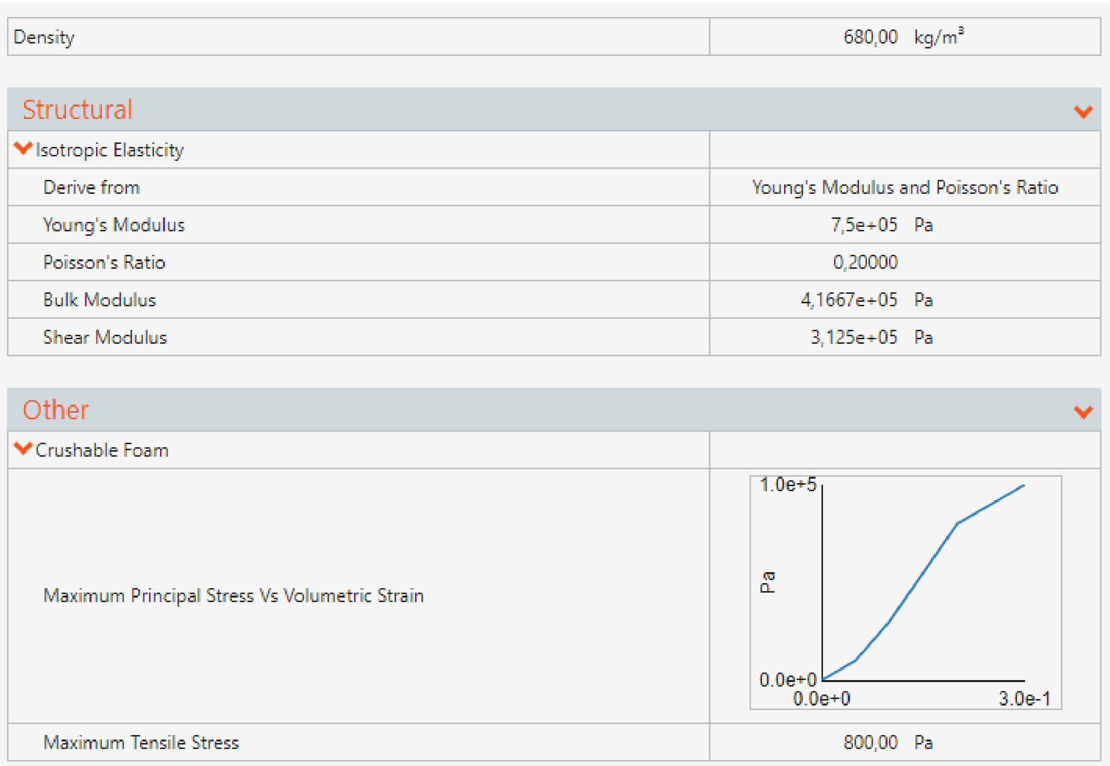

Density	680,00 kg/m³
Structural	
Isotropic Elasticity	
Derive from	Young's Modulus and Poisson's Ratio
Young's Modulus	7,5e+05 Pa
Poisson's Ratio	0,20000
Bulk Modulus	4,1667e+05 Pa
Shear Modulus	3,125e+05 Pa
Other	
Crushable Foam	
Maximum Principal Stress Vs Volumetric Strain	1.0e+5 Pa 0.0e+0 0.0e+0 3.0e-1
Maximum Tensile Stress	800,00 Pa

Figure 3.4 – Material Model Parameters for Foam Stemming (Crushable Foam Model)

For the material that stems the domain, we used a Lagrangian Solver to solve it. In this case, a Mesh will be able to move and change shape along with the material, thus making it very suitable for simulating the response of solid/semi-solid materials, such as sand and foam gel. The Lagrangian approach provides the ability to track exactly where an element is deforming (or compacting or failing) during the explosive load, and therefore provides a true representation of both the stress wave propagation and the material interaction within the borehole.

Variant 1

The geometry of the rock mass in the first model is implemented as a rectangular parallelepiped with a square base measuring 2 meters on each side and a height of 5.3 meters. The borehole geometry is represented as a cylindrical region within the rock mass, with a diameter of 110 mm and a height of 5 meters, extending to the surface of the rock mass. The lower 3.3 meters of the borehole is filled with explosive material (EM), while the upper 1.7 meters, up to the surface, is filled with stemming material.

The finite element mesh of the model includes 114,504 nodes and 98,556 elements (Fig. 3.6). The element size is 0.1 m for the rock mass and 0.01 m for the stemming. The Eulerian computational mesh is characterized by an element size of 0.025 m.

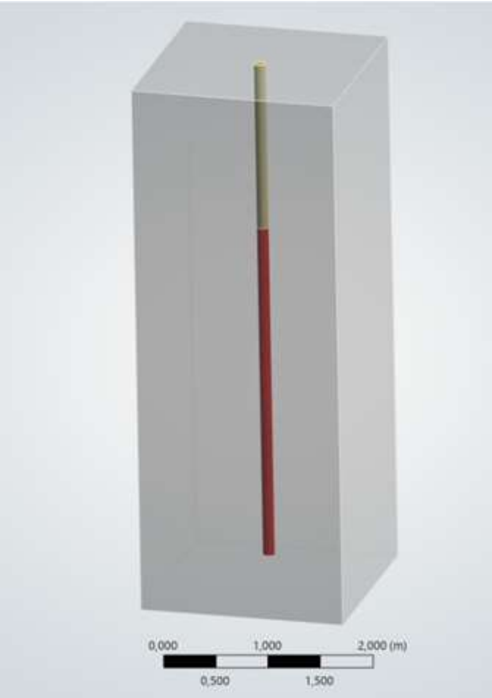

Figure 3.5. Geometry of the model

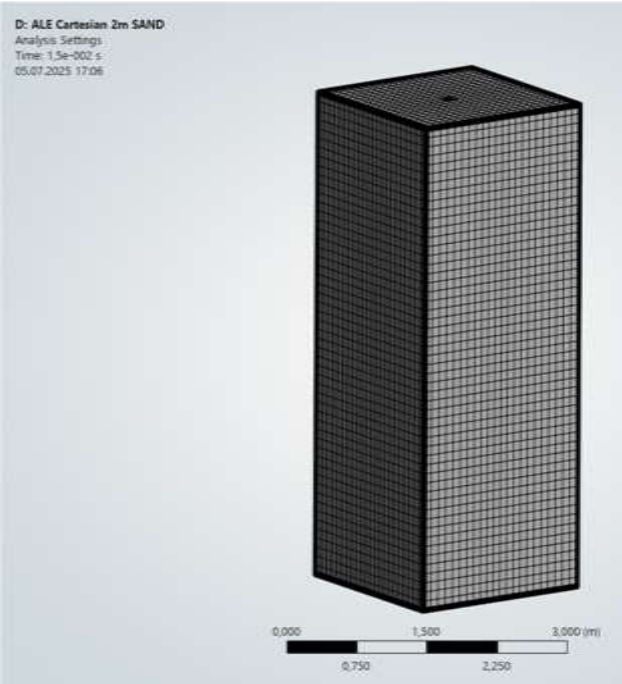

Figure 3.6. Finite element mesh of the model

To account for the contact interaction between the rock mass and the stemming, a contact group was defined for the contact surfaces between these bodies, with a friction coefficient of 0.55 (Fig. 3.7).

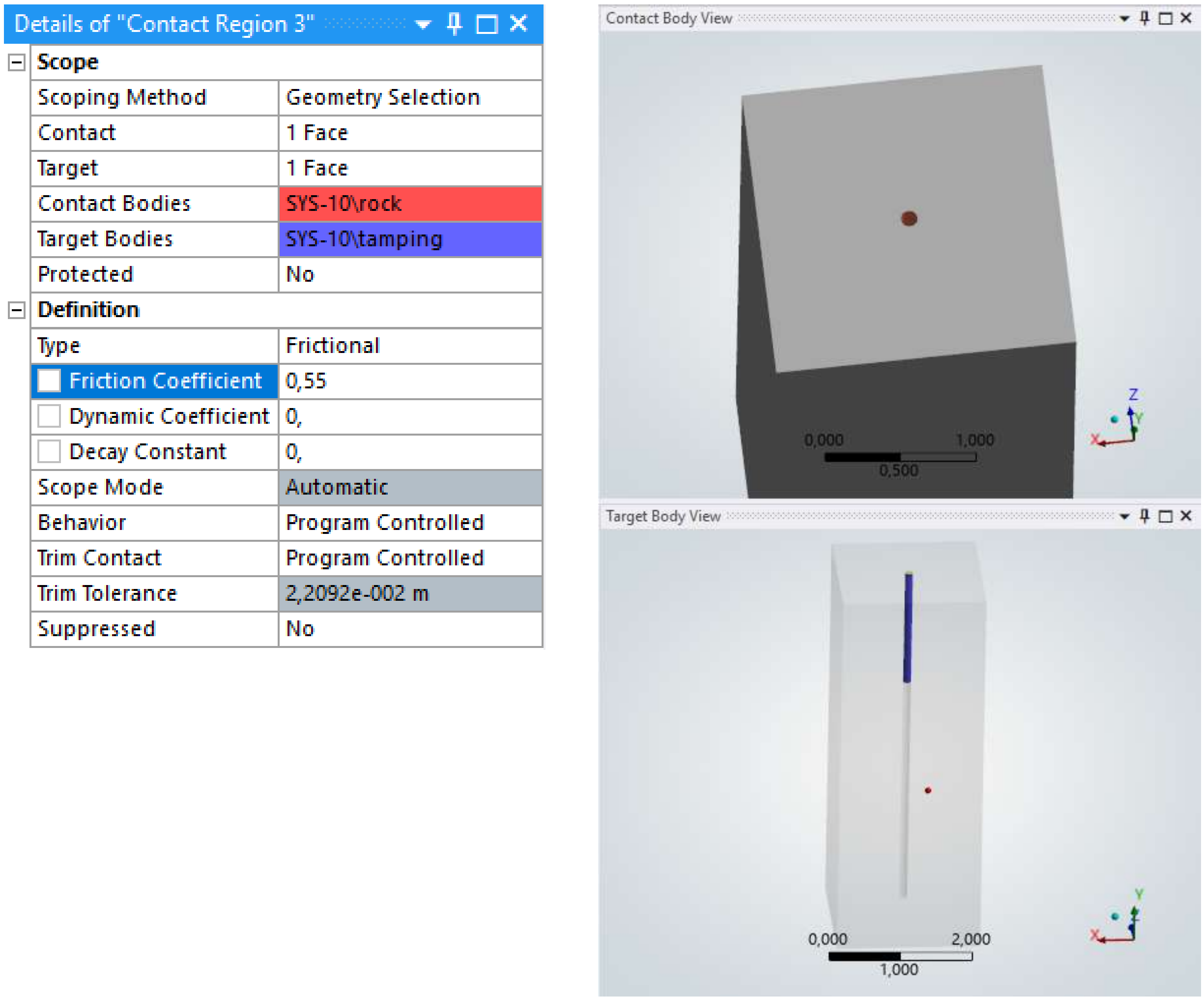

Figure 3.7. Contact group for the contact surfaces between the rock mass and the stemming

Impedance boundaries were selected as the boundary conditions for the lateral and bottom surfaces of the model (Fig. 3.8), as well as for all sides of the Eulerian computational domain. These boundaries help to reduce the effect of reflected waves that occur at the edges of the computational area during the propagation of blast waves.

Impedance boundaries approximate the condition of free wave propagation based on the acoustic impedance of the medium (the product of density and sound velocity), and they allow the transmission of the normal component of velocity with minimal reflection.

In ANSYS, this type of boundary is implemented by accounting for changes in pressure and velocity along the characteristic line departing from the boundary, assuming zero reference values for an initially motionless medium.

Thus, the impact of potential wave reflections at the computational boundaries is minimized, considering the model size and the nature of blast wave propagation.

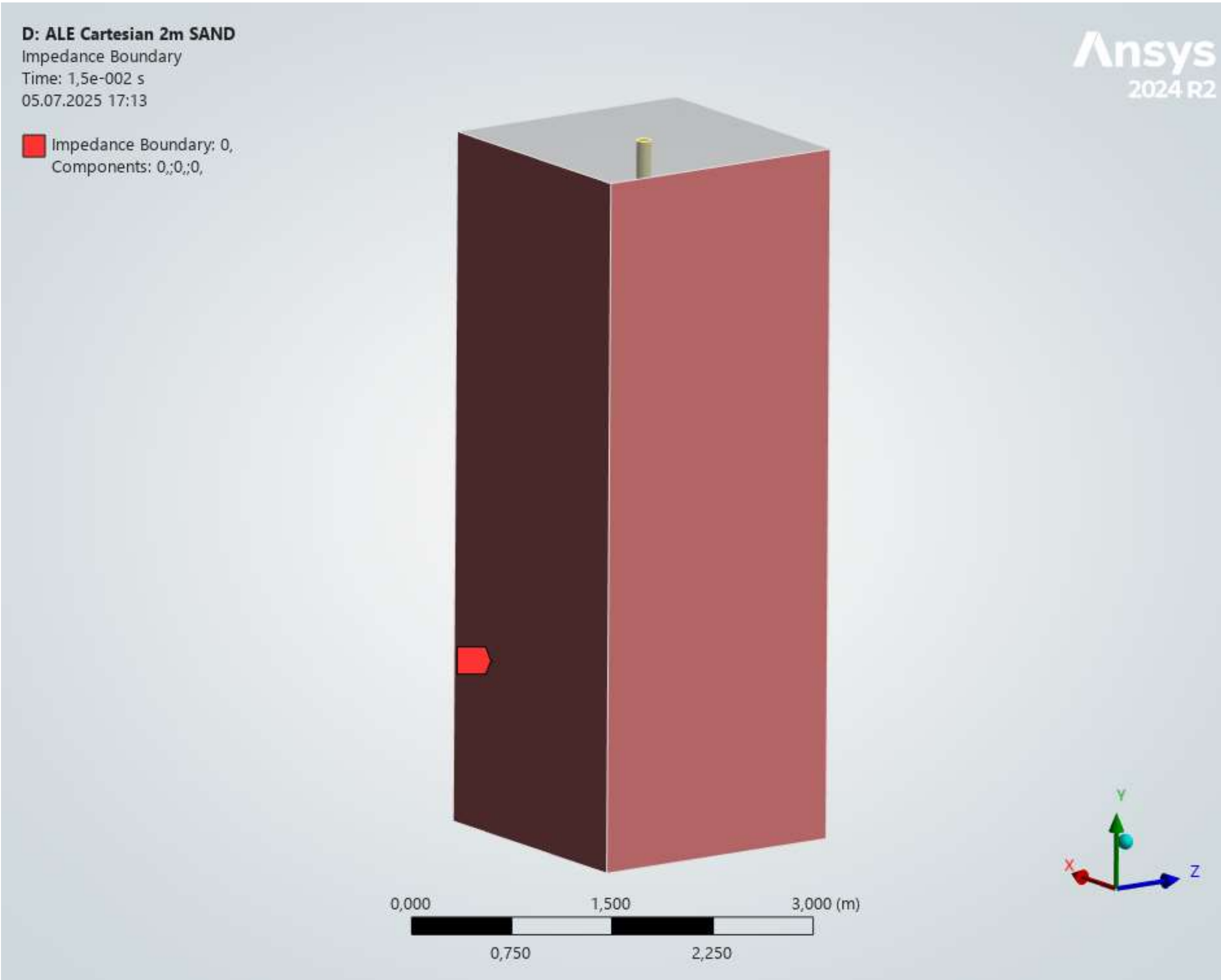

Figure 3.8. Impedance boundaries of the model

Variant 2. The geometry of the rock mass in the second model is implemented as a rectangular parallelepiped with a square base measuring 2 meters on each side and a height of 5.3 meters. The borehole geometry is represented as a cylindrical region within the rock mass, with a diameter of 110 mm and a height of 5 meters, extending to the surface of the rock mass. The lower 3.3 meters of the borehole is filled with explosive material (EM), while the upper 1.7 meters, up to the surface, is filled with stemming material.

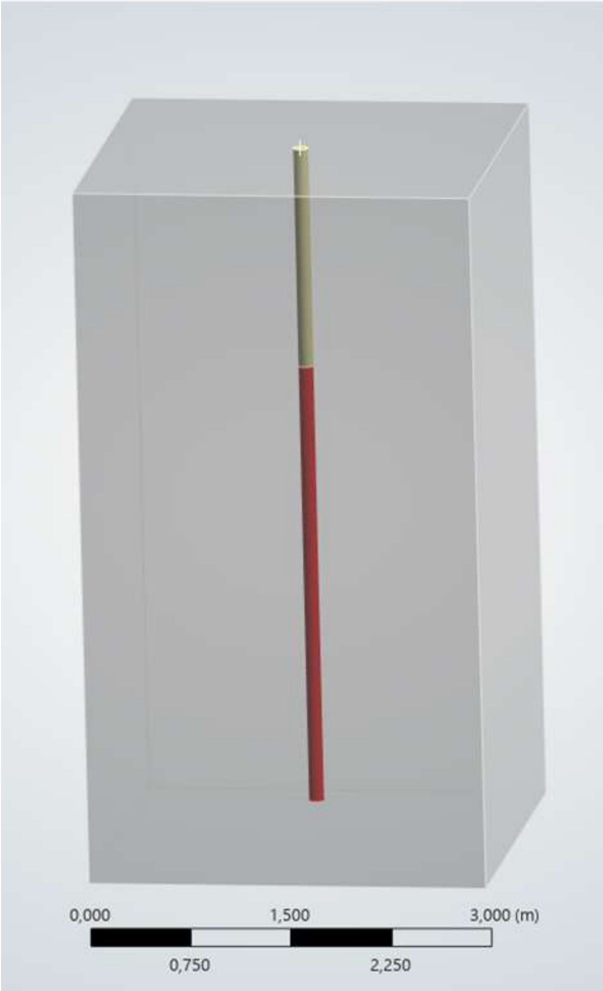

Figure 3.9. Geometry of the model

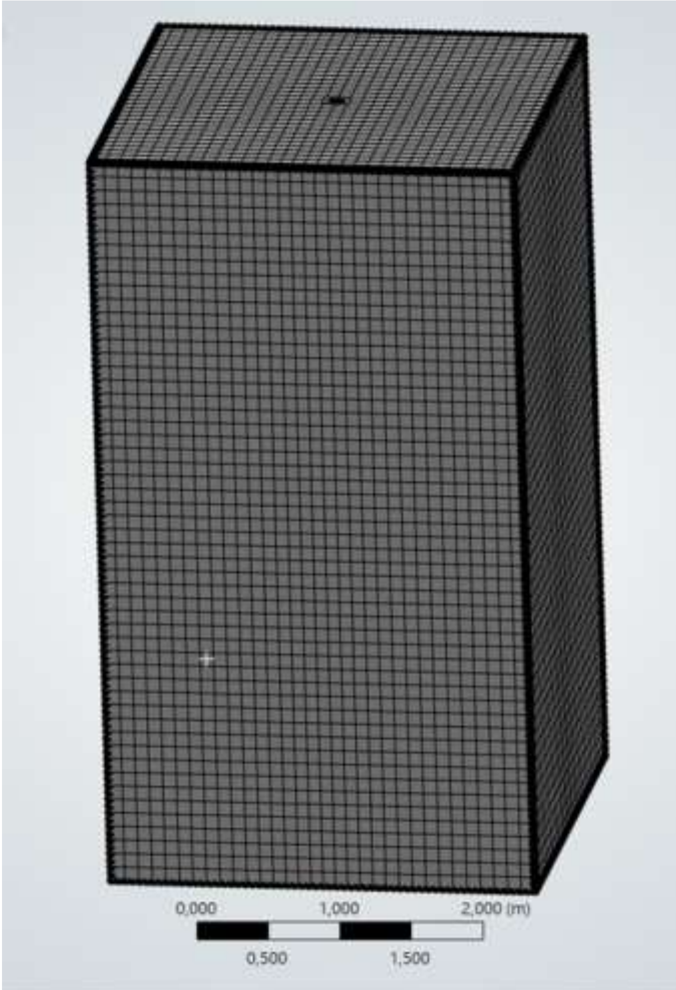

Figure 3.10. Finite element mesh of the model for the second variant

The finite element mesh of the model includes 144,744 nodes and 127,176 elements (Fig. 3.10). The element size is 0.1 m for the rock mass and 0.01 m for the stemming.

The Eulerian computational mesh is characterized by an element size of 0.05 m.

To account for the contact interaction between the rock mass and the stemming, a contact group was defined for the contact surfaces between these bodies, with a friction coefficient of 0.7 (Fig. 3.11).

Details of "Contact Region 3"	
Scope	
Scoping Method	Geometry Selection
Contact	1 Face
Target	1 Face
Contact Bodies	SYS-16\rock
Target Bodies	SYS-16\tamping
Protected	No
Definition	
Type	Frictional
Friction Coefficient	0,7
Dynamic Coefficient	0,
Decay Constant	0,
Scope Mode	Automatic
Behavior	Program Controlled
Trim Contact	Program Controlled
Trim Tolerance	1,6972e-002 m
Suppressed	No

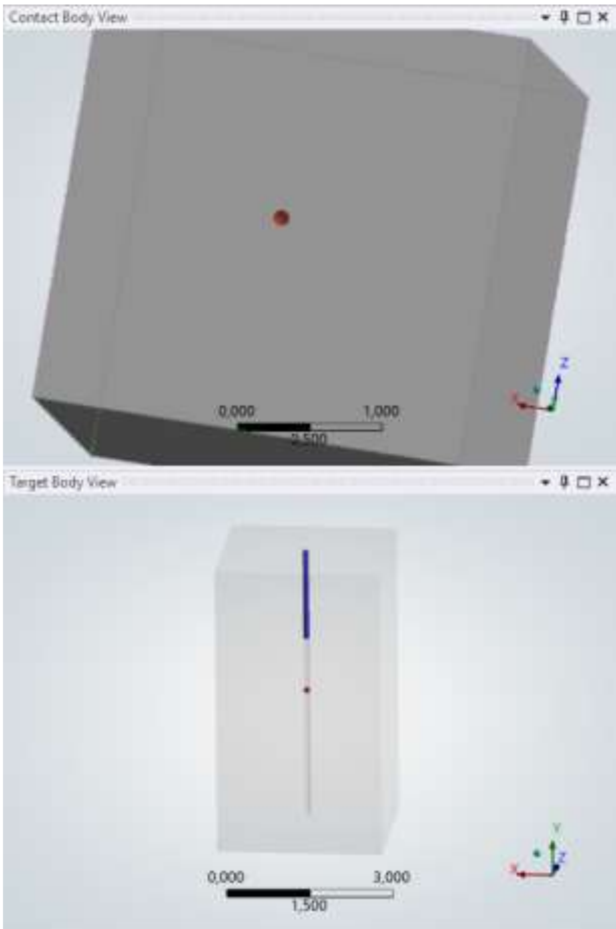

Figure 3.11. Contact group for the contact surfaces between the rock mass and the foam stemming

The impedance boundaries served as boundary conditions for the lateral bottom surfaces of the model (see Figure 3.12) and also represented boundary conditions for each of the boundaries of the Eulerian computational domain. Impedance boundaries help minimize the impact of reflected waves that emanate from the exterior edges of the computational domain when blast waves are travelling within the computational domain.

Impedance boundaries are being utilized to approximate the free wave condition of propagation and have been established with reference to the acoustic impedance of the medium, being the product of the density times the speed of sound of the medium. The normal component of velocity will, therefore, be largely transmitted through the impedance boundary with very little reflection.

The approach used by ANSYS software to implement the impedance boundary condition is essentially based on tracking the pressure and velocity changes on the characteristic line, which propagates away from the boundary. The two values of pressure and velocity will have zero reference values for initially stationary medium.

Thus, the impact of possible blast wave reflections at the computational boundaries is minimized, considering the model dimensions and the nature of wave propagation.

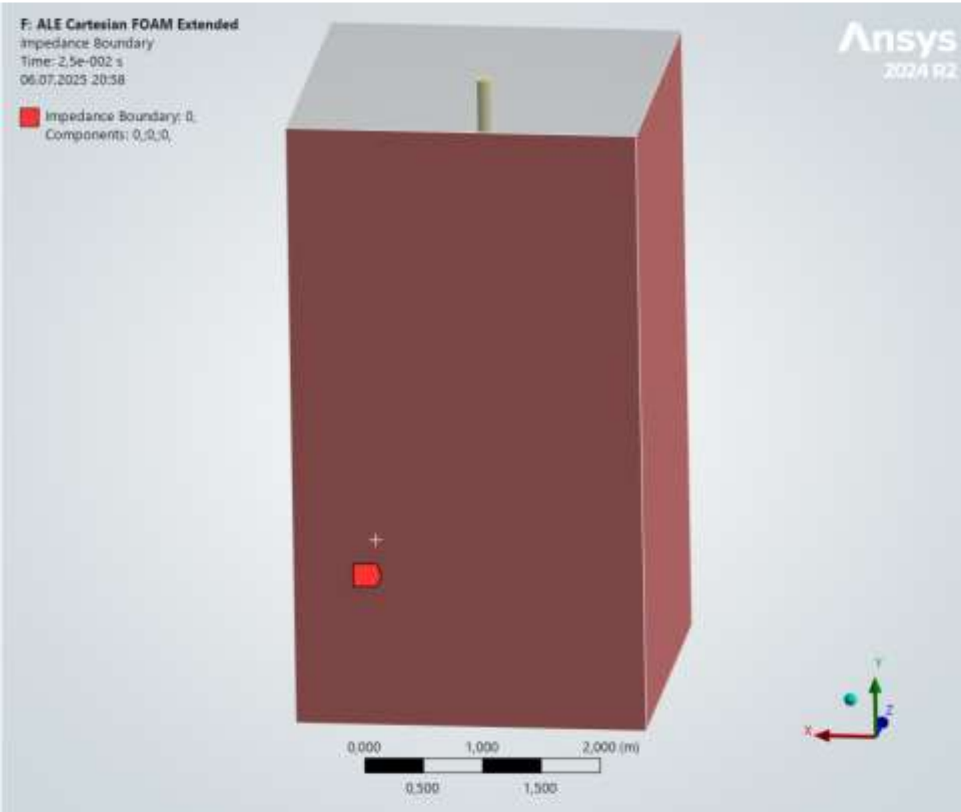

Figure 3.12. Impedance boundaries of the model for the second variant

As a result of analyzing the two variants — one using sand as stemming and the other using foam — simulation results were obtained. The calculations were carried out over a time interval of 15 milliseconds. Extending the simulation time would significantly increase the computational cost.

The main objective of the analysis was to determine the ejection time of the stemming material and to compare the results for both variants.

Total deformation for first variant present on the fig.3.13.

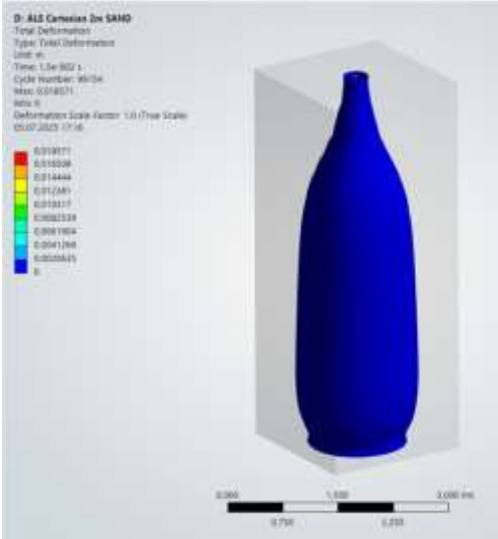

Figure 3.13. Element displacement (Deformation) at 15 ms with sand stemming

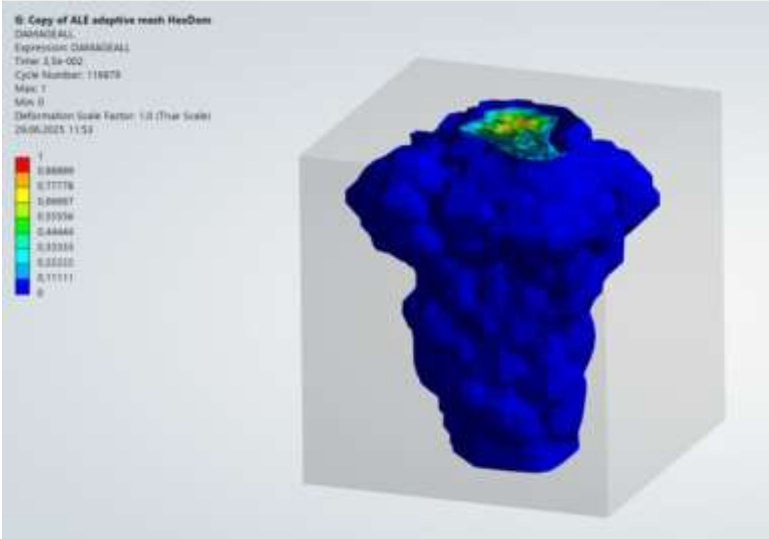

Figure 3.14. Element Damage at 35 ms with sand stemming

The simulation results of the model with foam stemming show a good illustration of how detonation stresses distribute over a given area. Compared to the case with sand stemming (see Figure 6a), the foam-based configuration has several advantages (see Figure 6b).

Pattern of Stress Distribution: The foam stemming model has a larger stress distribution area compared to sand stemming. The lines that show how much pressure is being distributed form an oval shape and have a distinct spreading pattern outward from the center of the borehole into the surrounding rock. This demonstrates the ability of the foam to retain explosive pressure for a longer period of time within the borehole which then transfers more energy in a lateral direction to surrounding rock.

The Uniformity of Distribution - Normally, explosive pressure exerts itself from the blast hole axis and forms a much wider symmetrical pattern. This is typical for releasing the explosive gases inside of the foam stemming very slowly and in a controlled manner.

The Stress Magnitude - The test results show that the maximum stress in the foam stemming case was found to be lower than in the sand case (3.41×10^{8} Pa vs. 5.49×10^{8} Pa). However, the area where the stresses were applied is much larger which could provide much better rock fragmentation.

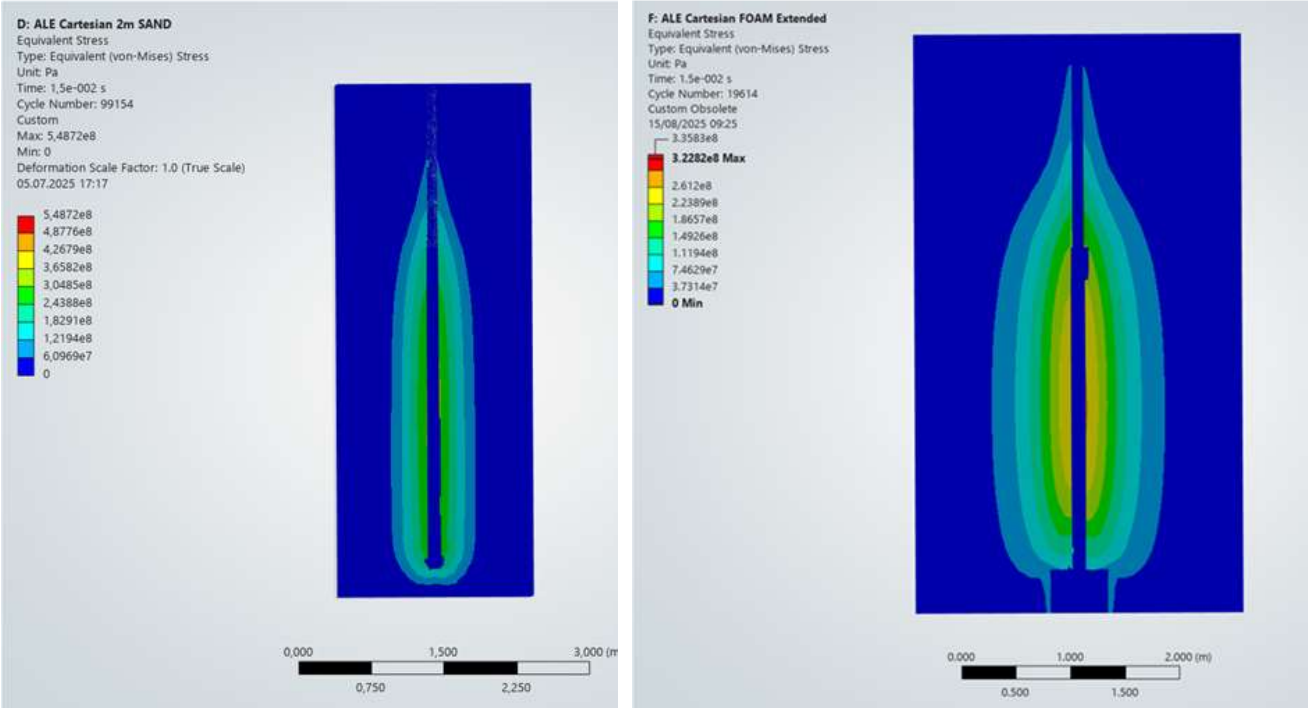

a) b)

Figure 6. (a) - Stress zones at 15 ms with sand stemming; (b) - Stress zones at 15 ms with foam stemming

The explosive impulse directs upward, which constitutes the movement of the stemming as depicted on the pressure-time graph.

The stress movement is mostly along the vertical direction where the blast is majorly inside the borehole column and there is very limited horizontal movement from the borehole to the surrounding rock.

The overall distribution of stress due to the use of foam stemming is more favorable, resulting in a more homogeneous energy transfer over a larger area of rock. This is likely to lead to a better performance of the blasting process with less loss of energy than the traditional sand stemming.

While ANSYS Explicit Dynamics demonstrates the simulation results in the form of equivalent (von Mises) stress, the equivalent (von Mises) stress (i.e., a scalar value) represents the amount of load applied to a given location in the material. The von Mises stress is calculated from the yield strength of a material and is used to determine whether the material at a particular location will yield or fracture under the loading conditions applied.

We calculate the von Mises stress according to the theory that ductile materials yield once the energy of distortion (or the energy of shape change) attains its critical level. This criterion has great popularity within engineering because it well correlates with experimental results for metals and other ductile materials.

When considering explosive simulations, where you are dealing with high strain rate materials under a wide variety of loads, von Mises stress can: a) provide you with a visualization of the areas of plastic deformation/failure, b) provide you with a basis for comparing the various magnitudes of stress within the different parts of the model and c) provide you with an indication of the behaviour of the material when loaded at high levels of stress.

Thus if you are viewing the results of "equivalent (von Mises) stress" in your simulations, you are looking at the material's state of stress simplified but it is a valid representation of the same, and thus offers a good way to evaluate the structural Integrity of the material under dynamic loading.

In the second version, with foam stemming, the stemming material began ejecting at approximately 1.4 milliseconds and completed ejecting by 11.5 milliseconds. the total duration of ejection was slightly greater than in the sand stemming case, which can be attributed to the lower density and different mechanical qualities of the foam compared to sand, altering the physical resistance provided by the material to detonation gas pressure.

A pressure-time plot was produced based on the simulation results shown in the attached figures in order to compare and graphically represent the pressure-time performance of the detonation products with varying stemming conditions fig. 3.16.

Pressure dynamics assessment. The initial peak pressure is indicated by rapid rise in pressure over the first several milliseconds in both curves showing the instantaneous nature of the detonation process. The maximum pressures result from sand stemming and foam stemming with a sand stemming peak near 2.4 to 2.5 x 10^9 Pa and a foam stemming peak near 2.3 x 10^9 Pa, Stabilization Phase: When the pressure reaches its maximum, it drops rapidly due to sand stemming because the heavier stemming material is ejected at a faster rate. As a result, the system experience less pressure retention time.

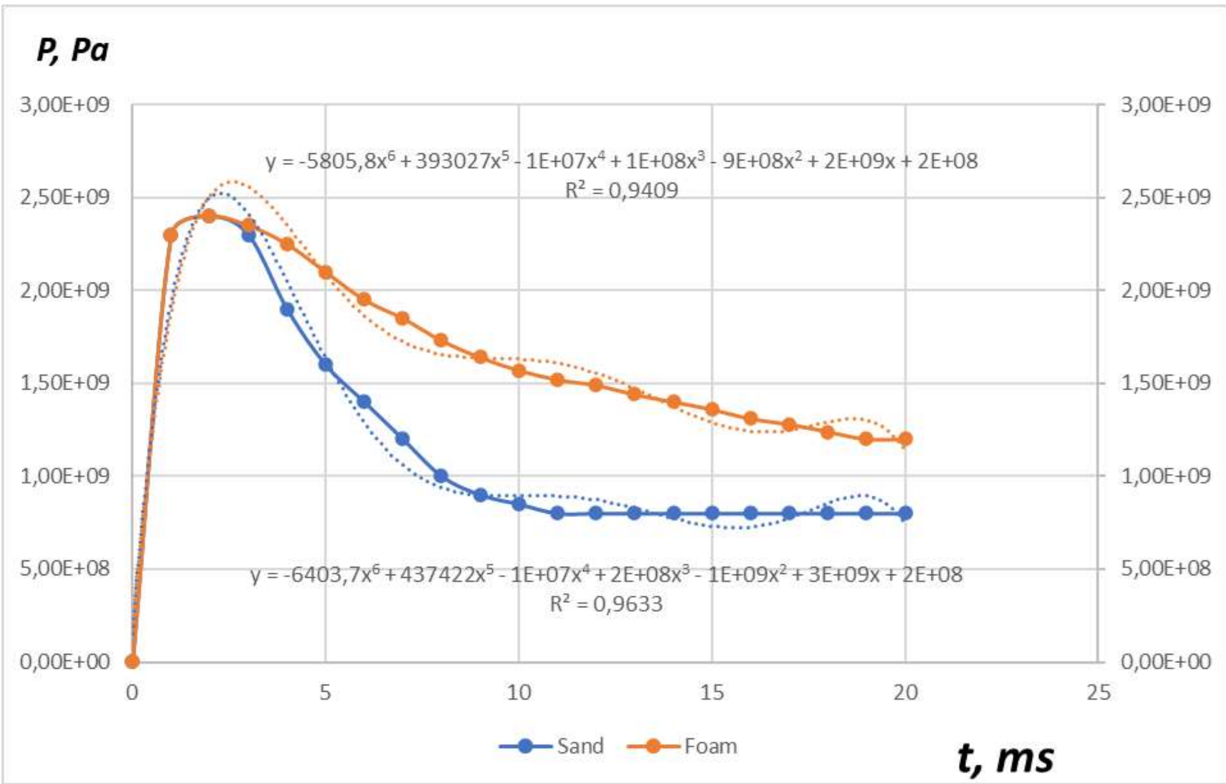

Figure 3.16 Change in the detonation products pressure of a borehole charge over time: 1 – with a sand stemming; 2 – with a foam stemming.

In the case of foam stemming, on the other hand, pressure drops at a slower rate; it stays at a much higher level for most of the simulation time. The slow rate at which gases are released and the slow rate at which the cavity is expanded.

Both curves decrease gradually in pressure after 5 to 6 milliseconds. The blue curve (foam stemming), remains greater than the red curve (sand stemming) until the end of 15 ms, which means that the pressure effect remains for much longer duration in the rock mass.

Interpretation of Physical Aspects: When foam is used to stem a detonation, it prolongs the retention of the pressure produced during detonation, and this prolonged retention of pressure also increases the ability to transfer impulse to surrounding rock, and therefore, the foam stemming can produce detonations that are controlled in how much energy is released; furthermore, the use of foam stemming reduces the possibility of premature ejection of the stemming and the resulting loss of energy through the atmosphere. Stemming the same material with sand creates a larger initial pressure spike, but the pressure decays and is removed much more quickly, producing much less stable pressure over the entire time.

Conclusion Recommendations: Based on the analysis discussed above, stemming with foam has a longer lasting and more consistent effect of the detonation pressure applied to the rocks. Thus, the resulting fragmentation of the rock can be much more efficient than stemming with sand, as the pressure-time graph in stemming with sand is characterized by lower peaks and a shorter time span of high pressure than that of stemming with foam.

The graph shows that for both types of stemming, the ANFO detonation produces a maximum detonation pressure during the initial few milliseconds of detonation, i.e. within a few milliseconds of the charge being detonated"

The pressure in sand stemming reaches it's peak almost immediately and also drops very quickly! This tells us the stemming material was ejected quickly, and as a result of that, the pressure was lost.

With the foam stemming, the pressure decreases more gradually after it's peak, which suggests that the detonation products are expanding more controlled because the system keeps the pressure for a longer period of time.

The pressure in the foam variant during the complete study time (to 20 ms) is always more than the sand variant. This may mean that the explosive energy is used more for breaking the rock.

Thus, the foam method produces a steady, longer-lasting pressure force applied to the rock, and that can help make blasting better and achieve higher quality.

According to the results of computer modeling, time-dependent relationships of the detonation products pressure were constructed for two stemming variants. Analysis of the graphs shows that in both cases the peak pressure is approximately the same and reaches a value of $P_{max} \approx 2.4 \cdot 10^9$ Pa. Accordingly, the maximum force exerted by the detonation products on the stemming is:

$F_{max} = A \cdot P_{max} = 9.5 \cdot 10^{-3} \cdot 2.4 \cdot 10^{9} = 2.28 \cdot 10^{7}$ N,

where A is the cross-sectional area of the borehole and is determined by the formula: $A = \frac{\pi d^2}{4} = \frac{\pi \cdot 0.11^2}{4} = 9.5 \cdot 10^{-3}$ m^2.

Based on the approximation of the pressure–time curves, the average pressure values were determined for the two stemming variants:

$\bar{P}_{sand} = 1.17 \cdot 10^{9}$ Pa, $\bar{P}_{foam} = 1.65 \cdot 10^{9}$ Pa.

The corresponding average forces exerted by the detonation products on the stemming are determined by the formula:

$$\bar{F} = A \cdot \bar{P} \qquad (3.6)$$

For sand stemming:

$\bar{F}_{sand} = A \cdot \bar{P}_{sand} = 9.5 \cdot 10^{-3} \cdot 1.17 \cdot 10^{9} = 11.12 \cdot 10^{6}$N.

For foam stemming:

$\bar{F}_{foam} = A \cdot \bar{P}_{foam} = 9.5 \cdot 10^{-3} \cdot 1.65 \cdot 10^{9} = 15.68 \cdot 10^{6}$N.

The relative increase in the average force in the case of using foam stemming is:

$$\delta_F = \frac{\bar{F}_{foam} - \bar{F}_{sand}}{\bar{F}_{sand}} \cdot 100\% = 41\%$$

The obtained result indicates that foam stemming provides a significantly longer retention of the high pressure of detonation products in the borehole.

The calculations demonstrated that the use of foam stemming increases the average force acting on the stemming by approximately 41% compared with sand stemming. This result confirms that foam stemming provides more effective confinement of detonation products within the borehole and significantly prolongs the period during which elevated pressure is maintained. In blasting practice, such a pressure retention effect is of fundamental importance, since it promotes a more complete transfer of explosive energy to the surrounding rock mass rather than allowing premature release of gases into the atmosphere.

Therefore, it can be concluded that the main advantage of foam stemming lies not in increasing the peak detonation pressure, but in extending the duration of its action.

Owing to the longer retention of detonation products in the borehole, foam stemming creates more favorable conditions for sustained loading of the borehole walls and for improved development of fracture processes in the rock mass. As a consequence, this contributes to more efficient fragmentation of gold-bearing quartzite, improves the utilization of explosive energy, and may enhance the overall effectiveness of drilling and blasting operations.

It is also possible to evaluate the work of the detonation products. To assess the energy effect of the detonation products acting along the stemming ejection path, the following relationship was used:

$$W = \bar{F} \cdot L_s = A \cdot \bar{P} \cdot L_s, \qquad (3.7)$$

where W — the work of the detonation products, J; L_s – the stemming length, m; $\bar{P}$ - the average pressure values, Pa; A - the cross-sectional area of the borehole, m^2.

For sand stemming:

$w_{sand} = A \cdot \bar{P}_{sand} \cdot L_s = 9.5 \cdot 10^{-3} \cdot 1.17 \cdot 10^9 \cdot 1.7 = 18.9 \cdot 10^6$J=18.9 MJ

For foam stemming:

$w_{foam} = A \cdot \bar{P}_{foam} \cdot L_s = 9.5 \cdot 10^{-3} \cdot 1.65 \cdot 10^9 \cdot 1.7 = 26.65 \cdot 10^6$ J=26.65 MJ

This indicates that when foam stemming is used, a significantly larger portion of the explosion energy can be directed toward rock mass fragmentation rather than being lost through the premature escape of gases from the borehole.

3.4 Conclusions to Chapter 3

In Chapter 3, a numerical model of explosive loading in a gold-bearing quartzite massif was developed and implemented using the ANSYS Explicit Dynamics software package. In order to accurately reproduce the physics of the process, a combined approach was applied: the Eulerian formulation for the ANFO explosive and its detonation products, and the Lagrangian formulation for the rock mass and the stemming. The RHT strength model was used for quartzite, the MO Granular model for sand stemming, and the Crushable Foam model for foam stemming, which made it possible to adequately account for the deformation, compaction, and failure characteristics of the materials under high-rate dynamic loading. The use of impedance boundary conditions minimized the influence of reflected waves and increased the reliability of the obtained results.

As a result of the modeling, it was established that the decisive factor affecting the efficiency of explosive rock breakage is not so much the peak pressure value as the duration of detonation product retention within the borehole. It was shown that, for both stemming variants, the maximum pressure of detonation products is close in magnitude; however, the subsequent pressure decay differs significantly. In the case of sand stemming, the pressure decreases much more rapidly, indicating earlier gas escape and the loss of part of the explosive energy. In contrast, in the case of foam stemming, a slower pressure decrease is observed, meaning a longer preservation of the force effect on the borehole walls and the surrounding rock mass.

An important scientific result of this chapter is the establishment of a polynomial relationship describing the variation of detonation product pressure over time for the two types of stemming. The obtained approximation made it possible to move from a qualitative analysis of the pressure curves to a quantitative assessment of the energy effect of the explosion. It was precisely on the basis of these polynomial relationships that the average pressure values, the average forces exerted by the detonation products on the stemming, and the work of the detonation products along the stemming ejection path were determined. Thus, the polynomial approximation served not only as a tool for describing the process dynamics, but also as the basis for further engineering calculations characterizing the efficiency of explosive energy utilization.

The quantitative assessment showed that the average pressure for foam stemming is higher than that for sand stemming, and accordingly, the average force exerted by the detonation products on the stemming is also greater. The calculations demonstrated that the average force in the case of foam stemming increases by approximately 41% compared with sand stemming. In addition, the evaluation of the work of the detonation products showed an increase in this parameter from 18.9 MJ for sand stemming to 26.65 MJ for foam stemming. This indicates that, when foam stemming is used, a significantly larger portion of the explosion energy is directed toward rock mass fragmentation rather than being lost due to the premature escape of gases from the borehole.

The analysis of the stress state of the rock mass showed that foam stemming forms a more favorable stress distribution pattern. While in the case of sand stemming the explosive effect is concentrated mainly along the borehole axis, the use of foam stemming results in a wider and more uniform radial propagation of the affected zone. Despite the somewhat lower maximum equivalent stress value, the effective area of stress distribution in the foam-stemming model is larger, which creates better conditions for uniform crack development and subsequent quartzite fragmentation.

Therefore, based on the results of the conducted modeling, it has been proven that foam stemming is more effective than traditional sand stemming in the open-pit mining of gold-bearing quartzites. Its main advantage lies not in increasing the peak pressure, but in prolonging the duration of detonation product action, improving blast energy retention within the borehole, and ensuring a more uniform transfer of energy into the rock mass. This contributes to improved fragmentation quality, a reduction in oversized fractions, and creates the preconditions for reducing the specific consumption of explosives under complex mining and geological conditions.

CHAPTER 4. JUSTIFICATION OF BOREHOLE CHARGE STEMMING PARAMETERS FOR IMPROVING THE QUALITY OF EXPLOSIVE ROCK FRAGMENTATION

The quality of drilling-and-blasting operations in open pits and underground workings is largely determined by the uniformity and size of rock fragmentation, the geometry of the muckpile (its width and height), and the condition of the bench floor. Taken together, these indicators directly affect the efficiency of subsequent excavation, loading, transportation, crushing, and sorting processes, and therefore influence equipment productivity and the cost of mining. The use of modern high-performance machinery and crushing-and-screening systems imposes increasingly stringent requirements on the quality of blast fragmentation, since non-uniform fragmentation leads to downtime, excessive energy consumption during crushing, increased wear of working components, and overloading of transport systems.

Despite the considerable attention paid to drilling-and-blasting issues, one of the key factors limiting productivity growth and cost reduction remains the non-uniform breakage of the rock mass, which is often accompanied by the formation of oversized fragments. The situation is especially complicated in the explosive breakage of strong rocks with borehole charges: typical problems include insufficient fragmentation efficiency in the upper part of the bench within the zone of uncontrolled breakage, as well as generally unsatisfactory control over the formation of the particle-size distribution throughout the bench height. This creates the need for a systematic approach that ensures coordinated intensification of explosive breakage in the upper, middle, and lower sections of the borehole charge, rather than merely local adjustment of individual parameters.

Under the conditions of the Tulallar open pit, where gold-bearing quartzites are mined, the requirements for fragmentation quality are particularly strict. The site uses relatively low benches with heights of 5–7 m, and under such geometric conditions the influence of borehole stemming on the blasting result increases significantly. It is the stemming that determines the efficiency of explosive energy utilization in the near-surface zone, affects the degree of fragmentation in the upper part of the bench, and influences the stability of fragmentation results as a whole. Accordingly, improving the design and parameters of stemming is one of the most effective tools for enhancing the quality of explosive fragmentation at small bench heights.

An additional factor underlying the relevance of the problem is the presence of oversize restrictions at the mine: the maximum fragment size must not exceed 60 cm, since exceeding this threshold leads to the need for additional breakage, increased costs and time losses, as well as a higher load on crushing equipment. Therefore, the technological task lies not only in the general improvement of the fragmentation degree, but also in the controlled limitation of the upper size class and the minimization of the oversize proportion in accordance with the requirements of further processing.

At the same time, the possibilities for regulating muckpile parameters and the nature of rock mass displacement solely through traditional initiation schemes are limited. Any borehole charge wiring scheme has a certain control range, in particular because of the relative symmetry of explosive load application to the rock mass, which reduces the effect of directed muckpile movement. In this regard, the use of diagonal blasting schemes appears to be a promising approach, since they provide longitudinal displacement of the blasted rock mass and contribute to more uniform muckpile formation without excessively high ridges. As one of the approaches to creating a controlled displacement vector, the placement of “locking” charges in the stemming zone with the direction of the main longitudinal displacement vector at an angle of 10–45° to the bench crest is considered. At the same time, many years of practice in blasting quartzite benches with borehole charges of asymmetric action using diagonal blasting schemes have not revealed any increased rock scatter, which confirms the expediency of this approach from the standpoint of safety and controllability.

4.1. Improving the efficiency of crushing a mineral through the use of modern explosives

Effective control of explosive breakage is impossible without prompt and reliable monitoring of fragmentation results. Rapid and accurate determination of the particle-size distribution of broken rock is critically important for optimizing drilling-and-blasting parameters and evaluating the efficiency of explosives, blasting schemes, and delay parameters. Traditional manual methods for measuring fragment sizes are often labor-intensive and subjective, limit the sample size, and complicate rapid decision-making under production conditions. In contrast, optical granulometry methods and photo-analysis systems make it possible to automate the assessment of particle-size distribution, eliminate subjectivity, avoid interrupting production processes, and obtain results within a short time. In addition, digital image analysis enables the processing of large datasets through expanded sampling and an increased number of photographic materials, which improves the representativeness of the assessment.

In this context, the use of WipFrag™ 4 software is a practical tool for controlling the quality of explosive fragmentation directly at the bench after drilling-and-blasting operations have been carried out. The use of an automated granulometry system based on digital image analysis makes it possible to obtain rapid and accurate results necessary for the prompt adjustment of blast parameters in order to reduce costs and decrease the share of oversized fragments. The results of photo-analysis can be used for monitoring and optimizing fragmentation, which reduces the risk of overloading transport systems and crushing equipment and increases the overall efficiency of the technological chain "drilling – blasting – excavation – transportation – crushing." [68, 69]

Thus, the relevance of the study stems from the need to ensure controlled fragmentation of gold-bearing quartzites at the Tulallar open pit with bench heights of 5–7 m, where the influence of stemming is especially significant and the requirements for limiting oversize to ≤ 70 cm are stringent. The combination of improved technological solutions in drilling-and-blasting operations, particularly stemming optimization and blasting schemes, with digital photo-analysis methods creates the basis for systematic control of the particle-size distribution of the blasted rock mass and for increasing the economic efficiency of explosive rock breakage.

Figure 4.1. Loading and Transportation of Fragmented Rock Mass at the Tulallar Gold Deposit

The management of the quality and parameters of explosive rock fragmentation in open-pit mines remains one of the most pressing practical problems in mining engineering. Despite the large number of scientific and applied studies, the issue of controlling the degree of fragmentation by adjusting drilling-and-blasting parameters still has no universal solution. This is explained by the fact that the fragmentation result is formed by the combined action of a number of factors: the physical and mechanical properties of the rocks and the structure of the rock mass, bench geometry, the design and arrangement of borehole charges, the initiation scheme, delay parameters, as well as unloading conditions and spatial constraints of the blast block. In practice, even with identical design parameters, differences in the yield of oversized fragments may occur due to the natural heterogeneity of rocks, changes in fracturing and layering, and local weak zones, which differently "govern" crack propagation and the pattern of rock failure.

The requirements for the quality of explosive fragmentation are determined primarily by the geometric parameters of mining, hauling, crushing, and screening equipment, as well as by the energy characteristics of the processes within quarry production flows. The geometry of excavator buckets, the dimensions of receiving hoppers, feeder parameters, the width of receiving openings, and crusher gap sizes determine the allowable fragment sizes that can be loaded, transported, and processed without obstruction. In the design of drilling-and-blasting operations, the calculated yield of oversized material should, as a rule, not exceed 5%, since even a slight increase in the proportion of coarse fragments leads to technological delays, overloading of crushing equipment, and increased costs for secondary crushing or repeated blasting. Under production conditions, such consequences are manifested in the form of downtime of the excavation-and-haulage system and reduced stability of crushing-and-screening lines.

At the same time, energy consumption depends not only on the proportion of oversized material, but also on the average fragment size in the blasted rock mass: an excessively large average size increases the load on crushers, whereas an overly fine size may result in mineral losses, dust generation, and reduced efficiency of individual operations. Therefore, fragmentation quality must be coordinated with the type of transport and crushers used; both the average fragment size and the upper size class must be treated as controlled parameters for a specific technological chain.

The efficiency of drilling-and-blasting operations is the subject of numerous studies analyzing the influence of various factors on rock fragmentation, including the type of explosive, charge design, initiation schemes and methods, the use of in-hole delays, and the parameters of borehole charges and their arrangement within the blast block [69]. To ensure the technological compatibility of blasting results with subsequent processes during mass blasts, the following requirements must be met: (1) achieving high-quality rock fragmentation; (2) preserving the design level of the bench floor; (3) forming a compact muckpile of fragmented rock; and (4) minimizing seismic impact, air blast, and flyrock. In real production conditions, these requirements are often interrelated and partially conflicting; for example, increasing the intensity of rock breakage may affect flyrock. Therefore, they require a balanced engineering approach.

Scientific research aimed at improving the process of explosive fragmentation is developing along several directions. One of the most effective approaches in surface mining is the control of blast impulse parameters by modifying charge design [3]. In particular, studies are being carried out to prolong the action of the explosion on the rock mass through improved charge configurations, the use of air decks, combined charges, and optimization of initiation parameters. A separate area of interest is the improvement of the composition and design of stemming, since stemming significantly affects the duration of explosive loading and, accordingly, the parameters of the stress field and the nature of material failure. In addition, the shape and dimensions of the charge cross-section influence the parameters of stress waves, as well as the intensity of crack formation in the near-surface zone of the bench, where the instability of fragmentation results is most often observed.

Multi-row short-delay blasting generates stress waves in the rock mass that propagate in all directions. In the time interval between the explosions of adjacent groups of charges, a system of cracks is formed in the rock under the action of stress waves, while an additional mechanism for increasing fragmentation efficiency is the collision of rock masses during explosive breakage. This effect can be enhanced by the use of appropriate blasting schemes and by organizing favorable unloading conditions. The adjustment of spacing between boreholes also has a significant influence, as it can improve the technical and economic performance of drilling-and-blasting operations by balancing drilling volumes and fragmentation quality.

During the detonation of an elongated charge in a borehole, complex gas-dynamic processes take place. The methods for calculating drilling-and-blasting parameters that are still in use today and form the basis of many software products were developed in the last century. Such methods often lack sufficiently rigorous theoretical substantiation and do not fully take into account the real properties of rocks and the heterogeneity of the rock mass. As a result, the calculated parameters are approximate and require refinement based on the results of experimental industrial blasts, particularly on the basis of actual data on oversized yield and particle-size distribution. In practice, this means the need for constant “feedback” between the design blast parameters and the actual fragmentation result at the bench.

Drilling-and-blasting operations significantly affect technological processes, from the initial separation of rock from the massif to subsequent stages culminating in the production of marketable output. During the mining of gold-bearing quartzites with complex morphology and heterogeneous layering, there is an increased risk of forming significant volumes of coarse fragments. This leads to additional costs for repeated blasting or secondary crushing of insufficiently fragmented rock masses, as well as to the risk of technological bottlenecks in the loading and hauling zones.

Figure 4.2. Examples of the formation of oversized fragments after mass blasting that require additional secondary breakage: (a) oversized boulders in the muck pile on the bench; (b) large oversized fragments in the muck pile (view under actual quarry operating conditions).

The given examples (Fig. 4.2) illustrate the practical nature of the problem of the “upper size class,” where some fragments exceed the allowable dimensions and generate additional costs for bringing the material to the required condition.

To obtain an objective forecast of the particle-size distribution, it is necessary to accumulate statistical data based on blast results, while reducing the yield of oversized fragments remains one of the key tasks solved through the optimization of drilling-and-blasting parameters. In this case, the largest proportion of oversized material is usually formed along the separation line of the design block and within the zone of the first row of boreholes, where the conditions of unloading and breakage differ from those in the central part of the block due to the presence of a free face, asymmetry of the stress–strain state, and a different nature of shear and tensile failure.

Works [68] present modern technical solutions and software products aimed at minimizing the yield of oversized fragments and improving borehole placement with due regard to the structural heterogeneity of the blasted rock mass. In particular, a comprehensive approach to improving the borehole drilling pattern has been proposed based on the use of a fracture intensity index obtained by means of digital solutions and specialized systems. Such an approach increases the controllability of fragmentation results, makes it possible to move from a “uniform” drilling grid to a zonal one, and ensures a reduction in the proportion of off-specification fractions, as demonstrated, in particular, for the Tulallar deposit.

Under the conditions of the studied deposit, experimental work was carried out to improve drilling-and-blasting technology by replacing traditional sand stemming with foam stemming. The foam was used with an increased chalk content in order to enhance the effect of gas and dust suppression (details are provided in Chapter 2). In addition to its environmental effect, namely dust suppression, foam stemming is considered a technological factor that may influence the duration of explosive loading in the collar zone and the quality of breakage in the upper part of the bench. Figure 4.3 shows the practical stage of preparing and supplying the mixture, as well as organizing the stemming process, which is important for the reproducibility of the experiments and for the correct comparison of the results.

Figure 4.3 Preparation and Application of Foam Stemming under Production Conditions (Foam with Increased Chalk Content) as an Alternative to Sand Stemming

As a result, two comparable test areas were formed for which the particle-size distribution was evaluated and the efficiency of sand stemming and foam stemming was compared. At the same time, it was found that fragmentation analysis using simple methods such as a tape measure and visual assessment is of low efficiency, since it requires considerable time, is highly labor-intensive, and depends on subjective factors, including the selection of fragments for measurement, visual estimation of the average size, and the limited sample size. Therefore, for the quantitative evaluation of fragmentation, a reference scale element was selected, after which digital processing of the photographic materials was carried out using specialized software. Such an approach ensures the reproducibility of the results and makes it possible to obtain statistically justified estimates of the particle-size distribution without interrupting the production process. The scale element is necessary for the correct calibration of the image and the subsequent determination of fragment sizes during digital processing (Fig. 4.5).

Figure 4.5. Field assessment of the particle-size distribution of blasted rock mass using a reference scale element (measuring tape) for subsequent digital photo analysis in specialized software

The evaluation of blast fragmentation is one of the key stages in assessing the efficiency of drilling-and-blasting operations, because the size distribution of broken rock directly affects loading, hauling, primary crushing, grinding performance, equipment wear, and the overall economics of mining and quarrying. In practical terms, fragmentation quality determines whether explosive energy has been converted efficiently into rock breakage or has been partially lost through excessive fines, oversized boulders, or poor size uniformity. For this reason, modern mines increasingly rely on quantitative fragmentation assessment methods rather than subjective visual inspection of muckpiles. WipFrag is one of the most established systems developed for this purpose and is widely used as a photo-based fragmentation analysis tool in mining, aggregates, and research applications.

WipFrag is an image-based granulometry system that uses photographs or digital images of blasted rock to estimate particle size distribution (PSD). In essence, the software transforms a visual image of a muckpile, stockpile, bench face, or haul truck load into numerical fragmentation data. According to WipWare, WipFrag is designed to measure particle size distribution rapidly from digital images collected in the field, underground, or at a desktop workstation, and it is intended to replace subjective estimates with repeatable, data-driven measurement. Earlier technical literature describing the system explains that WipFrag identifies visible particle boundaries, converts the delineated fragments into a size-distribution output, and generates charts that can be used for fragmentation evaluation and blast optimization. This makes the method especially valuable where rapid operational feedback is required [70].

From a methodological standpoint, the use of WipFrag typically begins with image acquisition. This stage is crucial, because the reliability of the final PSD results depends strongly on the quality and representativeness of the input photographs. Official WipWare guidance emphasizes several requirements: correct scaling, adequate lighting, sufficient image resolution, proper camera angle and distance, and the use of multiple images to capture the full variability of the rock pile. Images with excessive shadows, poor contrast, or insufficient coverage may distort fragment delineation and reduce analysis quality. In practical studies, several photographs are often taken at different stages of loading or from multiple zones of the muckpile in order to reduce sampling bias and improve representativeness. In this respect, WipFrag should not be understood merely as software, but as part of a structured measurement procedure in which image capture discipline is as important as the subsequent digital processing.

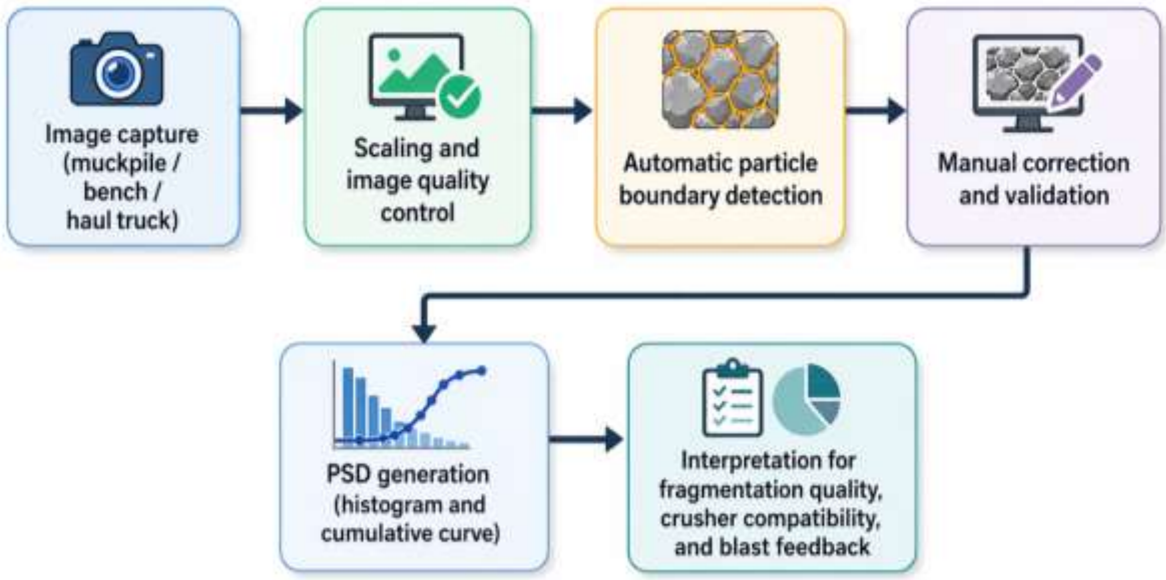

Figure 4.6 Typical WipFrag-based fragmentation assessment work

On Figure 4.6 illustrate the standard sequence of image capture, scaling, delineation, validation, PSD generation, and engineering interpretation. The workflow shown in the figure reflects the logic commonly used in WipFrag-based blast assessment: first, representative images are collected; second, the images are scaled and checked; third, particle boundaries are detected automatically; fourth, the operator corrects segmentation errors where needed; and finally, the software produces fragmentation outputs that can be interpreted in relation to crusher requirements, blast objectives, and downstream plant performance. This staged approach is important because fragmentation analysis is not limited to obtaining a graph; it is an integrated decision-support process that links field observation with blast evaluation and process control.

Once the images have been loaded into the system, WipFrag applies delineation algorithms to identify individual fragments and generate a polygonal network around visible block boundaries. The resulting segmented image is then converted into size data and presented in graphical and tabular form. Published descriptions of WipFrag note that the software can process images captured from camcorders, fixed cameras, photographs, and digital files, while modern WipWare materials describe advanced segmentation, scaling tools, and reporting functions for comparing results across blasts, shifts, and sites. As a result, the system is useful not only for one-time studies, but also for continuous monitoring and historical trend analysis. In mining operations, this capability is particularly important because blast quality should ideally be assessed as part of an ongoing improvement cycle rather than as an isolated event.

Figure 4.7. Application of the software at the quarry site using a tablet device.

WipFrag's main analysis results include the particle size distribution (Fig. 4.8). The result is typically displayed as a histogram as well as a cumulative passing curve. On the histogram one can determine which size range of the material accounts for a particular volume of blasted rock; on the cumulative curve, one can observe what percent of material is smaller than established threshold sizes (P50, P80, etc.) according to WipWare's Technical Guidance. These two types of output are instrumental in assessing fragmentation quality; they can be used by engineers to discern fine-dominated or coarse-dominated distributions from balanced fragmentation states. In the practical assessment process, a distribution dominated by fines likely results from over-fragmentation and the application of excessive energy or excessive energy concentration; conversely, a distribution dominated by very large fragments likely indicates poor blast performance and thus will create challenges for the loading and primary crushing process [54].

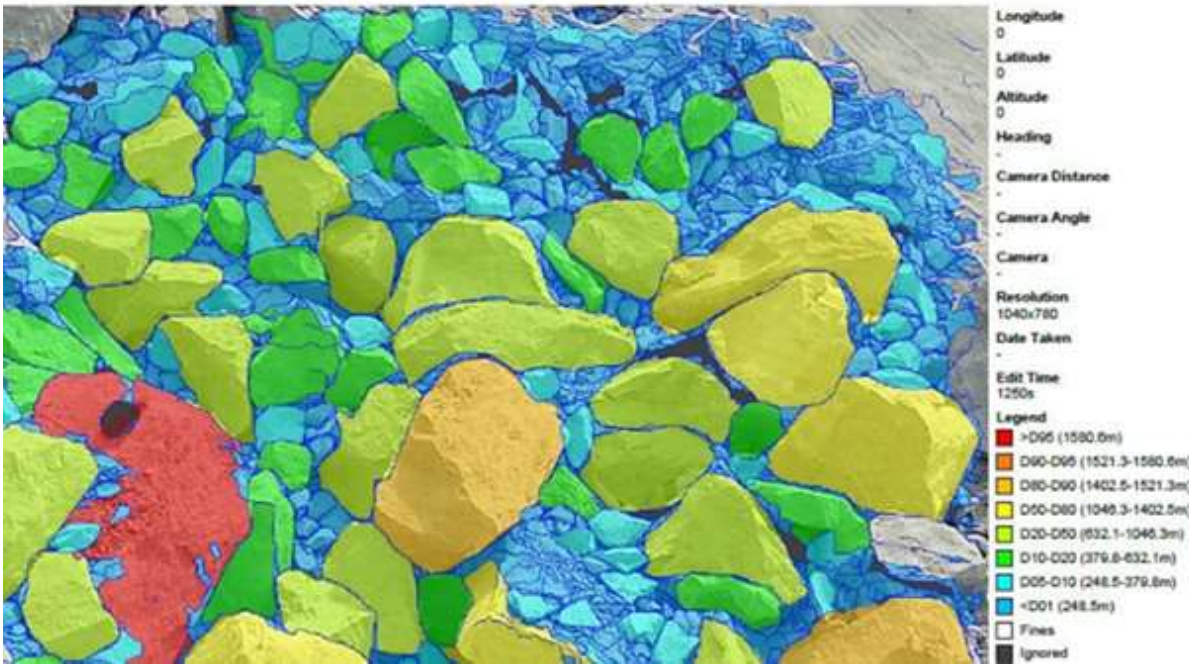

Figure 4.8. The main output of WipFrag analysis is the particle size distribution.

One of the major advantages of WipFrag is speed. Traditional sieve analysis is accurate but labor-intensive, time-consuming, and often impractical for routine production-scale blast assessment. Image analysis, by contrast, provides rapid results at relatively low cost and can be repeated frequently without interrupting production. Earlier literature on WipFrag describes it as a system that enables operations to measure fragmented particle sizes quickly, accurately, and economically, supporting blast optimization and process improvement. A commonly cited validation result in that literature reports that, in one comparison with other image-based systems, WipFrag was the closest to sieved results, and after calibration its D50 value came within 2% of sieving for the tested case. This does not eliminate the need for engineering judgment, but it does show why WipFrag became a widely accepted industrial tool.

Another important benefit of WipFrag is that it supports comparative blast evaluation. Because the software produces standardized PSD outputs, it can be used to compare the effects of different explosive charges, initiation schemes, burden and spacing combinations, or stemming materials. In published case studies and technical usage examples, WipFrag has been applied to assess blast performance, compare fragmentation results with empirical models such as Kuz-Ram, and evaluate whether blasted rock remains within acceptable size limits for a crusher. This comparative function is especially relevant in scientific research, where the aim is not only to describe fragmentation, but also to identify which blasting variables most strongly influence the final size distribution of broken rock. In such studies, WipFrag serves as a bridge between field blasting practice and quantitative engineering analysis.

At the same time, WipFrag has methodological limitations that must be acknowledged in academic work. The software evaluates visible surface fragments from a two-dimensional image, whereas the actual rock mass is a three-dimensional fragmented system. This means that image overlap, hidden fines, perspective distortion, poor illumination, and incorrect scaling may affect the results. In addition, automatic segmentation is not always perfect and may require manual correction, especially in complex muckpile images where boundaries between fragments are unclear. For this reason, careful sampling strategy, multiple photographs, and critical review of the delineation network remain essential. WipFrag should therefore be presented not as an infallible substitute for all direct measurements, but as a highly practical and sufficiently robust method for rapid blast fragmentation assessment under real operating conditions.

From the standpoint of explosive rock fragmentation quality assessment, the scientific and practical value of WipFrag lies in its ability to transform field images into objective, reproducible, and operationally useful data. It enables the evaluation of fragmentation not only through average fragment size, but also through distribution shape, percentage passing, coarse fraction content, and compatibility with downstream processing requirements. In this way, the system supports more rational blast design adjustment, improved control of oversized material, better prediction of crusher feed behavior, and more effective use of explosive energy. Consequently, WipFrag can be regarded as an effective modern tool for evaluating the quality of explosive rock fragmentation and for supporting the optimization of drilling-and-blasting operations in mining and quarrying practice.

4.2. Using the Wipfrag image analysis system to evaluate the quality of explosive rock fragmentation

During the experimental blasts, four key parameters were identified and taken into account: natural fracturing, borehole spacing, the delay interval between rows, and the type of stemming (foam instead of sand). The combination of these parameters was selected on the basis of previous studies [54]. As a result, areas with different degrees of blasted rock fragmentation were obtained, which confirms the expediency of the integrated approach “geology/rock mass structure – drilling pattern – initiation parameters – stemming design – оперативний контроль фракційності,” as shown in Figs. 4.9 and 4.10.

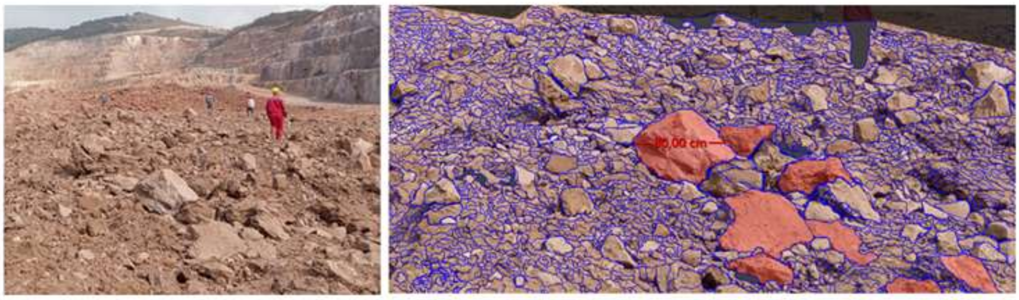

a) b)

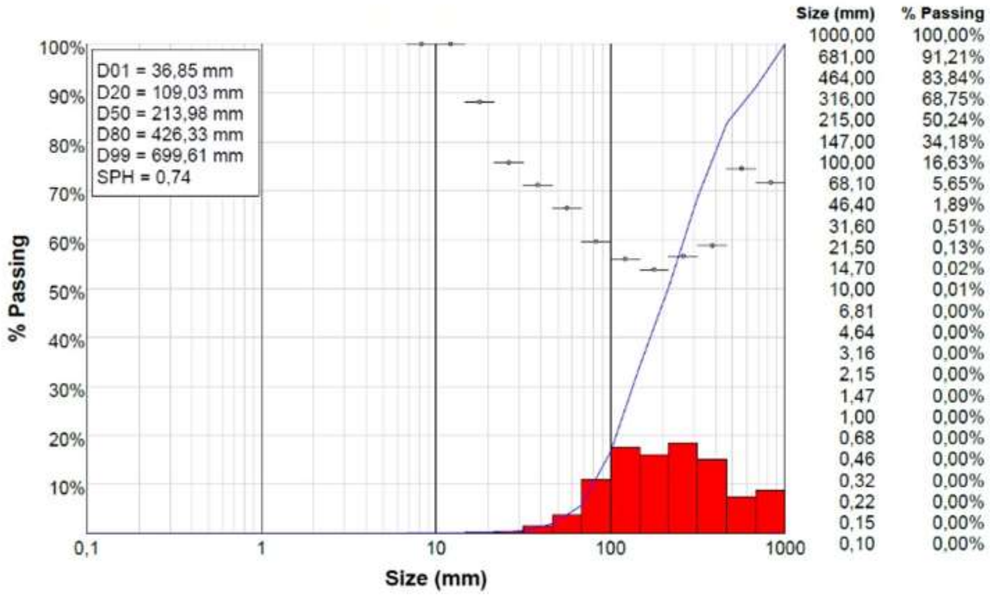

c)

Figure 4.9. a - Photograph of the site; b - Image processing according to the selected standard; c - Analysis of the granulometric composition distribution of the blasted rock mass (9%).

a)

b)

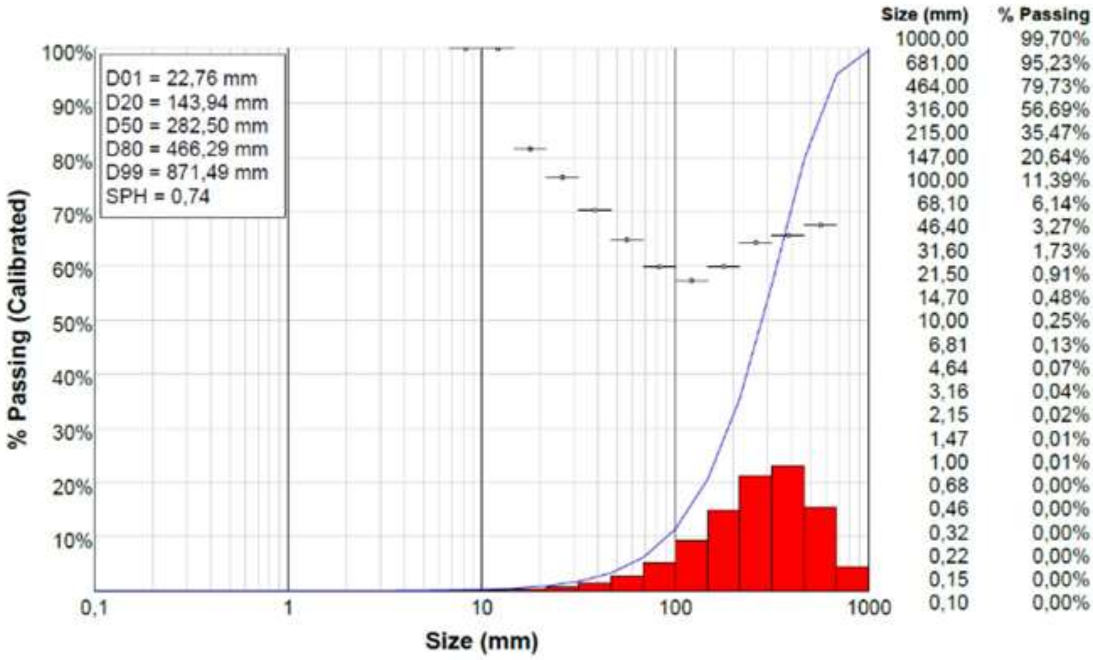

c)

Figure 4.10. a - Photograph of the site; b - Image processing according to the selected standard; c - Analysis of the granulometric composition distribution of the blasted rock mass (5%)

Based on the data obtained from the photo analysis, the particle-size distribution of the blasted rock mass was constructed. The following parameters were recorded: the average fragment size in the blasted rock mass, the percentage of oversized fractions, and the uniformity index of the fragmentation distribution. The limiting size of oversized material was determined in accordance with the technical characteristics of the crushing equipment. In this case, fractions larger than 60 mm were classified as oversized.

The collected data on the particle-size distribution before and after the implementation of the proposed solutions involving the use of a new stemming material—foam, compared with sand stemming—are presented in the graphs in Fig. 4.9 and Fig. 4.10.

Over the past three decades, significant progress has been achieved in the development of new blasting technologies. These advances include increasingly sophisticated computer models for blast design and performance prediction. Rock fragmentation is regarded as the most important aspect of production blasting, since it directly affects drilling and blasting costs, as well as the economics of subsequent operations such as loading, hauling, and crushing. Unfortunately, fragmentation depends on many variables, including rock mass properties, site geological conditions, fracturing parameters, and the parameters of blast-hole configuration and charge filling; therefore, at present there is no comprehensive theoretical solution for its accurate prediction.

The development of technical solutions aimed at improving the understanding of rock blast breakage mechanisms, advancing drilling equipment, and enhancing explosives, initiation systems, and modern stemming materials is ongoing. The use of modern fragmentation analysis methods under field conditions provides rapid, accurate, and cost-effective measurement of fragment sizes after blasting. Advanced granulometric analysis methods using the WipFrag software package are a powerful tool for optimizing quarry blasting operations and minimizing costs.

4.3. Conclusions to chapter 4

Chapter 4 summarizes the theoretical and applied aspects of controlling the quality of explosive rock fragmentation under open-pit mining conditions and substantiates the expediency of applying modern approaches to regulating the particle-size distribution of blasted rock mass. It is shown that fragmentation quality is determined by the combined action of geological and structural factors, including the physical and mechanical properties of rocks, fracturing, blockiness, and layering of the rock mass, as well as bench geometry, drilling parameters, charge design, initiation schemes, and unloading conditions. It has been established that, due to the multifactorial nature of the process, universal theoretical prediction of fragmentation without taking into account the actual heterogeneity of the rock mass and without verification based on the results of industrial or field blasts is limited. This confirms the need to combine design-based approaches with systematic monitoring of the actual results of drilling-and-blasting operations.

It has been confirmed that the requirements for the quality of explosive fragmentation are determined primarily by the parameters of mining, haulage, and crushing-and-screening equipment, while the main evaluation criteria are the yield of oversized fractions, the average fragment size, and the uniformity of the particle-size distribution. It has been established that exceeding the permissible fragment size or increasing the proportion of oversized material directly leads to higher costs for secondary crushing or repeated blasting, as well as to reduced efficiency of related processes such as loading, transportation, and crushing. In this regard, the need to accumulate statistical data from blasting results and to use these data for the prompt adjustment of drilling-and-blasting parameters at a specific deposit has been substantiated.

The main directions for improving the efficiency of explosive fragmentation have been systematized, among which the most significant are the control of blast impulse parameters by changing charge design, optimization of initiation schemes and delay intervals, adjustment of borehole spacing, and improvement of technological elements that affect the duration and nature of explosive loading. It is shown that the zones most problematic in terms of oversized fragment formation are the first row of boreholes and the block separation line, where the conditions of breakage and unloading differ significantly from those in the central part of the rock mass. The importance of stemming as a tool for controlling explosive loading in the collar zone of the borehole is also substantiated separately, since the upper part of the bench is often characterized by uncontrolled breakage and unstable fragmentation results.

Within the framework of this chapter, field studies were carried out on the use of foam stemming as an alternative to traditional sand stemming during the fragmentation of gold-bearing quartzites. A comparison of the two technological variants showed that the use of foam stemming provides a noticeable improvement in fragmentation performance. In particular, it was established that when foam stemming was used, the yield of oversized fractions decreased to 5%, whereas when conventional sand stemming was used, this indicator was 9%. Thus, the application of foam stemming made it possible to reduce the percentage yield of oversized material by 4 percentage points, which confirms its higher technological efficiency in comparison with traditional sand stemming. This result is of important practical significance, since it indicates a reduced need for secondary crushing, a lower load on crushing equipment, and improved stability of the entire technological chain.

To ensure the objectivity of the comparison, the chapter applied a methodology of digital photo analysis of particle-size distribution using specialized software. It has been substantiated that, unlike traditional methods such as visual estimation or manual measurements, digital photo analysis makes it possible to promptly obtain quantitative fragmentation characteristics, including average fragment size, the proportion of oversized material, and distribution uniformity indicators, as well as to expand the sample by analyzing multiple photographs. Importantly, such a methodology is suitable for field conditions, does not require interruption of the production process, and can be used to form a statistical database for the further optimization of drilling-and-blasting parameters.

Summarizing the results of the chapter, it has been established that improving the efficiency of explosive fragmentation and reducing the yield of oversized fractions should be achieved on the basis of an integrated approach that includes consideration of the structural heterogeneity of the rock mass when designing the drilling pattern; optimization of blasting parameters taking into account unloading conditions; improvement of stemming design as a means of controlling explosive loading in the upper part of the bench; and the introduction of operational digital fragmentation control using photo analysis. The practical significance of the chapter lies in the fact that the combination of field testing of technological solutions with digital granulometric assessment creates the basis for improving the stability of blasting results and reducing the costs of secondary crushing and repeated blasting. The scientific value of the obtained results lies in substantiating the transition from purely design-based schemes to a "calculation – experiment – digital verification" model, within which foam stemming has been confirmed as an effective means of reducing the yield of oversized material and increasing the controllability of explosive breakage of gold-bearing quartzites.

CONCLUSIONS

The dissertation is a completed scientific research work that provides a theoretical substantiation of the use of geographic information systems for optimizing the directions of mining operations under the conditions of gold-bearing deposits. The study also addresses an important scientific and practical problem related to the improvement of explosive fragmentation technology for gold-bearing quartzites through the selection of an effective stemming material aimed at enhancing fragmentation quality.

The main scientific and practical results of the dissertation are as follows:

1. A methodology for analyzing the Tulallar gold deposit was developed through the integration of geodetic monitoring data with GIS technologies. A digital geospatial model was created, making it possible to assess the spatial distribution of gold concentrations and substantiate promising directions for the further development of mining operations.

2. A mathematical model was developed to describe the influence of stemming material on the duration of detonation product confinement within the borehole. Polynomial relationships were obtained to characterize the time-dependent variation in detonation product pressure for borehole charges using sand and foam stemming.

3It was agreed upon that if to the foam stemming was added 5% chalk the gas neutralisation characteristics and the dust binding ability of thefoam stemming would also be improved, while at the same time, the porosity of the foam stemming would be reduced. By comparison to the conventional sand stemming, the use of the foam stemming reduced the highest concentrations of NO2 nearly by approximately 45%; CO by approximately 65%; and dust concentration by approximately 63%, hence improving the environmental safety of blasting.

4. The methodology for assessing the particle-size distribution of blasted rock mass over large rock volumes was improved through the application of digital photo analysis.

This approach makes it possible to quantitatively determine, under field conditions, the average fragment size, the yield of oversized fractions, and the uniformity of particle-size distribution.

5. The studies carried out in the dissertation confirm the effectiveness of foam stemming. Its application at the Tulallar deposit made it possible to reduce the yield of oversized material from 9% to 5%, demonstrating its practical efficiency in improving fragmentation quality, reducing the need for secondary crushing, and increasing the overall effectiveness of open-pit blasting operations.

6. The obtained results confirm the scientific and practical feasibility of using foam stemming in the blasting of gold-bearing quartzites. The proposed technological and methodological solutions can be applied to improve the controllability of explosive rock fragmentation, enhance operational efficiency, and reduce the environmental impact of blasting operations.

REFERENCES

1. Zuievska N., Hrebeniuk T., Zuievskyi Y. Application of GIS for analysis of environmental aspects of mineral deposits. Coll. res. pap. nat. min. univ. 2023. Vol. 75. P. 7–17. DOI: 10.33271/crpnmu/75.007.
2. Zuievska N., Kryvoruchko A., Shaidetska L., Shukurlu E. The Use of GIS to Improve the Parameters of Gold-Bearing Quartzite Extraction Technology. Geomining. Studies in Systems, Decision and Control. Cham : Springer, 2024. Vol. 224. P. 135–146. DOI: 10.1007/978-3-031-70725-4_10.
3. Takodjou Wambo J. D. T. Geostatistical and GIS analysis of the spatial variability of alluvial gold content in Eastern Cameroon: Implications for primary gold deposit exploration. Journal of African Earth Sciences. 2018. Vol. 142. P. 138–150. DOI: 10.1016/j.jafrearsci.2018.02.012.
4. Takodjou Wambo J. D., Ganno S., Djonthu L. Y. S. et al. Geostatistical and GIS analysis of the spatial variability of alluvial gold content in Ngoura-Colomines area, Eastern Cameroon: Implications for the exploration of primary gold deposit. Journal of African Earth Sciences. 2018. Vol. 142. P. 138–157. DOI: 10.1016/j.jafrearsci.2018.03.015.
5. Yang L., Deng J., Wang Z. et al. Relationships between gold and pyrite at the Xincheng gold deposit, Jiaodong Peninsula, China: Implications for gold source and deposition in a brittle epizonal environment. Economic Geology. 2016. Vol. 111, no. 1. P. 105–126. DOI: 10.2113/econgeo.111.1.105.
6. Jin X., Wang G., Tang P. et al. 3D geological modelling and uncertainty analysis for 3D targeting in Shanggong gold deposit. Journal of Geochemical Exploration. 2020. Vol. 210. Article 106442. DOI: 10.1016/j.gexplo.2020.106442.
7. Rahimi H., Asghari O., Hajizadeh F., Meysami F. Investigation of linear and non-linear estimation methods in highly-skewed gold distribution: A case from Qolqoleh deposit, Iran. Journal of Mining & Environment. 2018. Vol. 9, no. 4. P. 967–979. DOI: 10.22044/jme.2018.7023.1544.

8. Chen G., Zhankun L., Chen G. et al. Deep gold prospectivity modeling in the Jiaojia gold belt using kriging and block modeling. Frontiers in Earth Science. 2024. Vol. 12. DOI: 10.3389/feart.2024.1308426.
9. Lindi O. T., Aladejare A. E., Ozoji T. M. Uncertainty quantification in mineral resource estimation. Natural Resources Research. 2024. Vol. 33. P. 2503–2526. DOI: 10.1007/s11053-024-10394-6.
10. Samal A. R., Fifarek R. H. Modeling spatial anisotropy of gold concentration data using GIS-based interpolated maps and variogram analysis. Journal of Earth System Science. 2011. Vol. 120. P. 583–593. DOI: 10.1007/s12040-011-0091-4.
11. Pradhan B. A deep learning and GIS-based framework for gold mineralization potential mapping in India. Remote Sensing. 2022. Vol. 14, no. 18. Article 4486. DOI: 10.3390/rs14184486.
12. Liu Z., Guo Z., Wang J. et al. Three-Dimensional Mineral Prospectivity Modeling with the Integration of Ore-forming Simulation Data. Applied Sciences. 2023. Vol. 13, no. 18. Article 10277. DOI: 10.3390/app131810277.
13. Karl S. M., Kreiner D. C., Case G. N. D. et al. GIS-based identification of areas with resource potential for lode gold in Alaska. U.S. Geological Survey Open-File Report. 2021. No. 2021-1041. DOI: 10.3133/ofr20211041.
14. Xishihui D., Kefa Z., Yao C., Jinlin W., Shuguang Z. Mapping Mineral Prospectivity Using a Hybrid Genetic Algorithm–Support Vector Machine (GA–SVM) Model. ISPRS International Journal of Geo-Information. 2021. Vol. 10, no. 11. Article 766. DOI: 10.3390/ijgi10110766.
15. McKinley J. M., Zuo R. Geostatistical modelling of ore bodies in mineral exploration. Ore Geology Reviews. 2017. Vol. 86. P. 548–560. DOI: 10.1016/j.oregeorev.2016.11.015.
16. Mamuse A., Beresford S., Porwal A., Kreuzer O. Assessment of undiscovered nickel sulphide resources, Kalgoorlie Terrane, Western Australia: Part 1. Deposit and endowment density models. Ore Geology Reviews. 2010. Vol. 37. P. 141–157. DOI: 10.1016/j.oregeorev.2010.02.004.

17. Zhang X., Zhao X. 3D modeling of ore bodies using borehole data. Journal of Earth Science. 2019. Vol. 30, no. 3. P. 541–550. DOI: 10.1007/s12583-019-1189-y.
18. Huang D., Zuo R., Wang J. Geochemical anomaly identification and uncertainty quantification using Bayesian convolutional neural networks. Applied Geochemistry. 2022. Vol. 146. Article 105450. DOI: 10.1016/j.apgeochem.2022.105450.
19. Sobolevskyi R., Zuievska N., Korobiichuk V., Tolkach O., Kotenko V. Cluster analysis of fracturing in the deposits of decorative stone for the optimization of the process of quality control of block raw material. Eastern-European Journal of Enterprise Technologies. 2016. Vol. 5, no. 3 (83). P. 21–29. DOI: 10.15587/1729-4061.2016.80652.
20. Nykänen V., Ojala V. J. Spatial Analysis Techniques as Successful Mineral-Potential Mapping Tools for Orogenic Gold Deposits in the Northern Fennoscandian Shield. Natural Resources Research. 2007. Vol. 16. P. 85–92. DOI: 10.1007/s11053-007-9046-5.
21. Zuievska N., Kosenko T., Shukurlu E., Hajiyev P., Shukurlu N. Integration of GIS and geodetic monitoring for gold deposit modeling and mine planning. Geo-Technical Mechanics. 2025. No. 173. P. 175–185. DOI: 10.15407/geotm2025.173.175.
22. Kulawiak M. Client-side versus server-side geographic data processing performance comparison: Data and code. Data in Brief. 2019. Vol. 26. Article 104507. DOI: 10.1016/j.dib.2019.104507.
23. Worboys M. F. GIS: A Computing Perspective. 2nd ed. Boca Raton : CRC Press, 2020. 448 p. DOI: 10.1201/9781315374863.
24. Breunig M., Bradley P. E., Jahn M. et al. Geospatial Data Management Research: Progress and Future Directions. ISPRS International Journal of Geo-Information. 2020. Vol. 9, no. 2. Article 95. DOI: 10.3390/ijgi9020095.
25. Quliyev E. E., İsayev E. N. Tülallar qizil yatağinin perspektivliliyi və onun yaxin cinahlarinda potensial minerallaşma zonalarina dair qisa icmal. ANAS Transactions, Earth Sciences. 2022. No. 2. P. 88–97. (in Azerbaijani).

26. Zuievska N., Kosenko T., Shukurlu E., Korobiichuk V. Estimation of fractionation of minerals using geoinformation systems in engineering and geological prospecting. Technical Engineering. 2024. No. 1 (93). P. 332–338. DOI: 10.26642/ten-2024-1(93)-332-338.
27. Zuievska N., Shaidetska L., Kosenko T., Matviichuk I. Prognostication of zones with variable physical and mechanical characteristics of soil massifs. Coll. res. pap. nat. min. univ. 2024. No. 77. P. 118–125. DOI: 10.33271/crpnmu/77.118.
28. Kosenko T., Shukurlu E. Prospects for the development of gold deposits based on geodesic monitoring and GIS technologies. Coll. res. pap. nat. min. univ. 2024. No. 79. P. 38–48. DOI: 10.33271/crpnmu/79.038.
29. Abdullayeva S. F. Predictive estimate for the perspectives on the endogenic mineralization of Chovdar ore-magmatic system by extracting favourable lithologic horizons and structures. Baki Universitetinin Xəbərləri. GEOLOGİYA. Təbiət Elmləri Seriyası. 2011. No. 3. (in Azerbaijani).
30. Zaichenko S., Frolov O., Stovpnyk S., Veremiichuk Y. Investigation of the change in the strength properties of a soil mass by mechanical sensing. Eastern-European Journal of Enterprise Technologies. 2018. Vol. 3, no. 9 (93). P. 19–26. DOI: 10.15587/1729-4061.2018.132210.
31. Liqing L. Use of aluminum in perforating and stimulating a subterranean formation and other engineering applications : US Pat. No. 20030037692. 2003. URL: http://ip.com/patapp/US20030037692 (date of access: 20.05.2026).
32. Kravets V., Zakusylo R., Sydorenko Y., Shukurov A., Sałaciński T., Zakusylo D. Regularities of energy field formation in the explosion of a conical charge. Central European Journal of Energetic Materials. 2019. Vol. 16, no. 4. P. 533–546. URL: https://www.researchgate.net/publication/338245382 (date of access: 20.05.2026).
33. Kravets V., Shukurov A., Zakusylo R., Kovtun A. Technological applications of border effects by hole charges system explosion. Materialy Wysokoenergetyczne. 2019. Vol. 11, no. 2. P. 21–30. URL: https://www.researchgate.net/publication/348614222 (date of access: 20.05.2026).

34. Voitenko Y., Kravets V., Shukurov A., Drachuk O. Peculiarities of brittle and ductile materials destruction and deformation during the explosion of industrial shaped charges. Mining of Mineral Deposits. 2017. Vol. 11, no. 2. P. 12–20. DOI: 10.15407/mining11.02.012.
35. Giuliani A., Schmidt M. W., Torsvik T. H., Fedortchouk Y. Genesis and evolution of kimberlites. Nature Reviews Earth & Environment. 2023. Vol. 4, no. 11. P. 738–753. DOI: 10.1038/s43017-023-00481-2.
36. Field M., Stiefenhofer J., Robey J., Kurszlaukis S. Kimberlite-hosted diamond deposits of Southern Africa: A review. Ore Geology Reviews. 2008. Vol. 34, no. 1–2. P. 33–75. DOI: 10.1016/j.oregeorev.2007.11.002.
37. Lucapa Diamond Company Limited. Mothae Diamond Project in Lesotho. JORC Mineral Resource Statement and Competent Persons Report. 2017. URL: https://docplayer.net/99501355-Mothae-diamond-project-in-lesotho.html (date of access: 20.05.2026).
38. Giuliani A., Phillips D., Pearson D. G. et al. Diamond preservation in the lithospheric mantle recorded by olivine in kimberlites. Nature Communications. 2023. Vol. 14, no. 1. Article 6999. DOI: 10.1038/s41467-023-42888-x.
39. Korobiichuk V., Shamrai V., Levytskyi V. et al. Evaluation of the effectiveness of natural stone surface treatment from Ukraine by mechanical and chemical methods. Rudarsko-Geološko-Naftni Zbornik. 2018. Vol. 33, no. 4. P. 15–21. DOI: 10.17794/rgn.2018.4.2.
40. Sdvyzhkova O., Babets D., Moldabayev S. et al. Mathematical modeling a stochastic variation of rock properties at an excavation design. SGEM International Multidisciplinary Scientific GeoConference EXPO Proceedings. 2020. DOI: 10.5593/sgem2020/1.2/s03.021.
41. Shi X., Zhang Z., Qiu X., Luo Z. Experiment study of stemming length and stemming material impact on rock fragmentation and dynamic strain. Sustainability. 2023. Vol. 15, no. 17. Article 13024. DOI: 10.3390/su151713024.
42. Baluch K., Park H.-J., Kim J.-G., Ko Y.-H., Kim G. Enhancing rock blasting efficiency in mining and tunneling: a comparative study of shear-thickening fluid

stemming and plug device performance. Applied Sciences. 2024. Vol. 14. Article 5395. DOI: 10.3390/app14135395.

43. Konya C. J., Konya A. Effect of Hole Stemming Practices on Energy Efficiency of Comminution. Energy Efficiency in the Minerals Industry / ed. by K. Awuah-Offei. Cham : Springer, 2018. P. 31–53. DOI: 10.1007/978-3-319-54199-0_3.

44. Sharma S. K., Rai P. Investigation of Crushed Aggregate as Stemming Material in Bench Blasting: A Case Study. Geotechnical and Geological Engineering. 2015. Vol. 33, no. 6. P. 1449–1463. DOI: 10.1007/s10706-015-9911-7.

45. Kojovic T. Influence of aggregate stemming in blasting on the SAG mill performance. Minerals Engineering. 2005. Vol. 18, no. 15. P. 1398–1404. DOI: 10.1016/j.mineng.2005.02.012.

46. Lachamp M., Grannas S., Chavez R. Influence of Stemming Length and Initiation Sequence on Rock Movement and Dilution During a Blast. EFEE, 2020. Cited in: Oates T. E., Spiteri W. Stemming and best practice in the mining industry: A literature review. Journal of the Southern African Institute of Mining and Metallurgy. 2021. Vol. 121, no. 8. P. 415–425. DOI: 10.17159/2411-9717/1606/2021.

47. Zhang Z.-X., Qiao Y., Chi L., Hou D.-F. Experimental study of rock fragmentation under different stemming conditions in model blasting. International Journal of Rock Mechanics and Mining Sciences. 2021. Vol. 143. Article 104797. DOI: 10.1016/j.ijrmms.2021.104797.

48. Li X., Liu K., Sha Y., Yang J., Hong Z. Numerical investigation on blast-induced rock fragmentation with different stemming structures. Geomechanics and Geophysics for Geo-Energy and Geo-Resources. 2023. Vol. 9, no. 1. DOI: 10.1007/s40948-023-00654-9.

49. Chi L. Y., Zhang Z. X., Ylitalo R. M., Bergström P., Haugen S. Effects of aggregate sizes of stemming on blasting outcomes at the Kevitsa mine — a case study. Mining, Metallurgy & Exploration. 2025. DOI: 10.1007/s42461-025-01341-x.

50. Zuievska N., Ishchenko K., Vovk O., Novikov L., Semchuk R. Protection of Landscape Infrastructure Under Conditions of Dynamic Influences. Modern

Technologies in Energy and Transport II / ed. by S. Boichenko, A. Zaporozhets, I. Shkilniuk, A. Yakovlieva. Studies in Systems, Decision and Control. Cham : Springer, 2024. Vol. 574. P. 95–108. DOI: 10.1007/978-3-031-76650-3_8.

51. European Environment Agency : official website. URL: https://www.eea.europa.eu (date of access: 20.05.2026).

52. Health effects of particulate matter : Policy implications for countries in eastern Europe, Caucasus and central Asia. World Health Organization Regional Office for Europe, 2013. URL: https://www.euro.who.int/__data/assets/pdf_file/0006/189051/Health-effects-of-particulate-matter-final-Eng.pdf (date of access: 20.05.2026).

53. World-wide air quality monitoring data coverage. URL: https://aqicn.org/sources (date of access: 20.05.2026).

54. Moomivand H., Soltanalinejad S., Karwansara A. M. Assessment of the optimized stemming length considering rock fragmentation and escape of explosive gases using actual large-scale results. Results in Engineering. 2025. Vol. 25. Article 103575. DOI: 10.1016/j.rineng.2024.103575.

55. Lanari M., Fakhimi A. Numerical study of contributions of shock wave and gas penetration toward induced rock damage during blasting. Computational Particle Mechanics. 2015. Vol. 2, no. 2. P. 197–208. DOI: 10.1007/s40571-015-0053-8.

56. Zuievska N., Berezdetskyi V., Shukurlu E. Numerical simulation of sand and foam stemming for improved rock fragmentation in gold-bearing quartzites. Coll. res. pap. nat. min. univ. 2025. No. 82. P. 29–43. DOI: 10.33271/crpnmu/82.029.

57. Baranowski P., Mazurkiewicz Ł., Małachowski J., Pytlik M. Experimental testing and numerical simulations of blast-induced fracture of dolomite rock. Meccanica. 2020. Vol. 55, no. 12. P. 2337–2352. DOI: 10.1007/s11012-020-01223-0.

58. Gebretsadik A., Kumar R., Fissha Y. et al. Enhancing rock fragmentation assessment in mine blasting through machine learning algorithms: a practical approach. Discover Applied Sciences. 2024. Vol. 6, no. 5. DOI: 10.1007/s42452-024-05888-0.

59. Prasad S., Choudhary B. S., Mishra A. K. Effect of Stemming to Burden Ratio and Powder Factor on Blast Induced Rock Fragmentation — A Case Study. IOP Conference Series: Materials Science and Engineering. 2017. Vol. 225. Article 012191. DOI: 10.1088/1757-899X/225/1/012191.
60. Frolov O., Belteka M. Determination of the Radius of the Zone of Explosive Loosening of a Fractured Rock Mass When Blasting a Borehole Charge. Technical Engineering. 2020. No. 2 (86). P. 179–184. DOI: 10.26642/ten-2020-2(86)-179-184.
61. Jayasinghe L. B., Thambiratnam D. P., Perera N., Jayasooriya J. H. A. R. Computer simulation of underground blast response of pile in saturated soil. Computers & Structures. 2013. Vol. 120. P. 86–95. DOI: 10.1016/j.compstruc.2013.02.016.
62. Du H., Li Z. Numerical analysis of dynamic behavior of RC slabs under blast loading. Transactions of Tianjin University. 2009. Vol. 15, no. 1. P. 61–64. DOI: 10.1007/s12209-009-0012-7.
63. Zuievska N., Vovk O., Shaidetska L., Semchuk R. Computer simulation of the effect of an explosion on critical objects infrastructure. NATO Science for Peace and Security Series — E: Human and Societal Dynamics. 2024. Vol. 157. P. 14–27. DOI: 10.3233/NHSDP240003.
64. Zuievska N., Bronytskyi V., Hrebeniuk T. L., Semchuk R., Shlyk S. Forecasting the destruction of shallow subway stations by the action of an explosion. NATO Science for Peace and Security Series — E: Human and Societal Dynamics. 2024. Vol. 157. P. 28–41. DOI: 10.3233/NHSDP240004.
65. Huang B., Gao Q. C., Wang J. G., Jiang X. Z., Wang X. Y., Jiang B., Wu W. Dynamic analysis of pile–soil–structure interaction system under blasting load. Applied Mechanics and Materials. 2014. Vol. 638–640. P. 433–436. DOI: 10.4028/www.scientific.net/AMM.638-640.433.
66. Morales-Alonso G., Cendón D. A., Gálvez F., Erice B., Sánchez-Gálvez V. Blast response analysis of reinforced concrete slabs: Experimental procedure and numerical simulation. Journal of Applied Mechanics. 2011. Vol. 78, no. 5. Article 051010. DOI: 10.1115/1.4004278.

67. Karmakar S., Shaw A. Response of R.C. plates under blast loading using FEM–SPH coupled method. Engineering Failure Analysis. 2021. Vol. 125. Article 105409. DOI: 10.1016/j.engfailanal.2021.105409.
68. Maerz N. H., Palangio T. C., Franklin J. A. WipFrag image based granulometry system. Proceedings of the FRAGBLAST Workshop on Measurement of Blast Fragmentation, Montreal, Quebec, Canada, 23–24 Aug. 1996. P. 91–99. URL: https://www.researchgate.net/publication/239531885 (date of access: 20.05.2026).
69. Berezdetskyi V., Shukurlu E. Using the WipFrag image analysis system to evaluate the quality of explosive rock fragmentation. Coll. res. pap. nat. min. univ. 2024. No. 79. P. 7–14. DOI: 10.33271/crpnmu/79.007.
70. Korobiichuk V., Temchenko A., Zuievska N., Temchenko O. Determination of the Impact of Methods and Schemes for Opening a Deposit and Individual Quarry Horizons on the Efficiency of Open-Pit Mining Technology. Geomining. Studies in Systems, Decision and Control. Cham : Springer, 2024. Vol. 224. P. 43–54. DOI: 10.1007/978-3-031-70725-4_3.

APPENDIX A

AZƏRBAYCAN RESPUBLİKASI
AZƏRBAYCAN GEOLOGİYASI MMC

Az 1012, Bakı şəhəri,
Yeni Yasamal-1, ev 12, mənzil 155

AZGEO
AZƏRBAYCAN GEOLOGİYASI

AZERBAİJAN REPUBLİC
AZERBAİJAN GEOLOGY LLC

New Yasamal-1, 12,
apartment 155, Baku, 1012 az

VÖEN: 1303160161

№ AG-73/2026

"19" may 2026 il

ACT

In accordance with the recommendations of the dissertation by ELNUR SHUKURLU, "Scientific Substantiation of the Technology of Explosive Demand of Gold-Bearing Quartzite," industrial trials were carried out at the Tullalar open-pit mine (Azerbaijan) involving the replacement of the borehole stemming material from sand to foam during blasting operations. The commission has established that this measure resulted in a 4% reduction in the proportion of oversized rock fragments within the test section.

The commission of "Azerbaijan Geology" LLC the company performing blasting operations at the Tullalar open-pit mine, hereby certifies that the improvement of the borehole stemming material, scientifically substantiated in the dissertation by ELNUR SHUKURLU "Scientific Substantiation of the Technology of Explosive Demand of Gold-Bearing Quartzite," has practical value. Its implementation makes it possible to reduce the volume of secondary crushing of oversized rock and to obtain an economic effect in the form of an increase in the company's gross annual profit by 192 000,00 housand US dollars.

Chief Engineer ____________________

Chief Surveyor ____________________

Director of the Company ____________________

AZGEO